



HHS Public Access

Author manuscript

Eur J Med Chem. Author manuscript; available in PMC 2020 December 01.

Published in final edited form as:

Eur J Med Chem. 2019 December 01; 183: 111673. doi:10.1016/j.ejmech.2019.111673.

Structure Activity Relationship Towards Design of *Cryptosporidium* Specific Thymidylate Synthase Inhibitors

D.J. Czyzyk^{a,‡}, M. Valhondo^{b,‡}, L. Deiana^b, J. Tirado-Rives^b, W.L. Jorgensen^{b,*}, K.S. Anderson^{a,c,*}

^aDepartment of Pharmacology, Yale University School of Medicine, 333 Cedar Street, New Haven, CT 06520, USA

^bDepartment of Chemistry, Yale University, 225 Prospect Street, PO Box 208107, New Haven, CT 06520, USA

^cDepartment of Molecular Biophysics and Biochemistry, Yale University, 225 Prospect Street, PO Box 208107, New Haven, CT 06520, USA

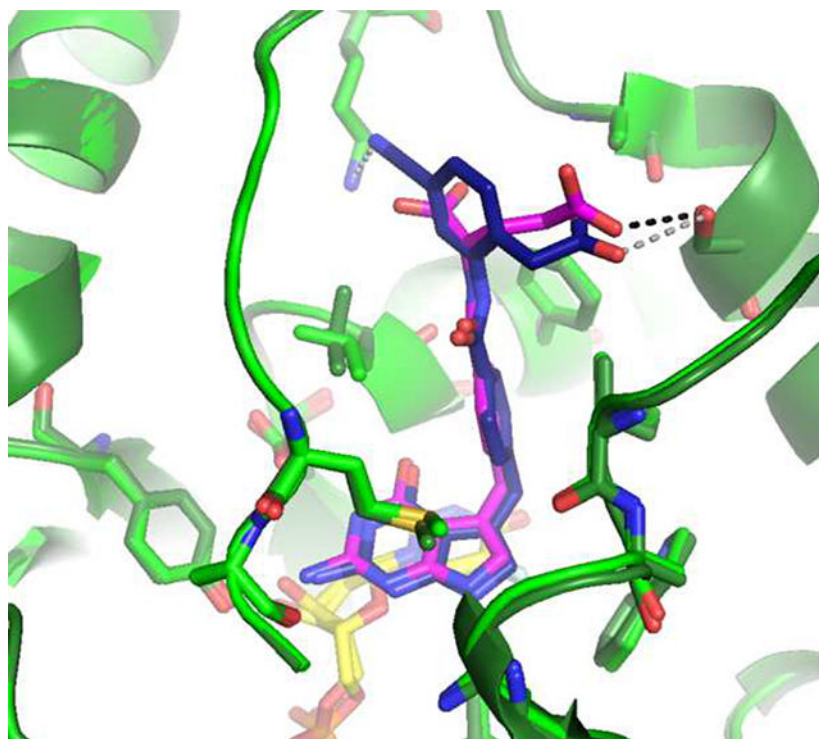
Abstract

Cryptosporidiosis is a human gastrointestinal disease caused by protozoans of the genus *Cryptosporidium*, which can be fatal in immunocompromised individuals. The essential enzyme, thymidylate synthase (TS), is responsible for *de novo* synthesis of deoxythymidine monophosphate. The TS active site is relatively conserved between *Cryptosporidium* and human enzymes. In previous work, we identified compound **1**, (2-amino-4-oxo-4,7-dihydro-pyrrolo[2,3-d]pyrimidin-methyl-phenyl-L-glutamic acid), as a promising selective *Cryptosporidium hominis* TS (*Ch*TS) inhibitor. In the present study, we explore the structure-activity relationship around **1** glutamate moiety by synthesizing and biochemically evaluating the inhibitory activity of analogues against *Ch*TS and human TS (hTS). X-Ray crystal structures were obtained for compounds bound to both *Ch*TS and hTS. We establish the importance of the 2-phenylacetic acid methylene linker in optimally positioning compounds **23**, **24**, and **25** within the active site. Moreover, through the comparison of structural data for **5**, **14**, **15**, and **23** bound in both *Ch*TS and hTS identified that active site rigidity is a driving force in determining inhibitor selectivity.

Graphical Abstract

*Corresponding authors. Tel.: +1 203 432 6278; fax: +1 203 432 6299 (W.L.J.); Tel.: +1 203 785 7670; fax: +1 203 785 7670 (K.S.A.), william.jorgensen@yale.edu (W.L. Jorgensen), karen.anderson@yale.edu (K.S. Anderson).

[‡]Authors have contributed equally to this work.



Keywords

SAR study; Antifolate; *Cryptosporidium hominis*; Thymidylate synthase; X-ray crystallography

1. Introduction

Cryptosporidiosis is a human gastrointestinal illness caused by protozoans of the genus *Cryptosporidium* and is the second leading cause of diarrheal disease and deaths in children <2 years old across Africa and South Asia.[1–3] Additionally, outbreaks have occurred in industrialized countries, with major outbreaks occurring in Milwaukee and New York City. [4, 5] Among the several *Cryptosporidium* species that can cause human disease, *Cryptosporidium hominis* (*C. hominis*) and *Cryptosporidium parvum* (*C. parvum*) are responsible for 90 % of the human disease and share a high sequence identity (95–97%) at the genome level.[6–8] *Cryptosporidium* is capable of surviving without a host for many months at a wide range of temperatures.[9] Infection occurs when an individual ingest oocyst in contaminated food or water. Healthy individuals experience gastrointestinal distress that can last for two or more weeks. However, infection rates are higher and more severe in children, the elderly, and immunocompromised individuals, where it leads to severe and life-threatening wasting disease.[8–10] Currently, nitazoxanide is the only FDA-approved drug for the treatment of cryptosporidiosis.[10] However, the efficacy of nitazoxanide is variable in immunocompetent patients, limited in children, and ineffective in immunocompromised patients, indicating a pressing need for improved therapies.[1, 9, 10]

The essential enzymes, thymidylate synthase (TS) and dihydrofolate reductase (DHFR), have long been chemotherapeutic targets for cancer and infectious diseases.[11, 12] In humans and most organisms, these two enzymes exist as separate polypeptide chains, whereas in *Cryptosporidium* both activities are encoded into a single bifunctional enzyme TS-DHFR.[13, 14] TS-DHFR has been extensively characterized and shown to be a promising target for the development of inhibitors.[12, 15, 16] TS catalyzes the *de novo* synthesis of deoxythymidine monophosphate (dTMP) from deoxyuridine monophosphate (dUMP) and the cofactor 5,10-methylenetetrahydrofolate (CH₂H₄F).[11, 17] The dihydrofolate produced as the other product of the TS reaction is then reduced by DHFR utilizing the cofactor NADPH, to produce tetrahydrofolate and NADP⁺. [11, 18] The TS active site is highly conserved for both the *C. hominis* and the human enzymes, however there are two distinct, variant amino acids in the region of the binding pocket that interact with the glutamate moiety of folate.[19] In *C. hominis* TS (*ChTS*) these residues are A287 and S290, versus F80 and G83 in human TS (hTS), respectively.[11, 19] Our earlier kinetic studies with bifunctional *ChTS*-DHFR together with mutational and structural analyses identified this novel folate binding region containing the two variant residues, A287 and S290. These residues are critical to properly position the folate substrate for efficient interaction with the second substrate dUMP for methyl transfer during catalysis.[11, 20] In other species such as human, a bulky phenylalanine residue is located in this region. These studies suggested that this region might be exploited to build in increased inhibitor specificity and affinity for the *ChTS*-DHFR.

In previous work we identified compound **1** (2-amino-4-oxo-4,7-dihydro-pyrrolo[2,3-d]pyrimidin-methylphenyl-L-glutamic acid), originally designed as an anticancer agent, that proved to be a promising *ChTS* inhibitor (see Figure 1).[12, 16, 21] We reported the X-ray crystal structure of *ChTS* complexed with **1**, in combination with inhibition activity of **1** demonstrating a 6-fold greater selectivity for the *ChTS* over the hTS enzyme.[12] This data suggested that these two variant active site residues might play an important role in determining selectivity. This concept was further supported by our recent work in which the X-ray crystal structure of **1** complexed with hTS was determined.[19] The variant *ChTS* residue S290 forms a hydrogen bond with the carboxylate of the glutamate moiety of **1** as well as hydrophobic interactions with A287, stabilizing this portion of compound **1** within the TS active site. In the case of hTS, a hydrogen bond with compound **1** glutamate moiety does not form, but rather hydrophobic interactions with F80 or interaction with solvent.

In this present study, we describe a computational and structure-guided lead optimization strategy to explore the structure-activity-relationship (SAR) of compound **1** with the aim of identifying compounds which take advantage of the variant *ChTS* and hTS active site residues in an effort to increase potency and selectivity. A series of 26 compounds were designed and synthesized for this effort. The compounds were tested for inhibitory activity against both *ChTS* and hTS enzymes. A total of 12 X-ray crystal structures were determined for a number of these compounds bound in the *ChTS* active site to evaluate interactions that may be important for inhibitor potency. Additionally, we compare the X-ray crystal structures of four compounds bound in both *ChTS* and hTS active sites to understand inhibitor selectivity.

2. Results and Discussion

2.1. Lead optimization guided by computational and structural analyses

The three-dimensional structure of compound **1** bound the *ChTS* active site is shown in Figure 1(A) along with several scaffolds showing potential regions of the molecule to be targeted in the lead optimization efforts (B). Analysis of the crystal structure of compound **1** indicates that the accommodation of the pyrrolo[2,3-d]pyrimidine fragment of **1** in the *ChTS* active site is nearly ideal. The pyrrolo[2,3-d]pyrimidine π -stackes with the uracil ring of the FdUMP, with hydrogen bonds of normal lengths for all of the heteroatoms except N3 (its closest contact is 4.32 Å with the side-chain N of N319), and the central benzyl ring is well situated in a hydrophobic region and has an edge-to-face aryl-aryl interaction with F433. However, the amide linker moiety and its attachments are not making notable contacts. The α -carboxylate of the glutamate moiety has one oxygen 4.30 Å from the ammonium group of K284, while the γ -carboxylate forms a hydrogen bond with S290 (Figure 1A). Thus, our initial focus for analogues was on the eastern region of compound **1**. Several possibilities were suggested by initial modeling based on the *ChTS* crystal structure with **1** (PDB: 40QE).[12] These include modifications which would retain the γ -carboxylate to preserve the hydrogen bond with S290 while substituting the α -carboxylic acid with an aryl ring to interact with hydrophobic pocket, changes to the amide linker, and additional functionalization of the aryl ring (Scaffold A, Fig. 1B). Modeling suggests that further elaboration of the aryl ring to substituted biphenyl compounds would also be viable (Scaffold B, Fig. 1B). Moreover, it has been shown that biphenyls are twisted 30° to provide some conformational variety.[22] This substitution pattern would feature a smaller group that projects towards K284, and a larger one for the opening between A287 and S290. The larger group could be used to control properties such as solubility as its terminus can project into the aqueous solvent. An example of a computed biphenyl structure is illustrated in Supplementary Figure S1.

2.2. Chemistry

A general outline of our synthetic strategy for the preparation of 2-amino-4-oxo-4,7-dihydro-pyrrolo[2,3-d]pyrimidin-methyl-phenyl-L-glutamic acid derivatives **2–26** is summarized in Schemes 1–3 and Experimental Section. A complete description of synthetic routes for the synthesis of the non-commercial amines is summarized in the Supplementary Information.

2.3. SAR Profiling using biochemical assays

A series of antifolate compounds were prepared to explore SAR based upon compound **1** and Scaffolds A and B (Figure 1B). The synthesized series of 26 antifolate compounds were biochemically evaluated against purified *ChTS* and hTS enzymes by monitoring the conversion of dUMP and CH₂H₄F to dTMP and H₂F. Compound **1** was utilized as a positive antifolate control. TS inhibitory activity is summarized in (Tables 1 and 2 and Supplementary Table S1), and the SAR of these compounds with *ChTS* was investigated.

As shown in Table 1 and Figure 2, the first compound synthesized, **2**, involved replacement of the α -carboxylate of the glutamic acid moiety with an aryl ring containing a carboxyl acid

at the ortho position to mimic the γ -carboxylate. Compound **2** had an $IC_{50} = 20 \mu M$. There was a ~ 5 -fold loss of potency, when the carboxylate was in either the meta or para positions of the aryl ring, compounds **3** and **4**, demonstrating a preference for the ortho position. The three-dimensional crystal structure for **2** in complex with the ChTS-DHFR protein was solved (see Supplementary Figure S2A). The structural analysis revealed that the ortho carboxylic acid was oriented toward S290, however the distance was too short to allow a hydrogen bond (see Figure 7, below). Accordingly, incorporation of a methylene linker to extend the ortho-carboxylate by one carbon unit from the aryl ring, in order to replicate the hydrogen bond observed in the crystal structure between **1** and S290, resulted in compound **5**, which did result in a small increase in potency. The increased linker length allowed formation of the hydrogen bond with S290 as verified by the determination of the crystal structure of **5** bound to the ChTS active site (see Figure 7, below, and Supplementary Figure S2B). However, the addition of the longer ethylene linker resulted in a ~ 6 -fold loss of potency for **6**. Isosteric replacement of the carboxylate moiety with other functional groups that could form a hydrogen bond, such as a tetrazole or a cyano, also resulted in an ~ 8 -fold and ~ 6 -fold loss of potency, respectively, compound **7** and **8**.

As illustrated in Table 2 and Figure 3, in general modifications made to the amide linker moiety resulted in substantial decrease in potency. The addition of a methyl group to produce a tertiary amine resulted in an ~ 11 -fold decrease in potency, compound **9**. Removing the amide linker and replacing with an ethylene linker resulted in a greater than 5-fold decrease in potency, compound **10**. Increasing the length of the linker region by inserting a methylene to elongate the linker region by one carbon unit resulted in a 6-fold loss in potency, compound **11**. Compound **12** demonstrated a greater than 25-fold decrease in potency. Here the loss of aromaticity is combined with the creation of a piperidine ring, which shortens the amide linker moiety by insertion of a secondary amine into the ring structure. However, the loss of aromaticity alone resulted in a 3-fold loss of potency, compound **13**.

Based on the ortho substituted compound **2**, a series of substituents were added to the C-4 position of the aryl ring to take advantage of the pocket surrounding K284 to improve potency as shown in Table 1 and Figure 4. Hydrophilic substituents in general were well tolerated, compounds **15**, **17** and **20**. While the addition of a carboxamide or carboxylate at C-4 maintained potency compared to **2**, where the addition of a cyano at this position enhanced potency 2-fold in compound **17**. This is confirmed by the crystal structure (Figure 9 and Supplementary Figure S3D), described below. However, the addition of a methoxy group or a hydroxymethyl group at the C-4 position resulted in a ~ 2.5 -fold and ~ 9 -fold decrease in potency, respectively, compound **16** and **18**. The addition of a chloride substituent to the C-4 position resulted in a small loss of potency, compound **14**. The addition of a methoxymethyl substituent to the C-4 position resulted in ~ 3.5 -fold loss in potency for compound **19**. Additionally, the addition of methoxymethyl or methoxy substituents to the aryl moiety at the C-3 and C-5 positions were not well tolerated, with a greater than 5-fold loss of potency, compound **21** and **22**.

As shown in Table 1 and Figure 5, the combination of an ortho-phenylacetic acid moiety with a substituent at the C-4 position of the aryl ring resulted in ~ 2 -fold increase in potency,

compounds **23–25**. These compounds were designed to form a hydrogen bond with S290 as well as interact with the pocket surrounding K284. These interactions are supported by the crystal structure (Figure 9 and Supplementary Figures S5 and S6), as described below.

Finally, as illustrated in Table 1 and Figure 6, elaboration of the aryl ring to a biphenyl, suggested by modeling to be favorable, resulted in a substantial drop in potency. The biphenyl moiety was poorly tolerated resulting in a loss of potency ~ 5-fold and greater than 25-fold for compounds **26** and **27** respectively.

2.4. X-ray crystal structures of antifolates complexed with ChTS

All 26 antifolate compounds were evaluated by biochemical assays to assess inhibition of *ChTS* catalytic activity. The compounds were then further evaluated with structural analyses. Co-crystal structures were obtained for 12 antifolate compounds: **2, 5, 6, 11, 14, 15, 16, 17, 20, 23, 24, and 25** with *ChTS*-DHFR. As further described in the Experimental section, structures of *ChTS*-DHFR complexed with antifolate compounds were obtained utilizing the same procedures. The resolution of the structures range from 2.5 to 3.3 Å and all twelve structures have been deposited in the Protein Data Bank. The co-crystal structures contained five protein molecules within the asymmetric subunit and crystallized as a C2 space group with a similar crystal lattice as reported for *ChTS*-DHFR complexed with **1**. [12]

The antifolate compounds bind into the 5,10-methylenetetrahydrofolate (CH₂H₄F) pocket where the pyrrolo[2,3-d]pyrimidine and centralbenzyl moieties form similar interactions with *ChTS* active site as previously described for **1** (Supplementary Figures S2–4). [12] However, the pyrrolo[2,3-d]pyrimidine of compounds **2, 6, 15, 17, and 20** form fewer hydrogen bonding interactions with the *ChTS* active site (Supplementary Figure S2A, S2C, S3B, S3D, and S4A). Compounds **6, 15** and **17** do not form hydrogen bonding interactions with the backbone N of G430. Additionally, **15** and **17** do not form hydrogen bonding interactions with D426. All five compounds do not form a hydrogen bond with Y466.

The carboxylate group of the benzoic acid, 2-phenylacetic acid, and 3-phenylpropanoic acid moieties are directed towards S290. With an average distance of ~ 3.9 Å, the carboxylate group for compounds containing a benzoic acid moiety were not within hydrogen bonding distance to S290. The carboxylate group for compounds containing either 2-phenylacetic acid, or 3-phenylpropanoic acid moieties, with an average distance of ~3.3 Å, were within hydrogen bonding distance to S290. Compounds **2, 5, and 6**, which contain a benzoic acid, 2-phenylacetic acid, and 3-phenylpropanoic acid moiety, respectively, illustrates the importance of linker length on inhibitor potency. Comparing the three compounds it is observed that the carboxylate of **2** is ~4.0 Å from S290, while the methylene linker of **5** extends the carboxylate within hydrogen bonding distance, ~ 3.3 Å, to S290 (Figure 7). The longer linker used in **6** enables the carboxylate to hydrogen bond with S290, however there is greater disorder due to the linker length resulting in the loss of two hydrogen bonds to the pyrrolo[2,3-d]pyrimidine moiety (Supplementary Figure S2C).

Compound **11** differs from **2** by the addition of a methylene to the amide linker moiety, which resulted in a 6-fold loss of potency. Comparing the two structures of **2** and **11**, the carboxylate of both compounds is ~ 4.0 Å from S290 (Figure 8A). In Figure 8B, we observe

the benzoic acid moiety shifts 1.4 Å into the pocket, while shifting the amide linker towards M519 by ~ 0.9 Å. The addition of the methylene to this region destabilizes the binding of **11** by increasing the compounds flexibility within the binding pocket.

C-4 substituents to either benzoic acid or 2-phenylacetic acid moieties were directed into a small pocket adjacent to K284. Cyano, carboxylate, or carboxamide C-4 substituents, **15** and **25**, **17** and **24**, or **20**, respectively, were within hydrogen bonding distance of the ammonium of K284, while the C-4 substituent of **20** was also within hydrogen bonding distance of the backbone carbonyl of I515 (Supplementary Figure S3B, S3D, S4A, S4C and S4D). Compounds **23**, **24**, and **25**, which combine a C-4 substituent, in this case a methoxy, cyano or carboxylate, respectively, with the 2-phenylacetic acid moiety, demonstrate the greatest *ChTS* potency for this series of compounds. A structural comparison of compounds **23**, **24**, and **25** with the benzoic acid moiety counterparts **16**, **17**, and **15**, respectively, reveals subtle differences in the way these compounds interact with the *ChTS* active site. First the carboxylate group of compounds **23**, **24**, and **25** is within hydrogen bonding distance of S290, while the carboxylate of the benzoic acid counterparts is an average ~ 3.8 Å away from this residue (Figure 9A and Supplementary Figure S5A and S6A). This hydrogen bond with S290 coupled with the C-4 substituents interactions within the pocket containing K284 stabilizes the 2-phenylacetic acid moiety within the *ChTS* active site. Secondly, the addition of the methylene linker in the 2-phenylacetic acid moiety of compounds **23**, **24**, and **25** produces ~ 22.0° clockwise rotation of this moiety with respect to their benzoic acid moiety counterparts (Figure 9B and Supplementary Figure S5B and S6B). This small rotation appears to transfer to the pyrrolo[2,3-d]pyrimidine moiety resulting in an average shift of ~ 0.3 Å into the pocket, stabilizing the hydrogen bonding interactions between the pyrrolo[2,3-d]pyrimidine and *ChTS* active site (Figure 9C and Supplementary Figure S5C and S6C).

2.5. X-ray crystal structures of antifolates complexed with hTS

All antifolate compounds were evaluated for structural analysis with hTS, however, co-crystal structures were obtained for antifolate compounds **5**, **14**, **15**, and **23**. A full description of the procedures used to obtain structures of hTS complexed with the antifolate compounds can be found in the Experimental section. The resolution of the structures range from 2.39 to 2.84 Å and all four structures have been deposited in the Protein Data Bank. The co-crystal structures contained four protein molecules within the asymmetric subunit, with **14** and **23**, **5**, and **15** crystalizing in a C2, P2₁2₁2₁, and P4₁2₁2 space groups, respectively. In all structures, density for the antifolate compounds was observed in all four chains of the asymmetric unit except for the structure for **15**, where density was only observed in chains B and C.

The antifolate compounds bind into the CH₂H₄F pocket where the pyrrolo[2,3-d]pyrimidine and central benzyl moieties form similar interactions with the hTS active site as previously described for **1**.^[19] However, the pyrrolo[2,3-d]pyrimidine of compounds **5**, **14**, and **23** form fewer hydrogen bonding interactions with the hTS active site (Supplementary Figure S7A, S7B, and S7D). Compound **5** does not form hydrogen bonding interactions with the backbone carbonyl of A312, but this could be an artifact due to a lack of density to visualize the neighboring residue V313. Compound **14** and **23** do not form hydrogen bonding

interactions with Q112. The carboxylate group of the benzoic acid, and 2-phenylacetic acid moieties are directed towards solvent, while C-4 substituents are directed towards the pocket containing residue K77. Additionally, the aryl ring of both the benzoic acid, and 2-phenylacetic acid moieties formed hydrophobic interactions with F80 (Supplementary Figure S7). Interestingly, unlike the positioning of the amide linker moiety for these compounds bound in *ChTS*, the amide linker moiety for all four compounds bound in the opposite orientation where the carbonyl points into the pocket near F225 (Supplementary Figure S7).

Comparing the structures of **5**, **14**, **15**, and **23** in both the *ChTS* and *hTS* active sites provides a possible explanation for the observed trend in inhibitory selectivity the antifolate compounds display for both enzymes (Supplementary Table S1). As previously reported in our work with *R*- and *S*- enantiomers of **1**, we observed that the *ChTS* active site is more rigid than the *hTS* active site.[19] Similarly here the *hTS* residue F225 rotates $\sim 75^\circ$ clockwise, as compared to its corresponding *ChTS* residue F433 for all four compound structures (Figure 10A and Supplementary Figure S8A, S9A, and S10A). The space afforded by the rotation of F225 allows the central benzyl moiety to shift back into the pocket towards F225 by $\sim 0.8 \text{ \AA}$, while providing space for the compound's amide linker moiety carbonyl (Figure 10B and Supplementary Figure S8B, S9B, and S10B). The reverse orientation of the amide linker moiety appears to position the benzoic acid, and 2-phenylacetic acid moieties aryl rings towards F80, allowing for a more optimal position to hydrophobically interact with F80. The positioning of the compounds towards F80 provides space for the sidechain of L221 to rotate $\sim 180^\circ$ into the pocket as compared to its *ChTS* counterpart L429 (Figure 10C and Supplementary Figure S8C, S9C, and S10C). Taken together, *hTS* structural data and IC_{50} values indicate that with few exceptions the *hTS* active site is capable of accommodating most alterations in the compounds used in this SAR.

3. Conclusions

We have designed, synthesized and evaluated a series of anti-cryptosporidium agents based on the chemical structure of lead compound **1**, where the glutamate moiety is replaced by a benzoic acid. Structure-activity relationship analysis indicates (1) *ChTS* prefers an ortho-phenylacetic acid moiety over an ortho-benzoic acid or ortho-phenylpropanoic acid moieties (2) hydrophilic C-4 substituents on the 2-phenylacetic acid moieties increase potency (3) changes to the amide linker moiety are not tolerated. X-ray crystal structures of compounds **23**, **24**, and **25** bound to the *ChTS* active site reveal the key interactions that are necessary for compound potency, as well as the role that the 2-phenylacetic acid methylene linker plays in optimally positioning these compounds into the active site. Comparison of structural data for compounds **5**, **14**, **15**, and **23** bound in both *ChTS* and *hTS* identified that active site structural rigidity is a driving factor in determining inhibitor selectivity. In summary, the results presented here provide a platform for further efforts to develop new anti-cryptosporidium agents.

4. Experimental section

4.1. General Information

NMR spectra were recorded on Agilent DD2 600 (600 MHz), DD2 500 (500 MHz) and DD2 400 (400 MHz) instruments. Column chromatography was carried out using CombiFlash over redisepp column cartridges employing Merck silica gel (Kieselgel 60, 63–200 μm). Pre-coated silica gel plates F-254 were used for thinlayer analytical chromatography. Mass determinations were performed using electrospray ionization on a Waters Micromass ZQ (LC-MS) and on an Agilent Technologies 6890N (GC-MS). HRMS (ESI-TOF) analyses were performed on Waters Xevo QTOF equipped with Z-spray electrospray ionization source. HRMS values agree within $\pm 0.4\%$ of the theoretical values. The purity of all final synthesized compounds was determined by reverse phase HPLC, using Waters 2487 dual λ absorbance detector with a Waters 1525 binary pump and a Phenomenex Luna 5 μ C18(2) 250 \times 4.6 mm column. Samples were run at 1 mL/min using gradient mixtures of 5–100% of water with 0.1% trifluoroacetic acid (TFA) (A) and 10:1 acetonitrile:water with 0.1% TFA (B) for 22 min followed by 3 min at 100% B. Additional details are provided in Supplementary Information.

4.2. General procedure for the synthesis of intermediates 29a-u. Method a.

Intermediates **29a-u** have been obtained through general method *a*. To a solution of corresponding amine (**28a-u**) (1eq) in anhydrous dichloromethane (3.16 mL/eq) and dry triethylamine (1.10 eq), was added 4-iodobenzoylchloride (1.10 eq). The reaction was stirred overnight at room temperature. Solvent was evaporated under reduced pressure and the desired intermediates purified by flash column chromatography.[23]

4.2.1. methyl 1-(4-iodobenzoyl)piperidine-2-carboxylate (29a)—(hexanes to ethyl acetate). White powder, 0.54 g, 1.44 mmol, 37% yield. ^1H NMR (400 MHz, CDCl_3) δ 7.79 – 7.73 (m, 2H), 7.21 – 7.16 (m, 2H), 5.51 – 5.44 (m, 1H), 3.78 (s, 3H), 3.62 – 3.56 (m, 1H), 3.31 – 3.18 (m, 1H), 2.37 – 2.31 (m, 1H), 1.78 – 1.74 (m, 3H), 1.43 – 1.35 (m, 2H). LC-MS (ESI) m/z 374.1 $[\text{M}+\text{H}]^+$.

4.2.2. methyl 2-(4-iodobenzamido)cyclohexane-1-carboxylate (29b)—(hexanes to hexanes/ dichloromethane 1:1). White powder, 0.54 g, 1.39 mmol, 32% yield. ^1H NMR (400 MHz, CDCl_3) δ 7.80 – 7.74 (m, 2H), 7.52 – 7.46 (m, 2H), 7.29 (s, 1H), 4.30 (qd, J = 9.0, 7.9, 4.4 Hz, 1H), 3.72 (s, 3H), 2.91 (q, J = 4.6 Hz, 1H), 2.24 – 2.13 (m, 1H), 1.83 – 1.51 (m, 5H), 1.51 – 1.40 (m, 1H), 1.33 – 1.20 (m, 1H). LC-MS (ESI) m/z 388.1 $[\text{M}+\text{H}]^+$.

4.2.3. methyl 2-(4-iodobenzamido)benzoate (29c)—(hexanes/dichloromethane 8:2 to dichloromethane). White powder, 0.66 g, 1.73 mmol, 87% yield. ^1H NMR (400 MHz, CDCl_3) δ 12.07 (s, 1H), 8.90 (d, J = 8.5 Hz, 1H), 8.12 – 8.06 (m, 1H), 7.91 – 7.86 (m, 2H), 7.80 – 7.74 (m, 2H), 7.65 – 7.58 (m, 1H), 7.17 – 7.11 (m, 1H), 3.97 (s, 3H). LC-MS (ESI) m/z 382.0 $[\text{M}+\text{H}]^+$.

4.2.4. methyl 3-(4-iodobenzamido)benzoate (29d)—(hexanes to ethyl acetate). White powder, 0.97 g, 2.55 mmol, 68% yield. ^1H NMR (400 MHz, CDCl_3) δ 8.16 – 8.09

(m, 1H), 8.05 – 8.01 (m, 1H), 7.92 (s, 1H), 7.88 – 7.80 (m, 3H), 7.63 – 7.58 (m, 2H), 7.46 (t, $J = 7.9$ Hz, 1H), 3.92 (s, 3H). LC-MS (ESI) m/z 382.1 [M+H]⁺.

4.2.5. methyl 4-(4-iodobenzamido)benzoate (29e)—(hexanes to ethyl acetate).

White powder, 0.29 g, 0.76 mmol, 20% yield. ¹H NMR (400 MHz, CDCl₃) δ 8.09 – 8.05 (m, 2H), 7.88 – 7.85 (m, 2H), 7.75 – 7.70 (m, 2H), 7.63 – 7.59 (m, 2H), 3.92 (s, 3H). LC-MS (ESI) m/z 382.1 [M+H]⁺.

4.2.6. methyl 2-(2-(4-iodobenzamido)phenyl)acetate (29f)—(hexanes/

dichloromethane 8:2 to dichloromethane). White powder, 1.15 g, 2.91 mmol, 78% yield. ¹H NMR (500 MHz, CDCl₃) δ 9.78 (s, 1H), 8.02 (d, $J = 8.1$ Hz, 1H), 7.90 – 7.84 (m, 2H), 7.80 – 7.74 (m, 2H), 7.39 – 7.35 (m, 1H), 7.27 – 7.22 (m, 1H), 7.18 – 7.13 (m, 1H), 3.76 (s, 3H), 3.68 (s, 2H). LC-MS (ESI) m/z 396.0 [M+H]⁺.

4.2.7. methyl 3-(2-(4-iodobenzamido)phenyl)propanoate (29g)—(hexanes to

ethyl acetate). White powder, 6.54 g, 15.99 mmol, 84% yield. ¹H NMR (400 MHz, CDCl₃) δ 9.75 (s, 1H), 7.93 – 7.80 (m, 5H), 7.31 – 7.24 (m, 1H), 7.23 – 7.13 (m, 2H), 3.67 (s, 3H), 2.91 (dd, $J = 7.1, 4.7$ Hz, 2H), 2.79 (dd, $J = 7.1, 4.6$ Hz, 2H) LC-MS (ESI) m/z 410.1 [M+H]⁺.

4.2.8. N-(2-cyanophenyl)-4-iodobenzamide (29h)—(hexanes to ethyl acetate).

White powder, 5.82 g, 16.7 mmol, 84% yield. ¹H NMR (400 MHz, CDCl₃) δ 8.56 (d, $J = 8.4$ Hz, 1H), 8.35 (s, 1H), 7.93 – 7.87 (m, 2H), 7.70 – 7.61 (m, 4H), 7.26 – 7.20 (m, 1H). LC-MS (ESI) m/z 349.1 [M+H]⁺.

4.2.9. methyl 2-((4-iodobenzamido)methyl)benzoate (29i)—(hexanes to hexanes/

ethyl acetate 6:4). White powder, 0.53 g, 1.35 mmol, 75% yield. ¹H NMR (400 MHz, CDCl₃) δ 7.99 (dd, $J = 7.8, 1.4$ Hz, 1H), 7.77 – 7.71 (m, 2H), 7.64 (dd, $J = 7.7, 1.4$ Hz, 1H), 7.60 (t, $J = 6.8$ Hz, 1H), 7.56 – 7.46 (m, 3H), 7.37 (td, $J = 7.6, 1.4$ Hz, 1H), 4.78 (d, $J = 6.5$ Hz, 2H), 3.95 (s, 3H). LC-MS (ESI) m/z 396.1 [M+H]⁺.

4.2.10. methyl 4-chloro-2-(4-iodobenzamido)benzoate (29j)—(hexanes/

dichloromethane 8:2 to dichloromethane). White powder, 0.96 g, 2.31 mmol, 62% yield. ¹H NMR (400 MHz, CDCl₃) δ 12.10 (s, 1H), 9.01 (d, $J = 2.0$ Hz, 1H), 8.02 (d, $J = 8.6$ Hz, 1H), 7.93 – 7.84 (m, 2H), 7.80 – 7.71 (m, 2H), 7.11 (dd, $J = 8.6, 2.1$ Hz, 1H), 3.97 (s, 3H). LC-MS (ESI) m/z 416.1 [M+H]⁺.

4.2.11. dimethyl 2-(4-iodobenzamido)terephthalate (29k)—(hexanes to hexanes/

ethyl acetate 8:2). White powder, 0.43 g, 0.98 mmol, 98% yield. ¹H NMR (400 MHz, CDCl₃) δ 12.03 (s, 1H), 9.52 (d, $J = 1.6$ Hz, 1H), 8.15 (d, $J = 8.3$ Hz, 1H), 7.92 – 7.87 (m, 2H), 7.81 – 7.75 (m, 3H), 4.00 (s, 3H), 3.96 (s, 3H). LC-MS (ESI) m/z 440.1 [M+H]⁺.

4.2.12. methyl 2-(4-iodobenzamido)-4-methoxybenzoate (29l)—(hexanes to

hexanes/ethyl acetate 8:2). White powder, 0.59 g, 1.43 mmol, 95% yield. ¹H NMR (400 MHz, DMSO-*d*₆) δ 11.93 (s, 1H), 8.32 (s, 1H), 8.02 – 7.99 (m, 2H), 7.87 (d, $J = 7.9$ Hz,

1H), 7.76 – 7.68 (m, 2H), 6.82 (d, $J = 7.9$ Hz, 1H), 3.88 (s, 3H), 3.86 (s, 3H). LC-MS (ESI) m/z 412.1 [M+H]⁺.

4.2.13. methyl 4-cyano-2-(4-iodobenzamido)benzoate (29m)—(hexanes to hexanes/ethyl acetate 8:2). White powder, 0.56 g, 1.34 mmol, 92% yield. ¹H NMR (400 MHz, DMSO-*d*₆) δ 11.41 (s, 1H), 8.72 (d, $J = 1.6$ Hz, 1H), 8.10 (d, $J = 8.1$ Hz, 1H), 8.02 – 8.00 (m, 2H), 7.74 – 7.71 (m, 3H), 3.89 (s, 3H). LC-MS (ESI) m/z 407.1 [M+H]⁺.

4.2.14. methyl 4-(hydroxymethyl)-2-(4-iodobenzamido)benzoate (29n)—(hexanes to hexanes/ethyl acetate 8:2). White powder, 0.95 g, 2.31 mmol, 45% yield. ¹H NMR (400 MHz, CDCl₃) δ 12.11 (s, 1H), 9.03 (d, $J = 1.7$ Hz, 1H), 8.10 (d, $J = 8.2$ Hz, 1H), 7.91 – 7.86 (m, 2H), 7.78 – 7.74 (m, 2H), 7.18 (dd, $J = 8.2, 1.7$ Hz, 1H), 5.41 (s, 2H), 3.97 (s, 3H). LC-MS (ESI) m/z 412.1 [M+H]⁺.

4.2.15. methyl 2-(4-iodobenzamido)-4-(methoxymethyl)benzoate (29o)—(hexanes to hexanes/ethyl acetate 8:2). White powder, 0.26 g, 0.62 mmol, 61% yield. ¹H NMR (400 MHz, DMSO-*d*₆) δ 11.60 (s, 1H), 8.52 (d, $J = 1.6$ Hz, 1H), 8.02 – 7.98 (m, 3H), 7.75 – 7.71 (m, 2H), 7.19 (dd, $J = 8.1, 1.6$ Hz, 1H), 4.51 (s, 2H), 3.89 (s, 3H), 3.35 (s, 3H). LC-MS (ESI) m/z 426.1 [M+H]⁺.

4.2.16. methyl 4-carbamoyl-2-(4-iodobenzamido)benzoate (29p)—(hexanes to dichloromethane). White powder, 0.25 g, 0.58 mmol, 13% yield. ¹H NMR (400 MHz, DMSO-*d*₆) δ 11.39 (bs, 1H), 8.80 (d, $J = 1.7$ Hz, 1H), 8.16 (bs, 1H), 8.05 – 7.98 (m, 3H), 7.77 – 7.72 (m, 2H), 7.69 (dd, $J = 8.2, 1.7$ Hz, 1H), 7.60 (bs, 1H), 3.88 (s, 3H). LC-MS (ESI) m/z 425.1 [M+H]⁺.

4.2.17. methyl 2-((4-iodophenyl)amino)-3-(methoxymethyl)benzoate (29q)—(hexanes to hexanes/ethyl acetate 1:1). White powder, 0.48 g, 1.18 mmol, 62% yield. ¹H NMR (400 MHz, DMSO-*d*₆) δ 11.39 (bs, 1H), 8.80 (d, $J = 1.7$ Hz, 1H), 8.16 (bs, 1H), 8.05 – 7.98 (m, 3H), 7.77 – 7.72 (m, 2H), 7.69 (dd, $J = 8.2, 1.7$ Hz, 1H), 7.60 (bs, 1H), 3.88 (s, 3H). LC-MS (ESI) m/z 425.1 [M+H]⁺.

4.2.18. methyl 2-(4-iodobenzamido)-5-methoxybenzoate (29r)—(hexanes to ethyl acetate). White powder, 1.17 g, 2.85 mmol, 86% yield. ¹H NMR (400 MHz, CDCl₃) δ 11.80 (s, 1H), 8.82 (d, $J = 9.3$ Hz, 1H), 7.88 – 7.84 (m, 2H), 7.77 – 7.72 (m, 2H), 7.57 (d, $J = 3.1$ Hz, 1H), 7.18 (dd, $J = 9.3, 3.1$ Hz, 1H), 3.97 (s, 3H), 3.84 (s, 3H). LC-MS (ESI) m/z 412.1 [M+H]⁺.

4.2.19. methyl 2-(2-(4-iodobenzamido)-4-methoxyphenyl)acetate (29s)—(hexanes to hexanes/ethyl acetate 8:2). White powder, 0.26 g, 0.6 mmol, 30% yield. ¹H NMR (400 MHz, CDCl₃) δ 9.83 (s, 1H), 7.91 – 7.84 (m, 2H), 7.80 – 7.73 (m, 2H), 7.71 (d, $J = 2.6$ Hz, 1H), 7.12 (d, $J = 8.5$ Hz, 1H), 6.70 (dd, $J = 8.5, 2.7$ Hz, 1H), 3.83 (s, 3H), 3.75 (s, 3H), 3.61 (s, 2H). LC-MS (ESI) m/z 426.1 [M+H]⁺.

4.2.20. methyl 2-(4-cyano-2-(4-iodobenzamido)phenyl)acetate (29t)—(hexanes to ethyl acetate). White powder, 2.38 g, 5.66 mmol, 82% yield. ¹H NMR (400 MHz, CDCl₃)

δ 9.96 (s, 1H), 8.45 (d, J = 1.2 Hz, 1H), 7.90 – 7.87 (m, 2H), 7.77 – 7.74 (m, 2H), 7.42 (dd, J = 7.9, 1.5 Hz, 1H), 7.35 (d, J = 7.9 Hz, 1H), 3.79 (s, 3H), 3.74 (s, 2H). LC-MS (ESI) m/z 421.1 [M+H]⁺.

4.2.21. methyl 3-(4-iodobenzamido)-4-(2-methoxy-2-oxoethyl)benzoate (29u)

—(hexanes to ethyl acetate). White powder, 2.38 g, 5.66 mmol, 82% yield. ¹H NMR (500 MHz, DMSO-*d*₆) δ 10.17 (s, 1H), 7.99 (d, J = 1.9 Hz, 1H), 7.96 – 7.92 (m, 2H), 7.82 (dd, J = 8.0, 1.8 Hz, 1H), 7.73 – 7.69 (m, 2H), 7.50 (d, J = 8.0 Hz, 1H), 3.86 (s, 3H), 3.85 (s, 2H), 3.51 (s, 3H). LC-MS (ESI) m/z 454.1 [M+H]⁺.

4.3. General procedure for the synthesis of intermediate 29c. Method b.

A mixture of methyl 2-(4-iodobenzamido)benzoate (**29c**). (0.823 mg, 2.16 mmol) and NaH (121 mg, 3 mmol, 60% in oil) in anhydrous DMF (20 mL) was stirred at 0 °C for 15 minutes. Then, MeI (366 mg, 2.6 mmol) was added and the reaction was stirred at room temperature until completion. Then reaction was quenched by addition of MeOH and concentrated under reduced pressure. Desired intermediate was purified by flash column chromatography (0–50 % EtOAc in hexanes) to provide 551 mg (1.39 mmol, 65% yield) of methyl 2-(4-iodo-*N*-methylbenzamido)benzoate (**29**) as yellow oil.

4.3.1. methyl 2-(4-iodo-*N*-methylbenzamido)benzoate (29)—¹H NMR (400 MHz, Methanol-*d*₄) δ 7.79 (d, J = 7.9 Hz, 1H), 7.58 (t, J = 7.6 Hz, 1H), 7.55 – 7.49 (m, 2H), 7.45 (d, J = 8.0 Hz, 1H), 7.36 (t, J = 7.6 Hz, 1H), 7.01 – 6.93 (m, 2H), 3.85 (s, 3H), 3.40 (s, 3H). LC-MS (ESI) m/z 396.0 [M+H]⁺.

4.4. General procedure for the synthesis of intermediates 30a-u. Method c.

The syntheses of compounds **30a-u** have been carried out according to general method *c*. To a solution of **29a-u** (1 eq) in anhydrous DMF (11 mL/mmol) allyl alcohol (1.10 eq), NaHCO₃ (2.5 eq), Pd(OAc)₂ (0.06 eq) and tetrabutylammonium chloride (0.5 eq) were added and the mixture was stirred at 70 °C overnight. The reaction was cooled to room temperature and then ethyl acetate (50 mL/mmol) was added and the solution washed with saturated aqueous NH₄Cl (3 × 100 mL/mmol). The organic phase was dried over anhydrous Na₂SO₄, filtered and concentrated under reduced pressure. The desired product was obtained as a brown solid and was used in subsequent reaction without purification.[12]

4.4.1. methyl 1-(4-(3-oxopropyl)benzoyl)piperidine-2-carboxylate (30a)—(390 mg, 1.29 mmol, 91% yield). ¹H NMR (400 MHz, CDCl₃) δ 9.83 (t, J = 1.3 Hz, 1H), 7.40 – 7.35 (m, 2H), 7.26 – 7.21 (m, 2H), 5.54 – 5.45 (m, 1H), 3.78 (s, 3H), 3.70 – 3.62 (m, 1H), 3.27 – 3.18 (m, 1H), 2.98 (t, J = 7.2 Hz, 2H), 2.80 (t, J = 7.5 Hz, 3H), 2.38 – 2.30 (m, 1H), 1.82 – 1.73 (m, 3H), 1.48 – 1.37 (m, 2H). LC-MS (ESI) m/z 304.1 [M+H]⁺.

4.4.2. methyl 2-(4-(3-oxopropyl)benzamido)cyclohexane-1-carboxylate (30b)—(406 mg, 1.28 mmol, 91% yield). ¹H NMR (400 MHz, CDCl₃) δ 9.82 (t, J = 1.3 Hz, 1H), 7.73 – 7.68 (m, 2H), 7.27 – 7.23 (m, 3H), 4.32 (qd, J = 9.4, 4.5, 3.8 Hz, 2H), 3.71 (s, 3H), 2.99 (t, J = 7.4

Hz, 2H), 2.95 – 2.88 (m, 2H), 2.84 – 2.75 (m, 2H), 2.23 – 2.18 (m, 2H), 1.80 – 1.41 (m, 4H). LC-MS (ESI) m/z 318.1 [M+H]⁺.

4.4.3. methyl 2-(4-(3-oxopropyl)benzamido)benzoate (30c)—(338 mg, 1.09 mmol, 58% yield). ¹H NMR (400 MHz, CDCl₃) δ 12.02 (s, 1H), 9.85 (t, J = 1.2 Hz, 1H), 8.93 (d, J = 8.5 Hz, 1H), 8.12 – 8.07 (m, 1H), 8.01 – 7.96 (m, 2H), 7.61 (t, J = 8.3 Hz, 1H), 7.38 – 7.32 (m, 2H), 7.12 (t, J = 7.5 Hz, 1H), 3.97 (d, J = 1.4 Hz, 3H), 3.04 (t, J = 7.5 Hz, 2H), 2.84 (t, J = 7.5 Hz, 2H). LC-MS (ESI) m/z 312.1 [M+H]⁺.

4.4.4. methyl 2-(N-methyl-4-(3-oxopropyl)benzamido)benzoate (30)—(414 mg, 1.16 mmol, 53% yield). ¹H NMR (400 MHz, CDCl₃) δ 9.73 (s, 1H), 7.76 (d, J = 8.0 Hz, 1H), 7.45 (t, J = 7.8 Hz, 1H), 7.32 – 7.20 (m, 2H), 7.17 – 7.12 (m, 2H), 6.96 – 6.90 (m, 2H), 3.86 (s, 3H), 3.42 (s, 3H), 2.82 (t, J = 7.5 Hz, 2H), 2.66 (t, J = 7.5 Hz, 2H). LC-MS (ESI) m/z 326.1 [M+H]⁺.

4.4.5. methyl 3-(4-(3-oxopropyl)benzamido)benzoate (30d)—(404 mg, 1.29 mmol, 51% yield). ¹H NMR (400 MHz, CDCl₃) δ 9.84 (s, 1H), 8.13 (t, J = 2.0 Hz, 1H), 8.05 (dd, J = 8.0, 2.3 Hz, 1H), 7.92 (s, 1H), 7.83 – 7.80 (m, 3H), 7.46 (t, J = 7.9 Hz, 1H), 7.33 (d, J = 7.9 Hz, 2H), 3.92 (s, 3H), 3.03 (t, J = 7.4 Hz, 2H), 2.84 (t, J = 7.4 Hz, 2H). LC-MS (ESI) m/z 312.1 [M+H]⁺.

4.4.6. methyl 4-(4-(3-oxopropyl)benzamido)benzoate (30e)—(45 mg, 0.15 mmol, 39% yield). ¹H NMR (500 MHz, CDCl₃) δ 9.84 (t, J = 1.3 Hz, 1H), 8.15 (s, 1H), 7.97 – 7.94 (m, 2H), 7.72 – 7.68 (m, 2H), 7.47 – 7.44 (m, 2H), 7.35 – 7.31 (m, 2H), 3.93 (s, 3H), 3.04 (t, J = 7.5 Hz, 2H), 2.84 (t, J = 7.5 Hz, 2H). LC-MS (ESI) m/z 312.1 [M+H]⁺.

4.4.7. methyl 2-(2-(4-(3-oxopropyl)benzamido)phenyl)acetate (30f)—(0.78 g, 2.4 mmol, 83% yield). ¹H NMR (400 MHz, CDCl₃) δ 9.84 (t, J = 1.2 Hz, 1H), 9.68 (bs, 1H), 8.02 (d, J = 7.9 Hz, 1H), 7.99 – 7.95 (m, 2H), 7.39 – 7.32 (m, 3H), 7.25 – 7.22 (m, 1H), 7.14 (t, J = 7.7 Hz, 1H), 3.76 (s, 3H), 3.69 (s, 2H), 3.04 (t, J = 7.4 Hz, 2H), 2.87 – 2.81 (m, 2H). LC-MS (ESI) m/z 326.1 [M+H]⁺.

4.4.8. methyl 3-(2-(4-(3-oxopropyl)benzamido)phenyl)propanoate (30g)—(3.93 g, 11.59 mmol, 72% yield). ¹H NMR (400 MHz, CDCl₃) δ 9.84 (t, J = 1.3 Hz, 1H), 9.57 (s, 1H), 8.05 – 8.01 (m, 2H), 7.83 (d, J = 8.1 Hz, 1H), 7.37 – 7.32 (m, 2H), 7.30 – 7.26 (m, 1H), 7.21 – 7.13 (m, 2H), 3.67 (s, 3H), 3.04 (t, J = 7.5 Hz, 2H), 2.94 – 2.89 (m, 2H), 2.87 – 2.81 (m, 2H), 2.80 – 2.75 (m, 2H). LC-MS (ESI) m/z 326.1 [M+H]⁺.

4.4.9. N-(2-cyanophenyl)-4-(3-oxopropyl)benzamide (30h)—(1.09 g, 3.93 mmol, 83% yield). ¹H NMR (400 MHz, CDCl₃) δ 9.84 (t, J = 1.1 Hz, 1H), 8.59 (d, J = 8.5 Hz, 1H), 8.38 (s, 1H), 7.89 – 7.84 (m, 2H), 7.68 – 7.61 (m, 2H), 7.39 – 7.33 (m, 2H), 7.25 – 7.18 (m, 1H), 3.04 (t, J = 7.5 Hz, 2H), 2.84 (t, J = 7.5 Hz, 2H). LC-MS (ESI) m/z 279.1 [M+H]⁺.

4.4.10. methyl 2-((4-(3-oxopropyl)benzamido)methyl)benzoate (30i)—(0.44 g, 1.34 mmol, 99 % yield). ¹H NMR (400 MHz, CDCl₃) δ 9.80 (t, J = 1.3 Hz, 1H), 8.02 – 7.95 (m, 1H), 7.85 – 7.80 (m, 1H), 7.72 – 7.68 (m, 2H), 7.62 – 7.58 (m, 1H), 7.54 – 7.49 (m, 1H),

7.39 – 7.33 (m, 1H), 7.25 – 7.49 (m, 2H), 4.79 (d, $J = 6.4$ Hz, 2H), 3.95 (s, 3H), 3.01 – 2.95 (m, 2H), 2.78 (t, $J = 7.5$ Hz, 2H). LC-MS (ESI) m/z 326.1[M+H]⁺.

4.4.11. methyl 4-chloro-2-(4-(3-oxopropyl)benzamido)benzoate (30j)—(0.4 g, 1.16 mmol, 53% yield). ¹H NMR (400 MHz, CDCl₃) δ 12.06 (bs, 1H), 9.85 (t, $J = 1.2$ Hz, 1H), 9.05 (d, $J = 2.0$ Hz, 1H), 8.01 (d, $J = 8.6$ Hz, 1H), 7.99 – 7.94 (m, 2H), 7.39 – 7.34 (m, 2H), 7.10 (dd, $J = 8.6, 2.1$ Hz, 1H), 3.97 (s, 3H), 3.04 (t, $J = 7.5$ Hz, 2H), 2.87 – 2.81 (m, 2H). LC-MS (ESI) m/z 346.1 [M+H]⁺.

4.4.12. dimethyl 2-(4-(3-oxopropyl)benzamido)terephthalate (30k)—(326 mg, 0.88 mmol, 92% yield). ¹H NMR (400 MHz, CDCl₃) δ 11.98 (s, 1H), 9.85 (t, $J = 1.2$ Hz, 1H), 9.55 (d, $J = 1.7$ Hz, 1H), 8.15 (d, $J = 8.3$ Hz, 2H), 8.02 – 7.97 (m, 2H), 7.77 (dd, $J = 8.3, 1.8$ Hz, 2H), 7.40 – 7.34 (m, 2H), 4.00 (s, 3H), 3.96 (s, 3H), 3.04 (t, $J = 7.5$ Hz, 2H), 2.88 – 2.81 (m, 2H). LC-MS (ESI) m/z 370.1 [M+H]⁺.

4.4.13. methyl 4-methoxy-2-(4-(3-oxopropyl)benzamido)benzoate (30l)—(330 mg, 0.97 mmol, 79% yield). ¹H NMR (400 MHz, DMSO-*d*₆) δ 11.96 (s, 1H), 9.73 (t, $J = 1.2$ Hz, 1H), 8.38 (d, $J = 2.7$ Hz, 1H), 8.00 (d, $J = 9.0$ Hz, 1H), 7.89 – 7.86 (m, 2H), 7.50 – 7.44 (m, 2H), 6.80 (dd, $J = 9.0, 2.6$ Hz, 1H), 3.89 (s, 3H), 3.86 (s, 3H), 2.95 (t, $J = 7.0$ Hz, 2H), 2.88 – 2.82 (m, 2H). LC-MS (ESI) m/z 342.1 [M+H]⁺.

4.4.14. methyl 4-cyano-2-(4-(3-oxopropyl)benzamido)benzoate (30m)—(381 mg, 1.13 mmol, 92% yield). ¹H NMR (400 MHz, DMSO-*d*₆) δ 11.44 (s, 1H), 9.71 (t, $J = 1.2$ Hz, 1H), 8.79 (d, $J = 1.6$ Hz, 1H), 8.10 (d, $J = 8.1$ Hz, 1H), 7.88 – 7.84 (m, 2H), 7.68 (dd, $J = 8.2, 1.7$ Hz, 1H), 7.47 – 7.43 (m, 2H), 3.88 (s, 3H), 2.94 (t, $J = 7.0$ Hz, 2H), 2.83 (t, $J = 7.2$ Hz, 2H). LC-MS (ESI) m/z 337.1 [M+H]⁺.

4.4.15. methyl 4-(hydroxymethyl)-2-(4-(3-oxopropyl)benzamido)benzoate (30n)—(400 mg, 1.17 mmol, 96% yield). ¹H NMR (400 MHz, CDCl₃) δ 12.05 (s, 1H), 9.83 (t, $J = 1.2$ Hz, 1H), 9.06 (d, $J = 1.6$ Hz, 1H), 8.12 – 8.07 (m, 1H), 8.06 – 8.02 (m, 1H), 8.01 – 7.95 (m, 2H), 7.38 – 7.33 (m, 2H), 7.18 (dd, $J = 8.4, 2.0$ Hz, 1H), 5.41 (s, 2H), 3.97 (s, 3H), 3.07 – 2.98 (m, 2H), 2.86 – 2.79 (m, 2H). LC-MS (ESI) m/z 342.1 [M+H]⁺.

4.4.16. methyl 4-(methoxymethyl)-2-(4-(3-oxopropyl)benzamido)benzoate (30o)—(150 mg, 0.422 mmol, 69% yield). ¹H NMR (400 MHz, CDCl₃) δ 12.05 (s, 1H), 9.85 (t, $J = 1.0$ Hz, 1H), 8.89 (s, 1H), 8.14 – 8.06 (m, 1H), 8.01 – 7.96 (m, 2H), 7.38 – 7.33 (m, 2H), 7.18 – 7.13 (m, 1H), 4.54 (s, 2H), 3.96 (s, 3H), 3.44 (s, 3H), 3.04 (t, $J = 7.4$ Hz, 2H), 2.84 (t, $J = 7.5$ Hz, 2H). LC-MS (ESI) m/z 356.1 [M+H]⁺.

4.4.17. methyl 4-carbamoyl-2-(4-(3-oxopropyl)benzamido)benzoate (30p)—(206 mg, 0.56 mmol, 96% yield). ¹H NMR (400 MHz, CDCl₃) δ 12.05 (s, 1H), 9.83 (t, $J = 1.2$ Hz, 1H), 9.06 (d, $J = 1.6$ Hz, 1H), 8.12 – 8.07 (m, 1H), 8.06 – 8.02 (m, 1H), 8.01 – 7.95 (m, 2H), 7.38 – 7.33 (m, 2H), 7.18 (dd, $J = 8.4, 2.0$ Hz, 1H), 5.41 (s, 2H), 3.97 (s, 3H), 3.07 – 2.98 (m, 2H), 2.86 – 2.79 (m, 2H). LC-MS (ESI) m/z 342.1 [M+H]⁺.

4.4.18. methyl 3-(methoxymethyl)-2-(4-(3-oxopropyl)benzamido)benzoate (30q)—(313 mg, 0.88 mmol, 75% yield). ¹H NMR (400 MHz, CDCl₃) δ 10.32 (s, 1H), 9.85 (t, *J* = 1.2 Hz, 1H), 7.97 – 7.90 (m, 3H), 7.78 – 7.74 (m, 1H), 7.37 – 7.33 (m, 2H), 7.30 (t, *J* = 7.8 Hz, 1H), 4.48 (s, 2H), 3.87 (s, 3H), 3.37 (s, 3H), 3.04 (t, *J* = 7.5 Hz, 2H), 2.87 – 2.81 (m, 2H). LC-MS (ESI) *m/z* 356.1 [M+H]⁺.

4.4.19. methyl 5-methoxy-2-(4-(3-oxopropyl)benzamido)benzoate (30r)—(835 mg, 2.45 mmol, 86% yield). ¹H NMR (400 MHz, CDCl₃) δ 11.75 (s, 1H), 9.84 (d, *J* = 1.3 Hz, 1H), 8.85 (d, *J* = 9.2 Hz, 1H), 7.99 – 7.94 (m, 2H), 7.57 (d, *J* = 3.1 Hz, 1H), 7.36 – 7.32 (m, 2H), 7.18 (dd, *J* = 9.3, 3.1 Hz, 1H), 3.97 (s, 3H), 3.84 (s, 3H), 3.03 (t, *J* = 7.5 Hz, 2H), 2.86 – 2.80 (m, 2H). LC-MS (ESI) *m/z* 342.1 [M+H]⁺.

4.4.20. methyl 2-(4-methoxy-2-(4-(3-oxopropyl)benzamido)phenyl)acetate (30s)—(189 mg, 0.53 mmol, 88% yield). ¹H NMR (400 MHz, DMSO-*d*₆) δ 12.05 (s, 1H), 9.73 (t, *J* = 1.2 Hz, 1H), 8.18 (d, *J* = 2.7 Hz, 1H), 7.98 – 7.90 (m, 2H), 7.85 – 7.78 (m, 3H), 7.50 – 7.44 (m, 2H), 6.98 (dd, *J* = 8.7, 2.0 Hz, 1H), 3.89 (s, 3H), 3.86 (s, 3H), 2.98 (t, *J* = 7.0 Hz, 2H), 2.88 – 2.82 (m, 2H). LC-MS (ESI) *m/z* 356.1 [M+H]⁺.

4.4.21. methyl 2-(4-cyano-2-(4-(3-oxopropyl)benzamido)phenyl)acetate (30t)—(625 mg, 1.78 mmol, 45% yield). ¹H NMR (400 MHz, CDCl₃) δ 9.84 (t, *J* = 1.2 Hz, 1H), 8.45 (d, *J* = 1.7 Hz, 1H), 7.98 – 7.94 (m, 2H), 7.41 (dd, *J* = 7.9, 1.7 Hz, 1H), 7.38 – 7.33 (m, 3H), 3.79 (s, 3H), 3.74 (s, 2H), 3.05 (t, *J* = 7.4 Hz, 2H), 2.88 – 2.82 (m, 2H). LC-MS (ESI) *m/z* 351.1 [M+H]⁺.

4.4.22. methyl 4-(2-methoxy-2-oxoethyl)-3-(4-(3-oxopropyl)benzamido)benzoate (30u)—(2.05 g, 5.35 mmol, 94% yield). ¹H NMR (400 MHz, CDCl₃) δ 9.74 (t, *J* = 1.3 Hz, 1H), 9.09 (s, 1H), 8.21 (d, *J* = 1.9 Hz, 1H), 7.91 – 7.85 (m, 2H), 7.77 (dd, *J* = 8.0, 1.9 Hz, 1H), 7.48 – 7.41 (m, 3H), 3.81 (s, 3H), 3.75 (s, 2H), 3.55 (s, 3H), 3.02 – 2.94 (m, 2H), 2.70 – 2.61 (m, 2H). LC-MS (ESI) *m/z* 384.1 [M+H]⁺.

4.5. General procedure for the synthesis of intermediates 31a-u. Method d.

Intermediates **31a-u** have been obtained through general method *d*. To a solution of 3-oxopropyl derivatives 30a-u (1 eq) in anhydrous THF (5 mL/mmol) 5,5-dibromo-2,2-dimethyl-1,3-dioxane-4,6-dione (0.5 eq) and HCl (35%) (8.15 μL/mmol) were added. The mixture reaction was stirred at room temperature for 18 h. 5% NaHCO₃ solution (20 mL/mmol) was added and the organic layer washed with H₂O (3 × 20 mL/mmol) and dried over anhydrous Na₂SO₄. After filtration solvent was evaporated under reduced pressure and the desired intermediates, obtained as a orange solid, were used in subsequent reaction without purification.[12]

4.5.1. methyl 1-(4-(2-bromo-3-oxopropyl)benzoyl)piperidine-2-carboxylate (31a)—(275 mg, 0.72 mmol, 49% yield). ¹H NMR (400 MHz, CDCl₃) δ 9.53 (d, *J* = 2.1 Hz, 1H), 7.40 – 7.35 (m, 2H), 7.26 – 7.21 (m, 2H), 5.54 – 5.45 (m, 1H), 4.49 (ddd, *J* = 14.5, 6.4, 2.2 Hz, 1H), 3.78 (s, 3H), 3.70 – 3.62 (m, 1H), 3.58 (dd, *J* = 14.7, 6.3 Hz, 1H), 3.27 –

3.18 (m, 2H), 2.38 – 2.30 (m, 1H), 1.82 – 1.73 (m, 3H), 1.48 – 1.37 (m, 2H). LC-MS (ESI) m/z 383.1 [M+H]⁺.

4.5.2. methyl 2-(4-(2-bromo-3-oxopropyl)benzamido)cyclohexane-1-carboxylate (31b)—(362 mg, 0.91 mmol, 60% yield). ¹H NMR (400 MHz, CDCl₃) δ 9.50 (d, J = 2.2 Hz, 1H), 7.76 – 7.72 (m, 2H), 7.31 – 7.27 (m, 3H), 4.48 – 4.42 (m, 1H), 4.38 – 4.27 (m, 2H), 3.73 (s, 3H), 3.53 (dd, J = 14.5, 6.3 Hz, 1H), 3.23 – 3.15 (m, 1H), 2.95 – 2.89 (m, 2H), 2.23 – 2.14 (m, 2H), 1.85 – 1.63 (m, 3H), 1.52 – 1.42 (m, 1H). LC-MS (ESI) m/z 397.1 [M+H]⁺.

4.5.3. methyl 2-(4-(2-bromo-3-oxopropyl)benzamido)benzoate (31c)—(93 mg, 0.24 mmol, 31% yield). ¹H NMR (400 MHz, CDCl₃) δ 12.05 (s, 1H), 9.53 (d, J = 2.1 Hz, 1H), 8.93 (d, J = 7.5 Hz, 1H), 8.12 – 8.07 (m, 2H), 8.03 (d, J = 8.4 Hz, 1H), 7.62 (t, J = 8.2 Hz, 1H), 7.43 – 7.36 (m, 2H), 7.14 (t, J = 7.8 Hz, 1H), 4.53 – 4.46 (m, 1H), 3.98 (s, 3H), 3.58 (dd, J = 14.8, 6.3 Hz, 1H), 3.24 (dd, J = 14.7, 8.0 Hz, 1H). LC-MS (ESI) m/z 391.1 [M+H]⁺.

4.5.4. methyl 2-(4-(2-bromo-3-oxopropyl)-N-methylbenzamido)benzoate (31)—(313 mg, 0.78 mmol, 61% yield). ¹H NMR (400 MHz, CDCl₃) δ 9.40 (s, 1H), 9.23 (s, 1H), 7.76 (d, J = 8.1 Hz, 1H), 7.45 (t, J = 7.7 Hz, 1H), 7.25 – 7.16 (m, 2H), 7.15 – 7.10 (m, 2H), 6.96 (d, J = 7.6 Hz, 1H), 4.35 – 4.28 (m, 1H), 3.86 (s, 3H), 3.43 (t, J = 4.9 Hz, 3H), 3.33 (dd, J = 14.8, 6.3 Hz, 1H), 3.03 (dd, J = 14.7, 8.0 Hz, 1H). LC-MS (ESI) m/z 406.0 [M+H]⁺.

4.5.5. methyl 3-(4-(2-bromo-3-oxopropyl)benzamido)benzoate (31d)—(450 mg, 1.15 mmol, 88% yield). ¹H NMR (400 MHz, CDCl₃) δ 9.53 (d, J = 2.1 Hz, 1H), 8.15 – 8.13 (m, 1H), 8.06 – 8.03 (m, 1H), 7.90 (s, 1H), 7.87 – 7.82 (m, 3H), 7.49 – 7.45 (m, 1H), 7.40 – 7.35 (m, 2H), 4.48 (ddd, J = 8.3, 6.3, 2.1 Hz, 1H), 3.93 (s, 3H), 3.57 (dd, J = 14.7, 6.3 Hz, 1H), 3.24 (dd, J = 14.7, 8.1 Hz, 1H). LC-MS (ESI) m/z 391.1 [M+H]⁺.

4.5.6. methyl 4-(4-(2-bromo-3-oxopropyl)benzamido)benzoate (31e)—(53 mg, 0.14 mmol, 91% yield). ¹H NMR (400 MHz, CDCl₃) δ 9.53 (d, J = 2.1 Hz, 1H), 8.15 (s, 1H), 7.97 – 7.94 (m, 2H), 7.72 – 7.68 (m, 2H), 7.47 – 7.44 (m, 2H), 7.35 – 7.31 (m, 2H), 4.48 (ddd, J = 8.3, 6.3, 2.1 Hz, 1H), 3.93 (s, 3H), 3.57 (dd, J = 14.7, 6.3 Hz, 1H), 3.24 (dd, J = 14.7, 8.1 Hz, 1H). LC-MS (ESI) m/z 391.1 [M+H]⁺.

4.5.7. methyl 2-(2-(4-(2-bromo-3-oxopropyl)benzamido)phenyl)acetate (31f)—(386.7 mg, 0.96 mmol, 40% yield). ¹H NMR (400 MHz, CDCl₃) δ 9.73 (bs, 1H), 9.53 (d, J = 2.2 Hz, 1H), 8.04 – 7.98 (m, 3H), 7.41 – 7.33 (m, 3H), 7.26 – 7.22 (m, 1H), 7.16 (t, J = 7.7 Hz, 1H), 4.49 (ddd, J = 8.3, 6.4, 2.2 Hz, 1H), 3.76 (s, 3H), 3.69 (s, 2H), 3.57 (dd, J = 14.6, 6.4 Hz, 1H), 3.24 (dd, J = 14.7, 8.1 Hz, 1H). LC-MS (ESI) m/z 406.0 [M+H]⁺.

4.5.8. methyl 3-(2-(4-(2-bromo-3-oxopropyl)benzamido)phenyl)propanoate (31g)—(2.23 g, 5.33 mmol, 46% yield). ¹H NMR (400 MHz, CDCl₃) δ 9.63 (s, 1H), 9.53 (d, J = 2.2 Hz, 1H), 8.11 – 8.07 (m, 2H), 7.84 (d, J = 8.0 Hz, 1H), 7.40 – 7.37 (m, 2H), 7.30 – 7.27 (m, 1H), 7.21 – 7.17 (m, 2H), 4.50 (ddd, J = 8.5, 6.6, 2.3 Hz, 1H), 3.97 (s, 3H), 3.58

(dd, $J = 14.6, 6.5$ Hz, 1H), 3.25 (dd, $J = 14.7, 8.0$ Hz, 1H), 2.95 – 2.92 (m, 2H), 2.81 – 2.79 (m, 2H). LC-MS (ESI) m/z 418.1 [M+H]⁺.

4.5.9. 4-(2-bromo-3-oxopropyl)-N-(2-cyanophenyl)benzamide (31h)—(830 mg, 2.32 mmol, 59% yield). ¹H NMR (400 MHz, CDCl₃) δ 9.53 (d, $J = 2.1$ Hz, 1H), 8.57 (d, $J = 8.5$ Hz, 1H), 8.41 (s, 1H), 7.90 – 7.85 (m, 2H), 7.69 – 7.62 (m, 2H), 7.40 – 7.34 (m, 2H), 7.24 – 7.17 (m, 1H), 4.53 – 4.46 (m, 1H), 3.58 (dd, $J = 14.8, 6.3$ Hz, 1H), 3.24 (dd, $J = 14.7, 8.0$ Hz, 1H). LC-MS (ESI) m/z 358.1 [M+H]⁺.

4.5.10. methyl 2-((4-(2-bromo-3-oxopropyl)benzamido)methyl)benzoate (31i)—(183 mg, 0.56 mmol, 42% yield). ¹H NMR (500 MHz, CDCl₃) δ 9.71 (s, 1H), 9.48 (d, $J = 2.2$ Hz, 1H), 8.04 – 7.97 (m, 3H), 7.76 – 7.71 (m, 2H), 7.68 – 7.64 (m, 1H), 7.55 – 7.51 (m, 1H), 7.39 – 7.36 (m, 1H), 4.82 (s, 2H), 4.43 (ddd, $J = 8.4, 6.4, 2.3$ Hz, 1H), 3.97 (s, 3H), 3.55 – 3.48 (m, 1H), 3.17 (dd, $J = 14.7, 8.1$ Hz, 1H). LC-MS (ESI) m/z 406.1 [M+H]⁺.

4.5.11. methyl 2-(4-(2-bromo-3-oxopropyl)benzamido)-4-chlorobenzoate (31j)—(234.2 mg, 0.554 mmol, 48% yield). ¹H NMR (500 MHz, CDCl₃) δ 12.08 (s, 1H), 9.53 (d, $J = 2.1$ Hz, 1H), 9.04 (d, $J = 2.2$ Hz, 1H), 8.02 – 7.99 (m, 3H), 7.42 – 7.38 (m, 2H), 7.10 (dd, $J = 8.5, 2.1$ Hz, 1H), 4.49 (ddd, $J = 8.3, 6.4, 2.1$ Hz, 1H), 3.97 (s, 3H), 3.58 (dd, $J = 14.6, 6.5$ Hz, 1H), 3.24 (dd, $J = 14.7, 8.1$ Hz, 1H). LC-MS (ESI) m/z 424.1 [M+H]⁺.

4.5.12. dimethyl 2-(4-(2-bromo-3-oxopropyl)benzamido)terephthalate (31k)—(285 mg, 0.64 mmol, 73% yield). ¹H NMR (400 MHz, CDCl₃) δ 12.04 (s, 1H), 9.52 (d, $J = 2.1$ Hz, 1H), 8.18 – 8.14 (m, 1H), 8.07 – 8.03 (m, 1H), 7.81 – 7.76 (m, 2H), 7.59 – 7.55 (m, 2H), 7.40 (d, $J = 7.9$ Hz, 1H), 4.50 (ddd, $J = 8.3, 6.3, 2.1$ Hz, 1H), 4.01 (s, 3H), 3.97 (s, 3H), 3.58 (dd, $J = 14.7, 6.2$ Hz, 1H), 3.24 (dd, $J = 14.7, 8.2$ Hz, 1H). LC-MS (ESI) m/z 448.1 [M+H]⁺.

4.5.13. methyl 2-(4-(2-bromo-3-oxopropyl)benzamido)-4-methoxybenzoate (31l)—(324 mg, 0.88 mmol, 91% yield). ¹H NMR (400 MHz, DMSO-*d*₆) δ 11.96 (s, 1H), 9.54 (d, $J = 1.8$ Hz, 1H), 8.36 (d, $J = 2.8$ Hz, 1H), 8.00 (d, $J = 9.1$ Hz, 1H), 7.95 – 7.88 (m, 2H), 7.62 – 7.58 (m, 2H), 6.80 (dd, $J = 8.9, 2.7$ Hz, 1H), 5.06 (ddd, $J = 9.0, 5.7, 1.9$ Hz, 1H), 3.89 (s, 3H), 3.86 (s, 3H), 3.60 (dd, $J = 14.7, 5.7$ Hz, 1H), 3.21 (dd, $J = 14.8, 9.0$ Hz, 1H). LC-MS (ESI) m/z 422.1 [M+H]⁺.

4.5.14. methyl 2-(4-(2-bromo-3-oxopropyl)benzamido)-4-cyanobenzoate (31m)—(357 mg, 0.98 mmol, 87% yield). ¹H NMR (400 MHz, DMSO-*d*₆) δ 11.50 (s, 1H), 9.54 (d, $J = 1.9$ Hz, 1H), 8.81 (d, $J = 1.6$ Hz, 1H), 8.13 – 8.09 (m, 1H), 8.03 – 7.99 (m, 2H), 7.74 – 7.71 (m, 2H), 7.54 (d, $J = 8.1$ Hz, 1H), 5.07 (ddd, $J = 9.0, 5.6, 1.8$ Hz, 1H), 3.89 (s, 3H), 3.61 (dd, $J = 14.7, 5.6$ Hz, 1H), 3.23 (dd, $J = 14.6, 5.6$ Hz, 1H). LC-MS (ESI) m/z 416.1 [M+H]⁺.

4.5.15. methyl 2-(4-(2-bromo-3-oxopropyl)benzamido)-4-(hydroxymethyl)benzoate (31n)—(77 mg, 0.17 mmol, 15% yield). ¹H NMR (500 MHz, DMSO-*d*₆) δ 11.62 (s, 1H), 9.57 (m, 1H), 8.70 (s, 1H), 8.04 – 7.87 (m, 6H), 7.51 (d, $J = 8.0$

Hz, 1H), 5.45 (s, 2H), 5.05 (ddd, $J = 14.5, 6.4, 2.2$ Hz, 1H), 3.90 (s, 3H), 3.63 – 3.56 (m, 1H), 3.25 – 3.19 (m, 1H). LC-MS (ESI) m/z 434.1 $[M+H]^+$.

4.5.16. methyl 2-(4-(2-bromo-3-oxopropyl)benzamido)-4-(methoxymethyl)benzoate (31o)—(137 mg, 0.315 mmol, 77% yield). ^1H NMR (400 MHz, CDCl_3) δ 12.08 (s, 1H), 9.53 (d, $J = 2.1$ Hz, 1H), 8.89 (s, 1H), 8.10 – 8.00 (m, 3H), 7.57 – 7.54 (m, 1H), 7.39 (dd, $J = 8.5, 2.1$ Hz, 1H), 7.18 – 7.14 (m, 1H), 4.54 (s, 2H), 4.49 (ddd, $J = 14.5, 6.4, 2.2$ Hz, 1H), 3.97 (s, 3H), 3.58 (dd, $J = 14.7, 6.3$ Hz, 1H), 3.44 (s, 3H), 3.24 (dd, $J = 14.7, 8.1$ Hz, 1H). LC-MS (ESI) m/z 434.1 $[M+H]^+$.

4.5.17. methyl 2-(4-(2-bromo-3-oxopropyl)benzamido)-4-carbamoylbenzoate (31p)—(167 mg, 0.39 mmol, 67% yield). ^1H NMR (500 MHz, $\text{DMSO}-d_6$) δ 11.45 (s, 1H), 9.53 (d, $J = 2.1$ Hz, 1H), 8.13 – 8.07 (m, 1H), 8.05 – 8.02 (m, 1H), 7.94 – 7.88 (m, 2H), 7.51 – 7.44 (m, 2H), 7.33 – 7.27 (m, Hz, 1H), 5.45 (s, 2H), 4.59 (ddd, $J = 14.5, 6.4, 2.2$ Hz, 1H), 3.89 (s, 3H), 3.62 – 3.55 (m, 1H), 3.25 – 3.19 (m, 1H). LC-MS (ESI) m/z 434.1 $[M+H]^+$.

4.5.18. methyl 2-(4-(2-bromo-3-oxopropyl)benzamido)-3-(methoxymethyl)benzoate (31q)—(289 mg, 0.66 mmol, 75% yield). ^1H NMR (500 MHz, $\text{DMSO}-d_6$) δ 10.03 (s, 1H), 9.42 (d, $J = 1.5$ Hz, 1H), 7.93 – 7.91 (m, 2H), 7.75 (d, $J = 8.1$ Hz, 1H), 7.67 (d, $J = 7.6$ Hz, 1H), 7.46 – 7.39 (m, 3H), 4.62 – 4.56 (m, 1H), 4.42 (s, 2H), 3.96 (s, 3H), 3.70 (s, 3H), 3.57 (dd, $J = 14.7, 5.9$ Hz, 1H), 3.19 (dd, $J = 14.7, 8.9$ Hz, 1H). LC-MS (ESI) m/z 435.1 $[M+H]^+$.

4.5.19. methyl 2-(4-(2-bromo-3-oxopropyl)benzamido)-5-methoxybenzoate (31r)—(888 mg, 2.11 mmol, 86% yield). ^1H NMR (400 MHz, CDCl_3) δ 11.78 (s, 1H), 9.52 (d, $J = 2.2$ Hz, 1H), 8.85 (d, $J = 9.4$ Hz, 1H), 8.01 – 7.98 (m, 2H), 7.57 (d, $J = 3.1$ Hz, 1H), 7.40 – 7.36 (m, 2H), 7.18 (dd, $J = 9.2, 3.2$ Hz, 1H), 4.53 – 4.44 (m, 1H), 3.97 (s, 3H), 3.84 (s, 3H), 3.57 (dd, $J = 14.7, 6.4$ Hz, 1H), 3.23 (dd, $J = 14.7, 8.1$ Hz, 1H). LC-MS (ESI) m/z 421.1 $[M+H]^+$.

4.5.20. methyl 2-(2-(4-(2-bromo-3-oxopropyl)benzamido)-4-methoxyphenyl)acetate (31s)—(141 mg, 0.32 mmol, 63% yield). ^1H NMR (400 MHz, CDCl_3) δ 10.98 (s, 1H), 9.56 (d, $J = 2.1$ Hz, 1H), 8.16 (d, $J = 2.7$ Hz, 1H), 7.91 – 7.86 (m, 2H), 7.41 (dd, $J = 7.9, 2.7$ Hz, 1H), 7.40 – 7.35 (m, 2H), 7.09 – 7.05 (m, 1H), 4.49 (ddd, $J = 14.5, 6.4, 2.2$ Hz, 1H), 3.95 (s, 3H), 3.80 (s, 3H), 3.74 (s, 2H), 3.58 (dd, $J = 14.5, 6.3$ Hz, 1H), 3.27 – 3.19 (m, 1H). LC-MS (ESI) m/z 435.1 $[M+H]^+$.

4.5.21. methyl 2-(2-(4-(2-bromo-3-oxopropyl)benzamido)-4-cyanophenyl)acetate (31t)—(688 mg, 1.60 mmol, 90% yield). ^1H NMR (400 MHz, CDCl_3) δ 9.90 (s, 1H), 9.53 (d, $J = 2.1$ Hz, 1H), 8.45 – 8.42 (m, 1H), 8.03 – 7.98 (m, 2H), 7.42 – 7.33 (m, 4H), 4.50 (ddd, $J = 8.3, 6.4, 2.1$ Hz, 1H), 3.79 (s, 3H), 3.74 (s, 2H), 3.55 (dd, $J = 14.7, 6.4$ Hz, 1H), 3.25 (dd, $J = 14.7, 8.0$ Hz, 1H). LC-MS (ESI) m/z 429.0 $[M+H]^+$.

4.5.22. methyl 3-(4-(2-bromo-3-oxopropyl)benzamido)-4-(2-methoxy-2-oxoethyl)benzoate (31u)—(1.05 g, 2.27 mmol, 42% yield). ^1H NMR (400 MHz, CDCl_3) δ 9.89 (s, 1H), 9.72 (d, $J = 1.9$ Hz, 1H), 8.25 – 8.19 (m, 1H), 7.91 – 7.86 (m, 2H), 7.64 –

7.58 (m, 2H), 7.00 – 6.96 (m, 2H), 4.45 (ddd, $J = 14.5, 6.4, 2.2$ Hz, 1H), 3.80 (s, 3H), 3.74 (s, 2H), 3.65 (s, 3H), 3.55 (ddd, $J = 14.5, 6.3$ Hz, 1H), 3.23 (ddd, $J = 14.5, 7.9$, 1H). LC-MS (ESI) m/z 462.1 [M+H]⁺.

4.6. General procedure for the synthesis of final compound 7 and intermediates 32a-g, 32i-32u. Method e.

Intermediates **31a-u** (1 eq) were added to solution of 2,6-diaminopyrimidin-4-ol (1.1 eq) and sodium acetate (2 eq) in water (3.13 mL/eq) and methanol (3.13 mL/eq). The reaction mixture was stirred at 45 °C for 2 hours. After solvent evaporation, intermediates were purified by flash column chromatography eluted initially with dichloromethane followed by 20% methanol in dichloromethane.[12]

4.6.1 4-((2-amino-4-oxo-4,7-dihydro-3H-pyrrolo[2,3-d]pyrimidin-5-yl)methyl)-N-(2-cyanophenyl)benzamide (7)—(101 mg, 0.26 mmol, 11% yield). ¹H NMR (400 MHz, DMSO-*d*₆) δ 12.27 (s, 1H), 10.72 (s, 1H), 10.27 (s, 1H), 8.80 – 8.75 (m, 1H), 8.20 (dd, $J = 7.8, 1.7$ Hz, 1H), 8.05 – 8.01 (m, 2H), 7.52 – 7.46 (m, 2H), 7.30 – 7.25 (m, 1H), 7.14 (td, $J = 7.5, 1.3$ Hz, 1H), 6.35 (d, $J = 1.8$ Hz, 1H), 6.04 (s, 2H), 4.02 (s, 2H). ¹³C NMR (101 MHz, DMSO-*d*₆) δ 166.4, 162.2, 157.8, 152.2, 147.3, 139.5, 134.5, 132.1, 128.1, 127.5, 127.1, 127.0, 126.6, 126.3, 123.5, 122.6, 122.1, 118.5, 48.2. HRMS (ESI): calc. for [M+H]⁺ C₂₁H₁₇N₆O₂⁺ 385.1408, found 385.1414.

4.6.2 methyl 1-(4-((2-amino-4-oxo-4,7-dihydro-3H-pyrrolo[2,3-d]pyrimidin-5-yl)methyl)benzoyl)piperidine-2-carboxylate (32a)—(60 mg, 0.147 mmol, yield 20% yield). ¹H NMR (400 MHz, DMSO-*d*₆) δ 10.72 (d, $J = 2.1$ Hz, 1H), 10.11 (s, 1H), 7.39 – 7.32 (m, 2H), 7.28 – 7.21 (m, 2H), 6.35 (d, $J = 2.2$ Hz, 1H), 5.99 (s, 2H), 4.47 – 4.36 (m, 1H), 3.96 (s, 2H), 3.71 (s, 3H), 3.59 – 3.50 (m, 1H), 3.13 – 3.02 (m, 1H), 2.20 – 2.12 (m, 1H), 1.71 – 1.63 (m, 1H), 1.58 – 1.48 (m, 1H), 1.44 – 1.36 (m, 1H), 1.30 – 1.23 (m, 1H), 1.20 – 1.13 (m, 1H). LC-MS (ESI) m/z 410.1 [M+H]⁺.

4.6.3. Methyl 2-(4-((2-amino-4-oxo-4,7-dihydro-3H-pyrrolo[2,3-d]pyrimidin-5-yl)methyl)benzamido) cyclohexane-1-carboxylate (32b)—(82.6 mg, 0.195 mmol, 20% yield). ¹H NMR (400 MHz, DMSO-*d*₆) δ 10.72 (s, 1H), 10.12 (s, 1H), 7.89 (d, $J = 8.3$ Hz, 1H), 7.65 – 7.59 (m, 2H), 7.37 – 7.31 (m, 2H), 6.32 (d, $J = 2.1$ Hz, 1H), 6.00 (s, 2H), 4.34 – 4.27 (m, 1H), 4.14 – 4.05 (m, 1H), 3.96 (s, 2H), 3.53 (s, 3H), 3.19 – 3.15 (m, 1H), 2.85 – 2.80 (m, 1H), 1.99 – 1.91 (m, 1H), 1.83 – 1.74 (m, 1H), 1.73 – 1.50 (m, 2H), 1.43 – 1.29 (m, 2H). LC-MS (ESI) m/z 424.1 [M+H]⁺.

4.6.4. methyl 2-(4-((2-amino-4-oxo-4,7-dihydro-3H-pyrrolo[2,3-d]pyrimidin-5-yl)methyl)benzamido)benzoate (32c)—(27 mg, 0.06 mmol, 25% yield). ¹H NMR (400 MHz, DMSO-*d*₆) δ 11.68 (s, 1H), 10.76 (d, $J = 1.9$ Hz, 1H), 10.14 (s, 1H), 8.72 (d, $J = 2.1$ Hz, 1H), 8.02 (d, $J = 8.6$ Hz, 1H), 7.85 – 7.80 (m, 2H), 7.53 – 7.49 (m, 2H), 7.30 (dd, $J = 8.6, 2.1$ Hz, 1H), 6.39 (d, $J = 1.7$ Hz, 1H), 6.02 (s, 2H), 4.03 (s, 2H), 3.90 (s, 3H). LC-MS (ESI) m/z 418.1 [M+H]⁺.

4.6.5. methyl 2-(4-((2-amino-4-oxo-4,7-dihydro-3H-pyrrolo[2,3-d]pyrimidin-5-yl)methyl)methyl)-N-methyl benzamido)benzoate (32)—(50 mg, 0.116 mmol, 15% yield). ¹H NMR (400 MHz, DMSO-*d*₆) δ 11.68 (s, 1H), 10.76 (d, *J* = 1.9 Hz, 1H), 10.14 (s, 1H), 8.72 (d, *J* = 2.1 Hz, 1H), 8.02 (d, *J* = 8.6 Hz, 1H), 7.85 – 7.80 (m, 2H), 7.53 – 7.49 (m, 2H), 7.30 (dd, *J* = 8.6, 2.1 Hz, 1H), 6.39 (d, *J* = 1.7 Hz, 1H), 6.02 (s, 2H), 4.03 (s, 2H), 3.90 (s, 3H). LC-MS (ESI) *m/z* 433.0 [M+H]⁺.

4.6.6. methyl 3-(4-((2-amino-4-oxo-4,7-dihydro-3H-pyrrolo[2,3-d]pyrimidin-5-yl)methyl)benzamido)benzoate (32d)—(57 mg, 0.13 mmol, 13 % yield). ¹H NMR (400 MHz, DMSO-*d*₆) δ 10.74 (d, *J* = 1.8 Hz, 1H), 10.33 (s, 1H), 10.14 (s, 1H), 8.45 (t, *J* = 2.0 Hz, 1H), 8.07 – 8.03 (m, 1H), 7.87 – 7.84 (m, 2H), 7.70 – 7.66 (m, 1H), 7.49 (t, *J* = 7.9 Hz, 1H), 7.46 – 7.43 (m, 2H), 6.36 (d, *J* = 2.2 Hz, 1H), 6.01 (s, 2H), 4.01 (s, 2H), 3.87 (s, 3H). LC-MS (ESI) *m/z* 418.1 [M+H]⁺.

4.6.7. methyl 4-(4-((2-amino-4-oxo-4,7-dihydro-3H-pyrrolo[2,3-d]pyrimidin-5-yl)methyl)benzamido)benzoate (32e)—(12 mg, 0.027 mmol, 20 % yield). ¹H NMR (600 MHz, DMSO-*d*₆) δ 10.74 (d, *J* = 1.8 Hz, 1H), 10.44 (s, 1H), 10.14 (s, 1H), 7.95 – 7.92 (m, 4H), 7.85 – 7.82 (m, 2H), 7.46 – 7.43 (m, 2H), 6.37 (d, *J* = 2.3 Hz, 1H), 6.01 (s, 2H), 4.01 (s, 2H), 3.83 (s, 3H). LC-MS (ESI) *m/z* 418.1 [M+H]⁺.

4.6.8. methyl 2-(2-(4-((2-amino-4-oxo-4,7-dihydro-3H-pyrrolo[2,3-d]pyrimidin-5-yl)methyl)benzamido)phenyl)acetate (32f)—(194 mg, 0.45 mmol, 47% yield). ¹H NMR (400 MHz, DMSO-*d*₆) δ 10.71 (d, *J* = 1.9 Hz, 1H), 9.87 (s, 1H), 7.81 – 7.77 (m, 2H), 7.44 – 7.40 (m, 2H), 7.39 – 7.36 (m, 1H), 7.34 – 7.29 (m, 2H), 7.21 (t, *J* = 7.4 Hz, 1H), 6.54 (s, 1H), 6.40 (s, 2H), 6.33 (d, *J* = 2.0 Hz, 1H), 4.00 (s, 2H), 3.72 (s, 3H), 3.50 (s, 2H). LC-MS (ESI) *m/z* 432.2 [M+H]⁺.

4.6.9. methyl 3-(2-(4-((2-amino-4-oxo-4,7-dihydro-3H-pyrrolo[2,3-d]pyrimidin-5-yl)methyl)benzamido) phenyl)propanoate (32g)—(300 mg, 0.67 mmol, 13% yield). ¹H NMR (400 MHz, DMSO-*d*₆) δ 10.76 (d, *J* = 1.6 Hz, 1H), 10.14 (s, 1H), 9.84 (s, 1H), 7.90 – 7.80 (m, 2H), 7.48 – 7.38 (m, 2H), 7.32 – 7.17 (m, 4H), 6.37 (d, *J* = 1.8 Hz, 1H), 6.02 (s, 2H), 4.01 (s, 2H), 3.54 (s, 3H), 2.85 (t, *J* = 7.7 Hz, 2H), 2.59 (t, *J* = 7.7 Hz, 2H). LC-MS (ESI) *m/z* 446.1 [M+H]⁺.

4.6.10. methyl 2-(4-((2-amino-4-oxo-4,7-dihydro-3H-pyrrolo[2,3-d]pyrimidin-5-yl)methyl)benzamido) methyl)benzoate (32i)—(91 mg, 0.21 mmol, 47% yield). ¹H NMR (400 MHz, DMSO-*d*₆) δ 10.74 (d, *J* = 2.1 Hz, 1H), 10.16 (s, 1H), 8.86 (t, *J* = 6.0 Hz, 1H), 7.86 (d, *J* = 7.7 Hz, 1H), 7.80 – 7.74 (m, 2H), 7.55 (t, *J* = 7.5 Hz, 1H), 7.42 – 7.33 (m, 4H), 6.35 (d, *J* = 2.1 Hz, 1H), 6.02 (s, 2H), 4.77 (d, *J* = 5.9 Hz, 2H), 3.98 (s, 2H), 3.85 (s, 3H). LC-MS (ESI) *m/z* 432.2 [M+H]⁺.

4.6.11. methyl 2-(4-((2-amino-4-oxo-4,7-dihydro-3H-pyrrolo[2,3-d]pyrimidin-5-yl)methyl)benzamido)-4-chlorobenzoate (32j)—(140 mg, 0.31 mmol, 44% yield). ¹H NMR (400 MHz, DMSO-*d*₆) δ 11.68 (s, 1H), 10.76 (d, *J* = 1.9 Hz, 1H), 10.14 (s, 1H), 8.72 (d, *J* = 2.1 Hz, 1H), 8.02 (d, *J* = 8.6 Hz, 1H), 7.85 – 7.80 (m, 2H), 7.53 – 7.49 (m, 2H), 7.30

(dd, $J = 8.6, 2.1$ Hz, 1H), 6.39 (d, $J = 1.7$ Hz, 1H), 6.02 (s, 2H), 4.03 (s, 2H), 3.90 (s, 3H). LC-MS (ESI) m/z 452.1 [M+H]⁺.

4.6.12. dimethyl 2-(4-((2-amino-4-oxo-4,7-dihydro-3H-pyrrolo[2,3-d]pyrimidin-5-yl)methyl)benzamido) terephthalate (32k)—(19 mg, 0.039 mmol, 6% yield). ¹H NMR (400 MHz, DMSO-*d*₆) δ 11.49 (s, 1H), 10.77 (d, $J = 1.9$ Hz, 1H), 10.15 (s, 1H), 9.11 (d, $J = 1.7$ Hz, 1H), 8.10 (d, $J = 8.2$ Hz, 1H), 7.88 – 7.83 (m, 2H), 7.77 (dd, $J = 8.3, 1.7$ Hz, 1H), 7.54 – 7.47 (m, 2H), 6.39 (d, $J = 2.2$ Hz, 1H), 6.03 (s, 2H), 4.02 (s, 2H), 3.91 (s, 6H). LC-MS (ESI) m/z 476.1 [M+H]⁺.

4.6.13. methyl 2-(4-((2-amino-4-oxo-4,7-dihydro-3H-pyrrolo[2,3-d]pyrimidin-5-yl)methyl)benzamido)-4-methoxybenzoate (32l)—(60 mg, 0.13 mmol, 15% yield). ¹H NMR (400 MHz, DMSO-*d*₆) δ 11.95 (s, 1H), 10.77 (d, $J = 2.3$ Hz, 1H), 10.14 (s, 1H), 8.38 (d, $J = 2.6$ Hz, 1H), 8.00 (d, $J = 9.0$ Hz, 1H), 7.86 – 7.81 (m, 2H), 7.54 – 7.48 (m, 2H), 6.79 (dd, $J = 9.0, 2.6$ Hz, 1H), 6.39 (d, $J = 2.2$ Hz, 1H), 6.02 (s, 2H), 4.02 (s, 2H), 3.88 (s, 3H), 3.86 (s, 3H). LC-MS (ESI) m/z 449.1 [M+H]⁺.

4.6.14. methyl 2-(4-((2-amino-4-oxo-4,7-dihydro-3H-pyrrolo[2,3-d]pyrimidin-5-yl)methyl)benzamido)-4-cyanobenzoate (32m)—(60 mg, 0.14 mmol, 14% yield). ¹H NMR (400 MHz, DMSO-*d*₆) δ 11.45 (s, 1H), 10.77 (d, $J = 2.3$ Hz, 1H), 10.15 (s, 1H), 8.82 (d, $J = 1.7$ Hz, 1H), 8.11 (d, $J = 8.2$ Hz, 1H), 7.86 – 7.82 (m, 2H), 7.70 (dd, $J = 8.1, 1.7$ Hz, 1H), 7.53 – 7.49 (m, 2H), 6.39 (d, $J = 2.2$ Hz, 1H), 6.03 (s, 2H), 4.03 (s, 2H), 3.90 (s, 3H). LC-MS (ESI) m/z 443.1 [M+H]⁺.

4.6.15. methyl 2-(4-((2-amino-4-oxo-4,7-dihydro-3H-pyrrolo[2,3-d]pyrimidin-5-yl)methyl)benzamido)-4-(hydroxymethyl)benzoate (32n)—(77 mg, 0.172 mmol, 19% yield). ¹H NMR (400 MHz, DMSO-*d*₆) δ 11.63 (s, 1H), 10.77 (d, $J = 2.1$ Hz, 1H), 10.15 (s, 1H), 8.70 (s, 1H), 8.08 – 7.80 (m, 5H), 7.51 – 7.44 (m, 2H), 6.37 (d, $J = 2.1$ Hz, 1H), 6.02 (s, 2H), 5.44 (s, 2H), 4.01 (s, 2H), 3.89 (s, 3H). LC-MS (ESI) m/z 448.1 [M+H]⁺.

4.6.16. methyl 2-(4-((2-amino-4-oxo-4,7-dihydro-3H-pyrrolo[2,3-d]pyrimidin-5-yl)methyl)benzamido)-4-(methoxymethyl)benzoate (32o)—(13 mg, 0.028 mmol, 8% yield). ¹H NMR (400 MHz, DMSO-*d*₆) δ 11.63 (s, 1H), 10.76 (d, $J = 2.1$ Hz, 1H), 10.13 (s, 1H), 8.61 (d, $J = 1.5$ Hz, 1H), 8.00 (d, $J = 8.2$ Hz, 1H), 7.86 – 7.82 (m, 2H), 7.52 – 7.48 (m, 2H), 7.16 (dd, $J = 8.2, 1.6$ Hz, 1H), 6.38 (d, $J = 2.1$ Hz, 1H), 6.02 (s, 2H), 4.51 (s, 2H), 4.02 (s, 2H), 3.90 (s, 3H), 3.35 (s, 3H). LC-MS (ESI) m/z 462.1 [M+H]⁺.

4.6.17. methyl 2-(4-((2-amino-4-oxo-4,7-dihydro-3H-pyrrolo[2,3-d]pyrimidin-5-yl)methyl)benzamido)-4-carbamoylbenzoate (32p)—(22.7 mg, 0.049 mmol, 13% yield). ¹H NMR (400 MHz, DMSO-*d*₆) δ 11.44 (s, 1H), 10.78 (d, $J = 2.1$ Hz, 1H), 10.15 (s, 1H), 8.90 (d, $J = 2.3$ Hz, 1H), 8.17 (s, 1H), 8.03 – 8.01 (m, 1H), 7.87 – 7.83 (m, 2H), 7.61 – 7.58 (m, 2H), 7.53 – 7.48 (m, 2H), 6.39 (d, $J = 2.1$ Hz, 1H), 6.04 (s, 2H), 4.02 (s, 2H), 3.89 (s, 3H). LC-MS (ESI) m/z 461.1 [M+H]⁺.

4.6.18. methyl 2-(4-((2-amino-4-oxo-4,7-dihydro-3H-pyrrolo[2,3-d]pyrimidin-5-yl)methyl)benzamido)-3-(methoxymethyl)benzoate (32q)—(81.9 mg, 0.177 mmol,

27% yield). (400 MHz, DMSO- d_6) δ 10.77 (d, J = 2.2 Hz, 1H), 10.15 (s, 1H), 9.93 (s, 1H), 7.86 – 7.81 (m, 2H), 7.75 (dd, J = 7.6, 1.6 Hz, 1H), 7.68 (dd, J = 7.7, 1.6 Hz, 1H), 7.46 – 7.39 (m, 3H), 6.39 (d, J = 2.2 Hz, 1H), 6.03 (s, 2H), 4.45 (s, 2H), 4.01 (s, 2H), 3.69 (s, 3H), 3.29 (s, 3H). LC-MS (ESI) m/z 462.1 [M+H]⁺.

4.6.19. methyl 2-(4-((2-amino-4-oxo-4,7-dihydro-3H-pyrrolo[2,3-d]pyrimidin-5-yl)methyl)benzamido)-5-methoxybenzoate (32r)—(192.8 mg, 0.43 mmol, 20% yield). ¹H NMR (400 MHz, DMSO- d_6) δ 11.19 (s, 1H), 10.75 (d, J = 2.1 Hz, 1H), 10.13 (s, 1H), 8.39 (d, J = 9.1 Hz, 1H), 7.83 – 7.79 (m, 2H), 7.49 – 7.45 (m, 3H), 7.29 (dd, J = 9.2, 3.1 Hz, 1H), 6.37 (d, J = 2.1 Hz, 1H), 6.01 (s, 2H), 4.02 (s, 2H), 3.87 (s, 2H), 3.80 (s, 3H). LC-MS (ESI) m/z 448.1 [M+H]⁺.

4.6.20. methyl 2-(2-(4-((2-amino-4-oxo-4,7-dihydro-3H-pyrrolo[2,3-d]pyrimidin-5-yl)methyl)benzamido)-4-methoxyphenyl)acetate (32s)—(49 mg, 0.011 mmol, 34 % yield). ¹H NMR (600 MHz, DMSO- d_6) δ 10.74 (d, J = 1.9 Hz, 2H), 10.15 (s, 1H), 9.80 (s, 1H), 7.81 – 7.76 (m, 2H), 7.45 – 7.39 (m, 2H), 7.22 (d, J = 8.5 Hz, 1H), 7.02 (d, J = 2.6 Hz, 1H), 6.80 (dd, J = 8.4, 2.7 Hz, 1H), 6.36 (d, J = 2.1 Hz, 1H), 6.02 (s, 2H), 4.00 (s, 2H), 3.74 (s, 3H), 3.65 (s, 2H), 3.50 (s, 3H). LC-MS (ESI) m/z 462.1 [M+H]⁺.

4.6.21. methyl 2-(2-(4-((2-amino-4-oxo-4,7-dihydro-3H-pyrrolo[2,3-d]pyrimidin-5-yl)methyl)benzamido)-4-cyanophenyl)acetate (32t)—(316 mg, 0.691 mmol, 45% yield). ¹H NMR (400 MHz, DMSO- d_6) δ 10.74 (d, J = 2.2 Hz, 1H), 10.13 (s, 1H), 10.04 (s, 1H), 7.88 (d, J = 1.7 Hz, 1H), 7.82 – 7.77 (m, 2H), 7.69 (dd, J = 7.9, 1.8 Hz, 1H), 7.56 (d, J = 8.0 Hz, 1H), 7.46 – 7.42 (m, 2H), 6.37 (d, J = 2.1 Hz, 1H), 6.01 (s, 2H), 4.01 (s, 2H), 3.87 (s, 2H), 3.51 (s, 3H). LC-MS (ESI) m/z 457.1 [M+H]⁺.

4.6.22. methyl 3-(4-((2-amino-4-oxo-4,7-dihydro-3H-pyrrolo[2,3-d]pyrimidin-5-yl)methyl)benzamido)-4-(2-methoxy-2-oxoethyl)benzoate (32u)—(295 mg, 0.603 mmol, 47% yield). ¹H NMR (400 MHz, CDCl₃) δ 10.72 (d, J = 2.1 Hz, 1H), 10.13 (s, 1H), 10.05 (s, 1H), 8.07 (s, 1H), 7.82 – 7.77 (m, 2H), 7.78 (dd, J = 8.0, 1.7 Hz, 1H), 7.48 – 7.41 (m, 3H), 6.35 (d, J = 2.2 Hz, 1H), 6.01 (s, 2H), 4.02 (s, 2H), 3.86 (s, 3H), 3.74 (s, 2H), 3.60 (s, 3H). LC-MS (ESI) m/z 490.1 [M+H]⁺.

4.7. General procedure for the synthesis of final compounds 2–6, 9 and 11–25. Method f.

The synthesis of compounds 2–6, 9 and 11–25 has been carried out following general method *f*. The corresponding derivate **32a-g** or **32h-u** (1 eq) was dissolved in a mixture MeOH (33 mL/mmol) and 2N NaOH (33 mL/mmol) was added. The resulting mixture was stirred at 60 °C for 1h. The resulting solution was cooled in an ice bath, and the pH was adjusted to 3–4 using 1 N HCl. The resulting suspension was chilled in a dry ice/acetone bath and thawed to 4 °C overnight in a refrigerator. The precipitate was filtered, washed with cold water, and dried under reduced pressure.[12]

4.7.1. 2-(4-((2-amino-4-oxo-4,7-dihydro-3H-pyrrolo[2,3-d]pyrimidin-5-yl)methyl)benzamido)benzoic acid (2)—(4.4 mg, 0.011 mmol, 17% yield). ¹H NMR

(400 MHz, DMSO- d_6) δ 12.18 (s, 1H), 10.75 (s, 1H), 10.13 (s, 1H), 8.71 (d, J = 8.3 Hz, 1H), 8.05 (d, J = 7.7 Hz, 1H), 7.86 – 7.77 (m, 2H), 7.64 (t, J = 7.8 Hz, 1H), 7.56 – 7.43 (m, 2H), 7.19 (t, J = 7.5 Hz, 1H), 6.37 (s, 1H), 6.01 (s, 2H), 4.02 (s, 2H). ^{13}C NMR (101 MHz, DMSO- d_6) δ 169.9, 164.7, 159.2, 152.2, 151.2, 147.0, 141.2, 134.2, 131.8, 131.3, 129.0, 126.9, 122.7, 119.7, 116.6, 116.5, 114.2, 98.6, 31.6. HRMS (ESI): calc. for $[\text{M}+\text{H}]^+$ $\text{C}_{21}\text{H}_{18}\text{N}_5\text{O}_4^+$ 404.1353, found 404.1359.

4.7.2. 3-(4-((2-amino-4-oxo-4,7-dihydro-3H-pyrrolo[2,3-d]pyrimidin-5-yl)methyl)benzamido)benzoic acid (3)—(13 mg, 0.032 mmol, 24% yield) as a green pale solid. ^1H NMR (600 MHz, DMSO- d_6) δ 12.94 (s, 1H), 11.05 (s, 1H), 10.71 (s, 1H), 10.32 (s, 1H), 8.40 (t, J = 1.9 Hz, 1H), 8.02 (ddd, J = 8.2, 2.2, 1.0 Hz, 1H), 7.88 – 7.84 (m, 2H), 7.66 (dt, J = 7.7, 1.2 Hz, 1H), 7.46 (t, J = 7.9 Hz, 1H), 7.44 – 7.42 (m, 2H), 6.69 (s, 2H), 6.47 – 6.44 (m, 1H), 4.02 (s, 2H). ^{13}C NMR (151 MHz, DMSO- d_6) δ 168.6, 166.0, 162.9, 152.6, 149.0, 134.9, 133.1, 131.4, 127.0, 126.9, 126.5, 126.1, 124.0, 119.1, 117.4, 116.8, 116.7, 111.3, 30.8. HRMS (ESI): calc. for $[\text{M}+\text{H}]^+$ $\text{C}_{21}\text{H}_{18}\text{N}_5\text{O}_4^+$ 404.1353, found 404.1341.

4.7.3. 4-(4-((2-amino-4-oxo-4,7-dihydro-3H-pyrrolo[2,3-d]pyrimidin-5-yl)methyl)benzamido)benzoic acid (4)—(1.6 mg, 0.004 mmol, 15% yield) as a yellow-green solid. ^1H NMR (600 MHz, DMSO- d_6) δ 12.73 (s, 1H), 10.78 (s, 1H), 10.41 (s, 1H), 10.23 (s, 1H), 7.97 – 7.86 (m, 4H), 7.83 (d, J = 8.1 Hz, 2H), 7.44 (d, J = 8.0 Hz, 2H), 6.38 (d, J = 2.2 Hz, 1H), 6.10 (s, 2H), 4.01 (s, 1H). ^{13}C NMR (151 MHz, DMSO- d_6) δ 170.3, 166.3, 162.9, 152.6, 149.0, 138.9, 133.1, 131.4, 129.5, 126.7, 126.0, 122.6, 121.5, 119.7, 116.5, 111.3, 31.8. HRMS (ESI): calc. for $[\text{M}+\text{H}]^+$ $\text{C}_{21}\text{H}_{18}\text{N}_5\text{O}_4^+$ 404.1353, found 404.1348.

4.7.4. 2-(2-(4-((2-amino-4-oxo-4,7-dihydro-3H-pyrrolo[2,3-d]pyrimidin-5-yl)methyl)benzamido)phenyl) acetic acid (5)—(71.1 mg, 0.17 mmol, 73% yield) as a pink solid. ^1H NMR (500 MHz, DMSO- d_6) δ 12.34 (s, 1H), 10.75 (d, J = 1.9 Hz, 1H), 10.16 (s, 1H), 9.86 (s, 1H), 7.85 – 7.78 (m, 2H), 7.48 – 7.44 (m, 1H), 7.43 – 7.40 (m, 2H), 7.33 – 7.27 (m, 2H), 7.22 – 7.16 (m, 1H), 6.37 (d, J = 1.9 Hz, 1H), 6.04 (s, 2H), 4.00 (s, 2H), 3.65 (s, 2H). ^{13}C NMR (101 MHz, DMSO- d_6) δ 172.8, 165.2, 159.2, 152.2, 151.1, 146.3, 136.8, 131.8, 131.0, 130.5, 128.5, 127.5, 127.2, 126.2, 125.6, 116.9, 114.2, 98.6, 37.6, 31.6. HRMS (ESI): calc. for $[\text{M}+\text{H}]^+$ $\text{C}_{22}\text{H}_{20}\text{N}_5\text{O}_4^+$ 418.1510, found 418.1515.

4.7.5. 3-(2-(4-((2-amino-4-oxo-4,7-dihydro-3H-pyrrolo[2,3-d]pyrimidin-5-yl)methyl)benzamido)phenyl) propanoic acid (6)—(257 mg, 0.595 mmol, 89% yield) as a green pale solid. ^1H NMR (400 MHz, DMSO- d_6) δ 12.22 (s, 1H), 10.76 (d, J = 1.6 Hz, 1H), 10.15 (s, 1H), 9.89 (s, 1H), 7.91 – 7.78 (m, 2H), 7.48 – 7.39 (m, 2H), 7.34 (d, J = 7.2 Hz, 1H), 7.30 (dd, J = 7.6, 1.7 Hz, 1H), 7.27 – 7.16 (m, 2H), 6.37 (d, J = 1.6 Hz, 1H), 6.03 (s, 2H), 4.01 (s, 2H), 2.82 (t, J = 7.4 Hz, 2H), 2.53 (d, J = 7.4 Hz, 2H). ^{13}C NMR (151 MHz, DMSO- d_6) δ 168.5, 166.4, 158.9, 152.0, 145.8, 140.7, 132.0, 131.6, 130.3, 129.3, 128.4, 127.1, 127.1, 127.0, 126.6, 117.2, 114.5, 98.7, 41.1, 31.5. HRMS (ESI): calc. for $[\text{M}+\text{H}]^+$ $\text{C}_{23}\text{H}_{22}\text{N}_5\text{O}_4^+$ 432.1666, found 432.1657.

4.7.6. 2-(4-((2-amino-4-oxo-4,7-dihydro-3H-pyrrolo[2,3-d]pyrimidin-5-yl)methyl)-N-methylbenzamido) benzoic acid (9)—(27 mg, 0.065 mmol, 56% yield). ¹H NMR (400 MHz, DMSO-*d*₆) δ 13.10 (s, 1H), 10.67 (s, 1H), 10.09 (s, 1H), 7.70 (d, *J* = 7.7 Hz, 1H), 7.50 (t, *J* = 7.5 Hz, 1H), 7.35 (d, *J* = 7.9 Hz, 1H), 7.29 (t, *J* = 7.6 Hz, 1H), 7.11 – 6.95 (m, 4H), 6.11 (s, 1H), 5.98 (s, 2H), 3.80 (s, 2H), 3.26 (s, 3H). ¹³C NMR (151 MHz, DMSO-*d*₆) δ 169.2, 166.6, 159.2, 152.2, 151.1, 144.3, 143.3, 133.5, 133.0, 131.1, 130.2, 12.9, 127.8, 127.6, 127.4, 117.0, 114.0, 98.6, 37.8, 31.4. HRMS (ESI): calc. for [M+H]⁺ C₂₂H₂₀N₅O₄⁺ 418.1510, found 418.1522.

4.7.7. 2-((4-((2-amino-4-oxo-4,7-dihydro-3H-pyrrolo[2,3-d]pyrimidin-5-yl)methyl)benzamido)methyl) benzoic acid (11)—(39 mg, 0.093 mmol, 44% yield) as a yellow pale solid. ¹H NMR (600 MHz, DMSO-*d*₆) δ 13.00 (bs, 1H), 10.88 (d, *J* = 1.9 Hz, 1H), 10.40 (s, 1H), 8.85 (t, *J* = 6.0 Hz, 1H), 7.87 (dd, *J* = 7.7, 1.5 Hz, 1H), 7.81 – 7.77 (m, 2H), 7.51 (td, *J* = 7.6, 1.5 Hz, 1H), 7.40 – 7.32 (m, 4H), 6.39 (d, *J* = 2.2 Hz, 1H), 6.35 (s, 2H), 4.80 (d, *J* = 6.0 Hz, 2H), 3.99 (s, 2H). ¹³C NMR (151 MHz, DMSO-*d*₆) δ 168.5, 166.4, 158.9, 152.0, 145.8, 140.7, 132.0, 131.6, 130.3, 129.3, 128.4, 127.1, 127.1, 127.0, 126.6, 117.2, 114.5, 98.7, 41.1, 31.5. HRMS (ESI): calc. for [M+H]⁺ C₂₂H₂₀N₅O₄⁺ 418.1510, found 418.1517.

4.7.8. 1-(4-((2-amino-4-oxo-4,7-dihydro-3H-pyrrolo[2,3-d]pyrimidin-5-yl)methyl)benzoyl) piperidine-2-carboxylic acid (12)—(60 mg, 0.147 mmol, 20% yield) as a white-yellow solid. ¹H NMR (400 MHz, DMSO-*d*₆) δ 11.89 (s, 1H), 10.72 (d, *J* = 2.1 Hz, 1H), 10.11 (s, 1H), 7.39 – 7.32 (m, 2H), 7.28 – 7.21 (m, 2H), 6.35 (d, *J* = 2.2 Hz, 1H), 5.99 (s, 2H), 4.47 – 4.36 (m, 1H), 3.96 (s, 2H), 3.59 – 3.50 (m, 1H), 3.13 – 3.02 (m, 1H), 2.20 – 2.12 (m, 1H), 1.71 – 1.63 (m, 1H), 1.58 – 1.48 (m, 1H), 1.44 – 1.36 (m, 1H), 1.30 – 1.23 (m, 1H), 1.20 – 1.13 (m, 1H). ¹³C NMR (101 MHz, DMSO-*d*₆) δ 172.3, 170.4, 159.3, 152.2, 151.2, 144.0, 133.1, 128.5, 126.6, 117.0, 114.1, 98.7, 57.8, 51.7, 45.3, 31.5, 26.3, 24.8, 20.9. HRMS (ESI): calc. for [M+H]⁺ C₂₀H₂₂N₅O₄⁺ 396.1666, found 396.1675.

4.7.9. 2-(4-((2-amino-4-oxo-4,7-dihydro-3H-pyrrolo[2,3-d]pyrimidin-5-yl)methyl)benzamido)cyclohexan-1-carboxylic acid (13)—(4.1 mg, 0.010 mmol, 5% yield) as a white-green solid. ¹H NMR (400 MHz, DMSO-*d*₆) δ 12.17 (s, 1H), 10.73 (s, 1H), 10.16 (s, 1H), 7.85 (d, *J* = 8.3 Hz, 1H), 7.66 – 7.60 (m, 2H), 7.37 – 7.31 (m, 2H), 6.31 (s, 1H), 6.04 (s, 2H), 4.28 (s, 1H), 3.96 (s, 2H), 2.78 – 2.68 (m, 2H), 1.99 (s, 1H), 1.82 – 1.71 (m, 2H), 1.66 – 1.45 (m, 2H), 1.36 (s, 2H). ¹³C NMR (101 MHz, DMSO-*d*₆) δ 173.6, 166.0, 162.9, 153.6, 150.5, 132.9, 132.7, 126.2, 125.9, 119.1, 116.7, 111.3, 53.5, 47.9, 31.8, 25.8, 25.0, 23.6, 23.5. HRMS (ESI): calc. for [M+H]⁺ C₂₁H₂₄N₅O₄⁺ 410.1823, found 410.1828.

4.7.10. 2-(4-((2-amino-4-oxo-4,7-dihydro-3H-pyrrolo[2,3-d]pyrimidin-5-yl)methyl)benzamido)-4-chloro benzoic acid (14)—(92.4 mg, 0.21 mmol, 68% yield) as a white solid. ¹H NMR (400 MHz, DMSO-*d*₆) δ 12.36 (s, 1H), 10.76 (s, 1H), 10.14 (s, 1H), 8.82 (d, *J* = 2.0 Hz, 1H), 8.05 (d, *J* = 8.5 Hz, 1H), 7.85 – 7.79 (m, 2H), 7.52 – 7.46 (m, 2H), 7.25 (dd, *J* = 8.7, 2.0 Hz, 1H), 6.38 (d, *J* = 1.4 Hz, 1H), 6.02 (s, 2H), 4.02 (s, 2H). ¹³C NMR (151 MHz, DMSO-*d*₆) δ 169.3, 165.0, 159.3, 152.3, 151.3, 147.3, 142.3, 138.4,

133.0, 131.4, 130.1, 129.1, 127.0, 122.6, 119.0, 116.6, 114.3, 98.6, 31.7. HRMS (ESI): calc. for $[M+H]^+$ $C_{21}H_{17}ClN_5O_4^+$ 438.0964, found 438.0955.

4.7.11. 2-(4-((2-amino-4-oxo-4,7-dihydro-3H-pyrrolo[2,3-d]pyrimidin-5-yl)methyl)benzamido) terephthalic acid (15)—(10 mg, 0.022 mmol, 57% yield) as a white-green solid. 1H NMR (600 MHz, DMSO- d_6) δ 13.25 (s, 2H), 10.76 (d, $J=2.3$ Hz, 1H), 10.21 (s, 1H), 9.27 (d, $J=1.7$ Hz, 1H), 8.12 (d, $J=8.2$ Hz, 1H), 7.87 – 7.84 (m, 2H), 7.67 (d, $J=8.2$ Hz, 1H), 7.50 – 7.47 (m, 2H), 6.37 (d, $J=2.1$ Hz, 1H), 6.09 (s, 2H), 4.02 (s, 2H). ^{13}C NMR (151 MHz, DMSO- d_6) δ 169.3, 166.7, 164.8, 159.3, 152.3, 151.3, 147.1, 141.0, 135.0, 131.7, 131.5, 131.4, 129.1, 127.0, 123.1, 120.6, 116.7, 114.2, 98.6, 31.7. HRMS (ESI): calc. for $[M+H]^+$ $C_{22}H_{18}N_5O_6^+$ 448.1252, found 448.1257.

4.7.12. 2-(4-((2-amino-4-oxo-4,7-dihydro-3H-pyrrolo[2,3-d]pyrimidin-5-yl)methyl)benzamido)-4-methoxy benzoic acid (16)—(40 mg, 0.092 mmol, 69% yield) as a white-yellow solid. 1H NMR (400 MHz, DMSO- d_6) δ 13.48 (s, 1H), 12.38 (s, 1H), 10.77 (d, $J=1.9$ Hz, 1H), 10.16 (s, 1H), 8.42 (d, $J=2.7$ Hz, 1H), 8.00 (d, $J=8.9$ Hz, 1H), 7.86 – 7.81 (m, 2H), 7.52 – 7.46 (m, 2H), 6.76 (dd, $J=8.9, 2.7$ Hz, 1H), 6.38 (d, $J=2.2$ Hz, 1H), 6.04 (s, 2H), 4.02 (s, 2H), 3.85 (s, 3H). ^{13}C NMR (101 MHz, DMSO- d_6) δ 167.2, 166.0, 163.9, 158.3, 152.6, 159.0, 138.7, 133.1, 131.8, 128.7, 126.5, 127.1, 119.1, 116.9, 112.4, 111.3, 109.7, 101.2, 56.5, 31.8. HRMS (ESI): calc. for $[M+H]^+$ $C_{22}H_{20}N_5O_5^+$ 434.1459, found 434.1446.

4.7.13. 2-(4-((2-amino-4-oxo-4,7-dihydro-3H-pyrrolo[2,3-d]pyrimidin-5-yl)methyl)benzamido)-4-cyanobenzoic acid (17)—(50 mg, 0.117 mmol, yield 86% yield) as a white-brown solid. 1H NMR (400 MHz, DMSO- d_6) δ 12.09 (s, 1H), 10.77 (s, 1H), 10.16 (s, 1H), 9.09 (s, 1H), 8.16 – 8.05 (m, 3H), 7.87 – 7.82 (m, 2H), 7.65 – 7.54 (m, 1H), 7.49 (d, $J=8.0$ Hz, 1H), 6.38 (s, 1H), 6.04 (s, 2H), 4.02 (s, 2H). ^{13}C NMR (151 MHz, DMSO- d_6) δ 168.2, 166.0, 163.9, 153.8, 150.5, 138.3, 134.1, 132.4, 130.5, 127.8, 127.3, 127.1, 121.3, 120.1, 119.7, 117.4, 112.6, 112.3, 111.8, 31.8. HRMS (ESI): calc. for $[M+H]^+$ $C_{22}H_{17}N_6O_4^+$ 429.1306, found 429.1302.

4.7.14. 2-(4-((2-amino-4-oxo-4,7-dihydro-3H-pyrrolo[2,3-d]pyrimidin-5-yl)methyl)benzamido)-4-(hydroxymethyl)benzoic acid (18)—(40 mg, 0.092 mmol, 54% yield) as a white-green solid. 1H NMR (400 MHz, DMSO- d_6) δ 12.27 (s, 1H), 10.77 (s, 1H), 10.15 (s, 1H), 8.72 (s, 1H), 8.12 – 7.96 (m, 3H), 7.92 – 7.79 (m, 3H), 7.51 – 7.46 (m, 1H), 7.16 – 7.09 (m, 1H) 6.37 (d, $J=2.2$ Hz, 1H), 6.03 (s, 2H), 4.57 (s, 2H), 4.02 (s, 2H). ^{13}C NMR (151 MHz, DMSO- d_6) δ 168.2, 166.0, 163.9, 153.6, 150.2, 141.8, 137.5, 134.3, 131.3, 128.8, 127.5, 127.1, 125.5, 123.7, 120.3, 118.6, 117.5, 111.3, 61.5, 30.9. HRMS (ESI): calc. for $[M+H]^+$ $C_{22}H_{20}N_5O_5^+$ 434.1459, found 434.1446.

4.7.15. 2-(4-((2-amino-4-oxo-4,7-dihydro-3H-pyrrolo[2,3-d]pyrimidin-5-yl)methyl)benzamido)-4-(methoxymethyl)benzoic acid (19)—(62 mg, 0.143 mmol, 83% yield) as a white-pink solid. 1H NMR (600 MHz, DMSO- d_6) δ 13.74 (s, 1H), 12.19 (s, 1H), 10.76 (d, $J=2.3$ Hz, 1H), 10.14 (s, 1H), 8.72 (d, $J=1.5$ Hz, 1H), 8.02 (d, $J=8.1$ Hz, 1H), 7.84 – 7.81 (m, 2H), 7.50 – 7.47 (m, 2H), 7.12 (dd, $J=8.1, 1.6$ Hz, 1H), 6.38 (d, $J=2.1$ Hz, 1H), 6.02 (s, 2H), 4.50 (s, 2H), 4.02 (s, 2H), 3.34 (s, 3H). ^{13}C NMR (151 MHz, DMSO-

d_6) δ 169.9, 164.7, 159.3, 152.3, 151.3, 147.0, 145.2, 141.4, 131.8, 131.3, 129.1, 126.9, 121.2, 118.0, 116.6, 115.3, 114.2, 98.6, 73.1, 57.9, 31.6. HRMS (ESI): calc. for $[M+H]^+$ $C_{23}H_{22}N_5O_5^+$ 448.1615, found 448.1622.

4.7.16. 2-(4-((2-amino-4-oxo-4,7-dihydro-3H-pyrrolo[2,3-d]pyrimidin-5-yl)methyl)benzamido)-4-carbamoylbenzoic acid (20)—(10 mg, 0.022 mmol, 46% yield) as a white-brown solid. 1H NMR (400 MHz, DMSO- d_6) δ 12.20 (bs, 1H), 10.73 (s, 1H), 10.12 (s, 1H), 9.06 (d, $J = 1.7$ Hz, 1H), 8.09 – 8.01 (m, 2H), 7.83 – 7.79 (m, 2H), 7.56 (d, $J = 8.1$ Hz, 2H), 7.50 (bs, 1H), 7.47 – 7.44 (m, 2H), 6.35 (d, $J = 2.1$ Hz, 1H), 5.99 (s, 2H), 3.99 (s, 2H). ^{13}C NMR (101 MHz, DMSO- d_6) δ 168.5, 167.8, 166.0, 165.9, 155.6, 152.0, 138.2, 134.9, 133.8, 132.6, 128.1, 127.5, 127.3, 127.1, 120.2, 117.5, 117.6, 115.8, 111.3, 31.8. HRMS (ESI): calc. for $[M+H]^+$ $C_{22}H_{19}N_6O_5^+$ 447.1411, found 447.1416.

4.7.17. 2-(4-((2-amino-4-oxo-4,7-dihydro-3H-pyrrolo[2,3-d]pyrimidin-5-yl)methyl)benzamido)-3-(methoxymethyl)benzoic acid (21)—(43 mg, 0.096 mmol, 56% yield) as a white-brown solid. 1H NMR (400 MHz, DMSO- d_6) δ 12.88 (s, 1H), 10.76 (d, $J = 2.0$ Hz, 1H), 10.14 (s, 1H), 9.99 (s, 1H), 7.88 – 7.82 (m, 2H), 7.78 (dd, $J = 7.8, 1.6$ Hz, 1H), 7.66 (d, $J = 7.6$ Hz, 1H), 7.45 – 7.36 (m, 3H), 6.38 (d, $J = 2.2$ Hz, 1H), 6.03 (s, 2H), 4.41 (s, 2H), 4.00 (s, 2H), 3.28 (s, 3H). ^{13}C NMR (101 MHz, DMSO- d_6) δ 168.4, 166.7, 162.9, 152.6, 151.4, 145.5, 137.1, 136.7, 135.4, 134.7, 132.5, 130.5, 130.1, 126.9, 123.1, 120.7, 111.6, 111.3, 68.6, 56.0, 31.8. HRMS (ESI): calc. for $[M+H]^+$ $C_{23}H_{22}N_5O_5^+$ 448.1615, found 448.1611.

4.7.18. 2-(4-((2-amino-4-oxo-4,7-dihydro-3H-pyrrolo[2,3-d]pyrimidin-5-yl)methyl)benzamido)-5-methoxybenzoic acid (22)—(121 mg, 0.279 mmol, 65% yield) as a white-green solid. 1H NMR (400 MHz, DMSO- d_6) δ 13.77 (s, 1H), 11.80 (s, 1H), 10.76 (d, $J = 2.3$ Hz, 1H), 10.15 (s, 1H), 8.59 (d, $J = 9.2$ Hz, 1H), 7.83 – 7.79 (m, 2H), 7.51 (d, $J = 3.2$ Hz, 1H), 7.49 – 7.45 (m, 2H), 7.26 (dd, $J = 9.2, 3.2$ Hz, 1H), 6.37 (d, $J = 2.2$ Hz, 1H), 6.03 (s, 2H), 4.01 (s, 2H), 3.79 (s, 3H). ^{13}C NMR (151 MHz, DMSO- d_6) δ 169.5, 164.3, 159.3, 154.3, 152.3, 151.2, 146.8, 134.6, 132.0, 129.0, 126.8, 121.8, 120.3, 118.1, 116.7, 114.9, 114.2, 98.6, 55.4, 31.6. HRMS (ESI): calc. for $[M+H]^+$ $C_{22}H_{20}N_5O_5^+$ 434.1459, found 434.1465.

4.7.19. 2-(2-(4-((2-amino-4-oxo-4,7-dihydro-3H-pyrrolo[2,3-d]pyrimidin-5-yl)methyl)benzamido)-4-methoxyphenyl)acetic acid (23)—(27 mg, 0.061 mmol, 68% yield) as a white-pink solid. 1H NMR (400 MHz, DMSO- d_6) δ 12.32 (s, 1H), 10.75 (s, 1H), 10.15 (s, 1H), 9.82 (s, 1H), 7.86 – 7.76 (m, 2H), 7.46 – 7.37 (m, 2H), 7.20 (d, $J = 8.5$ Hz, 1H), 7.14 (d, $J = 2.2$ Hz, 1H), 6.77 (dd, $J = 8.5, 2.4$ Hz, 1H), 6.36 (s, 1H), 6.03 (s, 2H), 4.00 (s, 2H), 3.74 (s, 3H), 3.57 (s, 2H). ^{13}C NMR (101 MHz, DMSO- d_6) δ 171.6, 168.0, 162.9, 158.7, 152.6, 151.3, 142.8, 137.1, 135.4, 132.3, 129.5, 128.7, 123.1, 119.7, 118.1, 115.3, 110.5, 104.9, 56.5, 39.9, 31.8. HRMS (ESI): calc. for $[M+H]^+$ $C_{23}H_{22}N_5O_5^+$ 448.1615, found 448.1624.

4.7.20. 2-(2-(4-((2-amino-4-oxo-4,7-dihydro-3H-pyrrolo[2,3-d]pyrimidin-5-yl)methyl)benzamido)-4-cyanophenyl)acetic acid (24)—(106 mg, 0.239 mmol, 38% yield) as a green pale solid. 1H NMR (600 MHz, DMSO- d_6) δ 12.51 (bs, 1H), 10.82 (d, $J =$

2.3 Hz, 1H), 10.27 (s, 1H), 10.06 (s, 1H), 7.93 (d, $J = 1.7$ Hz, 1H), 7.84 – 7.79 (m, 2H), 7.67 (dd, $J = 7.9, 1.8$ Hz, 1H), 7.54 (d, $J = 8.0$ Hz, 1H), 7.46 – 7.40 (m, 2H), 6.39 (d, $J = 2.1$ Hz, 1H), 6.18 (s, 2H), 4.01 (s, 2H), 3.80 (s, 2H). ^{13}C NMR (151 MHz, DMSO- d_6) δ 171.8, 165.6, 159.1, 158.1, 152.1, 146.6, 137.8, 136.3, 132.5, 131.3, 129.4, 129.0, 128.5, 127.6, 118.5, 117.0, 114.3, 109.9, 98.6, 37.5, 31.6. HRMS (ESI): calc. for $[\text{M}+\text{H}]^+$ $\text{C}_{23}\text{H}_{19}\text{N}_6\text{O}_4^+$ 443.1462, found 443.1464.

4.7.21. 3-(4-((2-amino-4-oxo-4,7-dihydro-3H-pyrrolo[2,3-d]pyrimidin-5-yl)methyl)benzamido)-4-(carboxymethyl)benzoic acid (25)—(89 mg, 0.193 mmol, 38% yield) as a orange solid. ^1H NMR (600 MHz, DMSO- d_6) δ 12.85 (bs, 2H), 10.75 (d, $J = 2.3$ Hz, 1H), 10.15 (s, 1H), 10.03 (s, 1H), 8.05 (s, 1H), 7.84 – 7.81 (m, 2H), 7.76 (dd, $J = 8.0, 1.7$ Hz, 1H), 7.46 – 7.41 (m, 3H), 6.37 (d, $J = 2.2$ Hz, 1H), 6.03 (s, 2H), 4.01 (s, 2H), 3.74 (s, 2H). ^{13}C NMR (151 MHz, DMSO- d_6) δ 172.2, 166.9, 165.4, 159.3, 152.3, 151.2, 146.5, 137.0, 135.5, 131.6, 131.3, 129.8, 128.5, 127.5, 126.9, 126.3, 116.9, 114.1, 98.6, 37.7, 31.7. HRMS (ESI): calc. for $[\text{M}+\text{H}]^+$ $\text{C}_{23}\text{H}_{20}\text{N}_5\text{O}_6^+$ 462.1408, found 462.1414.

4.8. General procedure for the synthesis of final compound 8. Method g.

The synthesis of compound **8** has been carried out following for general method *g*. NaN_3 (76 mg, 1.16 mmol) was added to a solution of 4-((2-amino-4-oxo-4,7-dihydro-3H-pyrrolo[2,3-d]pyrimidin-5-yl)methyl)-*N*-(2-cyanophenyl)benzamide (**7**) (50 mg, 0.13 mmol) in DMSO (0.57 mL) and water (0.57 mL) and the reaction mixture stirred at 100 °C overnight. After solvent evaporation under reduced pressure the desired final compound was purified by flash column chromatography eluted initially with dichloromethane followed by 20% methanol in dichloromethane and finally 50% methanol in dichloromethane to give *N*-(2-(1*H*-tetrazol-5-yl)phenyl)-4-((2-amino-4-oxo-4,7-dihydro-3H-pyrrolo[2,3-d]pyrimidin-5-yl)methyl)benzamide (**8**) as a pale brown powder.

4.8.1. *N*-(2-(1*H*-tetrazol-5-yl)phenyl)-4-((2-amino-4-oxo-4,7-dihydro-3H-pyrrolo[2,3-d]pyrimidin-5-yl)methyl)benzamide (8)—(27 mg, 0.061 mmol, 49% yield). ^1H NMR (400 MHz, DMSO- d_6) δ 13.30 (s, 1H), 10.72 (s, 1H), 10.29 (s, 1H), 8.77 – 8.73 (m, 1H), 8.22 (dd, $J = 7.8, 1.7$ Hz, 1H), 8.07 – 8.02 (m, 2H), 7.50 – 7.44 (m, 2H), 7.29 – 7.25 (m, 1H), 7.10 (td, $J = 7.5, 1.3$ Hz, 1H), 6.35 (d, $J = 2.1$ Hz, 1H), 6.06 (s, 2H), 4.00 (s, 2H). ^{13}C NMR (101 MHz, DMSO- d_6) δ 164.4, 159.9, 159.1, 152.2, 150.3, 137.7, 136.5, 130.1, 129.1, 127.7, 127.3, 127.0, 126.8, 126.5, 123.9, 122.8, 122.7, 119.2, 48.6. HRMS (ESI): calc. for $[\text{M}+\text{H}]^+$ $\text{C}_{21}\text{H}_{18}\text{N}_9\text{O}_2^+$ 428.1578, found 428.1570.

4.9. Procedure for the synthesis of final compound 10.

4.9.1. Synthesis of intermediate 33—4,4,5,5-tetramethyl-2-vinyl-1,2,3-dioxaborolane (1.23 g, 8 mmol), K_2CO_3 (1.1 g, 8 mmol) and $\text{Pd}(\text{dppf})\text{Cl}_2$ (293 mg, 0.4 mmol) were added to a solution of methyl 2-bromobenzoate (0.86 g, 4 mmol) in dioxane/water (11 mL/0.5 mL) and the resulting mixture was stirred at 100 °C overnight. The mixture was diluted with water (15 mL) and extracted with ethyl acetate (3×25 mL). The combined organic layers were washed with brine (100 mL), dried over anhydrous Na_2SO_4 , filtered and concentrated under reduced pressure.[24] The residue was purified by flash

column chromatography (hexanes to ethyl acetate) to provide *methyl 2-vinylbenzoate* (**33**) as transparent oil.

4.9.2. Synthesis of intermediate **37**—*4-iodophenyl trifluoromethanesulfonate* (**34**)

Trifluoromethanesulfonic anhydride (34 mL, 5.64 g, 20 mmol) was slowly added at 0 °C to a solution of 4-iodophenol (4 g, 18.17 mmol) in dry pyridine (9.3 mL). The resulting mixture was stirred at the same temperature for 5 minutes and then allowed to warm to 25 °C and stirred for overnight. The reaction was poured into water and extracted with ethyl ether (50 mL). The organic layer was washed sequentially with water, 10% HCl (2x), water and brine, dried over anhydrous MgSO₄ and concentrated under reduced pressure. The crude was purified by flash column chromatography (hexanes to ethyl acetate) to provide *4-iodophenyl trifluoromethanesulfonate* (**34**) as transparent oil.

4.9.2.1. *4-(3-oxopropyl)phenyl trifluoromethanesulfonate* (**35**): Synthesized following Method *c*.

4.9.2.2. *4-(2-bromo-3-oxopropyl)phenyl trifluoromethanesulfonate* (**36**): Synthesized following Method *d*.

4.9.2.3. *4-((2-amino-4-oxo-4,7-dihydro-3H-pyrrolo[2,3-d]pyrimidin-5-yl)methyl)phenyl trifluoromethane sulfonate* (**37**): Synthesized following Method *e*.

4.9.3. Synthesis of intermediate **38**—Dry DMF (16 mL/eq), intermediates **37** (1eq) and **33** (1.25 eq), Pd(OAc)₂ (0.01 eq), PPh₃ (0.02 eq) and dry trimethylamine (4 eq) were added to a pressure vial. The reaction mixture was stirred at 100 °C for 16h. The crude reaction mixture was filtered through silica pad and washed with EtOAc.[25] The solvent was evaporated and the product was purified by flash column chromatography eluted initially with dichloromethane followed by 20% methanol in dichloromethane to give (*E*)-2-(4-((2-amino-4-oxo-4,7-dihydro-3H-pyrrolo[2,3-d]pyrimidin-5-yl)methyl)styryl) benzoate (**38**).

4.9.4. Synthesis of final compound **10**—Synthesized following Method *f*.

4.9.5. *methyl 2-vinylbenzoate* (33**)**—(286 mg, 1.76 mmol, 44% yield) ¹H NMR (400 MHz, Methanol-*d*₄) δ 7.87 (d, *J* = 7.6 Hz, 1H), 7.28–7.57 (m, 4H), 5.61 (d, *J* = 7.6 Hz, 1H), 5.35 (d, *J* = 1.2 Hz, 1H), 3.88 (s, 3H). LC-MS (ESI) *m/z* 163.1 [M+H]⁺.

4.9.6. *4-iodophenyl trifluoromethanesulfonate* (34**)**—(2.47 g, 7.02 mmol, 39% yield) ¹H NMR (400 MHz, CDCl₃) δ 7.81 – 7.75 (m, 2H), 7.07 – 7.00 (m, 2H). LC-MS (ESI) *m/z* 353.1 [M+H]⁺.

4.9.7. *4-(3-oxopropyl)phenyl trifluoromethanesulfonate* (35**)**—(1.86 g, 6.69 mmol, 55% yield). ¹H NMR (400 MHz, CDCl₃) δ 9.82 (t, *J* = 1.6 Hz, 1H), 7.30 – 7.24 (m, 2H), 7.21 – 7.17 (m, 2H), 3.02 – 2.94 (m, 2H), 2.84 – 2.77 (m, 2H). LC-MS (ESI) *m/z* 283.1 [M+H]⁺.

4.9.8. 4-(2-bromo-3-oxopropyl)phenyl trifluoromethanesulfonate (36).—(1.05 g, 4.02 mmol, 61% yield). $^1\text{H NMR}$ (400 MHz, CDCl_3) δ 9.51 (d, $J = 1.7$ Hz, 1H), 7.37 – 7.31 (m, 2H), 7.29 – 7.21 (m, 2H), 4.44 (ddt, $J = 8.0, 6.4, 1.7$ Hz, 1H), 3.56 – 3.50 (m, 1H), 3.18 (ddd, $J = 14.8, 8.0, 1.5$ Hz, 1H). LC-MS (ESI) m/z 262.1 $[\text{M}+\text{H}]^+$.

4.9.9. 4-((2-amino-4-oxo-4,7-dihydro-3H-pyrrolo[2,3-d]pyrimidin-5-yl)methyl)phenyl trifluoromethane sulfonate (37).—(704 mg, 1.81 mmol, 45% yield). $^1\text{H NMR}$ (400 MHz, $\text{DMSO}-d_6$) δ 10.76 (d, $J = 2.1$ Hz, 1H), 10.13 (s, 1H), 7.48 – 7.42 (m, 2H), 7.37 – 7.31 (m, 2H), 6.39 (d, $J = 2.1$ Hz, 1H), 6.01 (s, 2H), 3.97 (s, 2H). LC-MS (ESI) m/z 389.1 $[\text{M}+\text{H}]^+$.

4.9.10. (E)-2-(4-((2-amino-4-oxo-4,7-dihydro-3H-pyrrolo[2,3-d]pyrimidin-5-yl)methyl)styryl) benzoate (38)—(34.7 mg, 0.082 mmol, 62% yield). $^1\text{H NMR}$ (500 MHz, $\text{DMSO}-d_6$) δ 10.73(s, 1H), 10.13 (s, 1H), 7.98 – 7.64 (m, 3H), 7.62 – 7.00 (m, 6H), 6.36 – 6.23 (m, 2H), 6.03 (s, 2H), 3.97 (s, 2H), 3.88 (s, 3H). LC-MS (ESI) m/z 401.1 $[\text{M}+\text{H}]^+$.

4.9.11. (E)-2-(4-((2-amino-4-oxo-4,7-dihydro-3H-pyrrolo[2,3-d]pyrimidin-5-yl)methyl)styryl)benzoic acid (10).—(13.6 mg, 0.035 mmol, 41% yield). $^1\text{H NMR}$ (500 MHz, $\text{DMSO}-d_6$) δ 12.96 (bs, 1H), 11.03 (s, 1H), 10.69 (s, 1H), 7.84 – 7.74 (m, 3H), 7.59 – 7.25 (m, 4H), 7.16 – 7.03 (m, 2H), 6.81 – 6.68 (m, 2H), 6.38 (s, 2H), 3.94 (s, 2H). $^{13}\text{C NMR}$ (151 MHz, $\text{DMSO}-d_6$) δ 168.7, 158.5, 151.8, 149.0, 141.9, 137.9, 134.6, 131.9, 130.7, 130.3, 129.6, 129.0, 127.2, 126.5, 126.4, 126.3, 126.0, 114.6, 98.8, 31.3. HRMS (ESI): calc. for $[\text{M}+\text{H}]^+ \text{C}_{21}\text{H}_{19}\text{N}_4\text{O}_4^+$ 387.1452, found 387.1448.

4.10. General procedure for the synthesis of final compounds 26–27

4.10.1. Synthesis of intermediate 39—1-bromo-2-methoxyethane (205 μL , 2.21 mmol) was added to a solution of 3-bromo-5-methoxyphenol (373 mg, 1.84 mmol), K_2CO_3 (381 mg, 2.76 mmol) and anhydrous DMF (10 mL) and the reaction mixture was stirred overnight at 85 °C. The resulting mixture was then diluted in EtOAc and washed with water (3×50 mL). The organic phase was dried over anhydrous Na_2SO_4 , filtered and concentrated to give 1-bromo-3-methoxy-5-(2-methoxyethoxy)benzene (**41**) as a white powder. $n\text{-BuLi}$ (0.63 mL, 1.58 mmol) was added under nitrogen atmosphere to a solution of **41** (411 mg, 1.58 mmol) in dry THF (5 mL) at -78°C . and the reaction stirred for 30 minutes. Trimethoxyborane (0.21 mL, 1.9 mmol) in a THF solution was slowly added dropwise at 70°C , and the mixture warmed to room temperature and stirred for 16 hours. After the completion of the reaction, 20% HCl (2.7 mL) was added and stirred for 3 hours. The mixture was extracted with ethyl acetate, washed with water and brine, and dried over anhydrous Na_2SO_4 to provide (3-methoxy-5-(2-methoxyethoxy)phenyl)boronic acid (**39**) as pale brown solid.

4.10.2. Synthesis of intermediate 40— $\text{PdCl}_2(\text{dppf})$ (0.03eq), KOAc (2.9 eq) and bis(pinacolato)diboron (1.1 eq) were added to a solution of methyl 3-bromo-5-methoxybenzoate (1 eq) in dry dioxane (5.6 mL/mmol) under nitrogen. The solution was stirred at 80 °C for 2 hours and then was diluted with dichloromethane (25 mL) and washed

with water (25 mL). The organic layer was dried over anhydrous Na₂SO₄, filtered and the solvent was eliminated under reduced pressure to give *methyl 3-methoxy-5-(4,4,5,5-tetramethyl-1,3,2-dioxaborolan-2-yl)benzoate* (**42**). Crude arylboronic acid pinacol ester (1 eq) and sodium periodate (3 eq) were stirred in 8 mL/mmol of a 4:1 mixture of acetone and water for 30 min, at which time aqueous NH₄OAc (1eq) was added to the suspension. The reaction mixture was stirred at room temperature for 17 h and then diluted with water (30 ml) and extracted with ethyl acetate (2 × 60 ml). The combined extracts were washed with water (2 × 30 ml) and brine (30 ml), dried over anhydrous Na₂SO₄, filtered, and concentrated to dryness by rotary evaporation to give a colourless solid, *(3-methoxy-5-(methoxycarbonyl)phenyl)boronic acid* (**40**).

4.10.3. Synthesis of final compounds 26 and 27—Compounds **26** and **27** have been synthesized through the reaction between trifluoromethane sulfonate derivate **37** (1 eq) and the corresponding boronic acid **39** or **40** following general method *h* or *i*, respectively. Method *h*: A mixture of **39** (1.5 eq), **37** (1.0 eq), Pd(PPh₃)₄ (0.01 eq) and TEA (2.6 eq) in dioxane (10 mL/mmol) was stirred overnight at 90 °C. The solvent was evaporated under reduced pressure and the residue purified by flash column chromatography eluted initially with dichloromethane followed by 20% methanol in dichloromethane to give *2-amino-5-((3'-methoxy-5'-(2-methoxyethoxy)-[1,1'-biphenyl]-4-yl)methyl)-3,7-dihydro-4H-pyrrolo[2,3-d]pyrimidin-4-one* (**26**). Pale pink powder. General method *i*: A solution of **40** (2 eq), **37** (1.0 eq), Pd(PPh₃)₂Cl₂ (0.05 eq) and (2M) Na₂CO₃ (4 eq) in DMF (1 mL/mmol) was stirred for 2h at 100 °C. The solvent was evaporated under reduced pressure and the residue purified by flash column chromatography eluted initially with dichloromethane followed by 20% methanol in dichloromethane to give *4'-((2-amino-4-oxo-4,7-dihydro-3H-pyrrolo[2,3-d]pyrimidin-5-yl)methyl)-5-methoxy-[1,1'-biphenyl]-3-carboxylic acid* (**27**). Pale green powder.

4.10.4. 1-bromo-3-methoxy-5-(2-methoxyethoxy)benzene (41)—(411 mg, 1.58 mmol, 86% yield) ¹H NMR (400 MHz, CDCl₃) δ 6.73 – 6.64 (m, 2H), 6.45 – 6.39 (m, 1H), 4.07 (t, *J* = 4.7 Hz, 2H), 3.76 (s, 3H), 3.73 (t, *J* = 4.6 Hz, 2H), 3.44 (s, 3H). LC-MS (ESI) *m/z* 262,1 [M+H]⁺.

4.10.5. (3-methoxy-5-(2-methoxyethoxy)phenyl)boronic acid (39)—(223 mg, 0.99 mmol, 63% yield). ¹H NMR (400 MHz, CDCl₃) δ 7.38 – 7.32 (m, 1H), 6.76 – 6.67 (m, 1H), 6.52 – 6.48 (m, 1H), 4.12 (t, *J* = 4.7 Hz, 2H), 3.78 (s, 3H), 3.75 (t, *J* = 4.6 Hz, 2H), 3.45 (s, 3H). LC-MS (ESI) *m/z* 227,0 [M+H]⁺.

4.10.6. methyl 3-methoxy-5-(4,4,5,5-tetramethyl-1,3,2-dioxaborolan-2-yl)benzoate (42)—(651 mg, 2.23 mmol, 89% yield). ¹H NMR (400 MHz, DMSO-*d*₆) δ 7.86 – 7.84 (m, 1H), 7.54 (dd, *J* = 2.7, 1.5 Hz, 1H), 7.38 (dd, *J* = 2.7, 0.9 Hz, 1H), 3.86 (s, 3H), 3.83 (s, 3H), 1.31 (s, 12H). LC-MS (ESI) *m/z* 293,0 [M+H]⁺.

4.10.7. (3-methoxy-5-(methoxycarbonyl)phenyl)boronic acid (40)—(453 mg, 2.16 mmol, 97% yield). ¹H NMR (400 MHz, DMSO-*d*₆) δ 7.56 (t, *J* = 2.4, 1H), 7.51 (t, *J* =

2.4, 1H), 7.46 (t, $J=2.3$ Hz, 1H), 3.89 (s, 3H), 3.88 (s, 3H). LC-MS (ESI) m/z 211,1 [M+H]⁺.

4.10.8. 2-amino-5-((3'-methoxy-5'-(2-methoxyethoxy)-[1,1'-biphenyl]-4-yl)methyl)-3,7-dihydro-4H-pyrrolo [2,3-d]pyrimidin-4-one (26).—(49 mg, 0.117 mmol, 39% yield). ¹H NMR (600 MHz, Methanol-*d*₄) δ 7.48 (d, $J=7.7$ Hz, 2H), 7.34 (d, $J=7.7$ Hz, 2H), 6.73 (d, $J=6.2$ Hz, 2H), 6.47 (s, 1H), 6.31 (s, 1H), 4.14 (t, $J=4.5$ Hz, 2H), 4.08 (s, 2H), 3.81 (s, 3H), 3.75 (t, $J=4.6$ Hz, 2H), 3.43 (s, 3H). ¹³C NMR (151 MHz, DMSO-*d*₆) δ 164.9, 161.7, 160.5, 153.7, 150.6, 142.1, 136.3, 134.3, 126.9, 126.3, 122.1, 117.9, 113.3, 109.1, 107.9, 102.5, 70.6, 67.5, 59.0, 55.8, 31.5. HRMS (ESI): calc. for [M+H]⁺ C₂₃H₂₅N₄O₄⁺ 421.1870, found 421.1886.

4.10.9. 4'-((2-amino-4-oxo-4,7-dihydro-3H-pyrrolo[2,3-d]pyrimidin-5-yl)methyl)-5-methoxy-[1,1'-biphenyl]-3-carboxylic acid (27).—(32 mg, 0.082 mmol, 96% yield) ¹H NMR (600 MHz, DMSO-*d*₆) δ 12.85 (bs, 1H), 10.64 (d, $J=2.3$ Hz, 1H), 10.09 (s, 1H), 7.07–7.04 (m, 2H), 6.96–6.95 (m, 1H), 6.91–6.90 (m, 1H), 6.62–6.60 (m, 2H), 6.54 (t, $J=2.3$ Hz, 1H), 6.20 (s, $J=2.1$ Hz, 1H), 5.98 (s, 2H), 3.80 (s, 2H), 3.74 (s, 3H). ¹³C NMR (151 MHz, DMSO-*d*₆) δ 167.6, 160.8, 158.9, 155.5, 152.6, 151.5, 132.8, 129.8, 122.2, 120.0, 119.0, 115.2, 114.0, 109.3, 106.1, 105.6, 99.1, 55.6, 31.3. HRMS (ESI): calc. for [M+H]⁺ C₂₁H₁₉N₄O₄⁺ 391.1401, found 391,1393.

4.11. Protein Preparation

ChTS-DHFR was expressed, purified and estimation of protein concentration was determined as reported in previous study.[13] His6-human TS was expressed, purified and estimation of protein concentration was determined as previously described.[26] 7–29 human TS deletion mutant (mhTS) was expressed, and an estimation of protein concentration was determined as previously reported.[19]

4.12. Enzyme assay, and data analysis

TS activity was determined by following the conversion of substrates dUMP and 5,10-methylenetetrahydrofolate to products dTMP and dihydrofolate at 340 nm ($\epsilon = 6400 \text{ M}^{-1} \text{ cm}^{-1}$) at 25°C.[13] Reaction conditions used to determining IC₅₀ values for TS are as described in a previous study.[12] Compound 1 was utilized as a positive antifolate control. Changes in absorption were determined on a SpectroMax M5 plate reader (Molecular Devices). Data were fitted to an [Inhibitor] vs normalized response with variable slope equation using GraphPad Prism software (version 7.01).

4.13. Protein crystallography

The purified ChTS-DHFR enzyme was co-crystallized with inhibitor compounds by hanging drop vaporization with a protein:well solution ratio of 2:1 to screen crystallization conditions. Reservoir conditions for crystallization included 16–22 % (v/v) PEG 6000, 200 mM ammonium sulfate, 60 mM lithium sulfate, and 100 mM Tris, pH 8.0. ChTS-DHFR enzyme (approximately 24 mg/ml) was incubated with 100 mM Tris, pH 8.0, 1.5 mM NADPH, 1.5 mM FdUMP, 0.5 mM methotrexate, and 5 mM inhibitor compounds on ice for 1 h before setting up drops. Crystals grew in approximately 2 days at 18°C. All crystals were

frozen with a cryosolution containing 25 % (v/v) ethylene glycol and 5 mM of the appropriate inhibitor compounds and flash cooled with liquid nitrogen.

The purified mhTS enzyme was co-crystallized with **14** or **23** by hanging drop vaporization with a protein:well solution ratio of 1:1 to screen crystallization conditions. Reservoir conditions included 16–18 % (v/v) PEG monomethyl ether 5000, and 100 mM Bis-Tris, pH 7.0. mhTS enzyme was co-crystallized with **5** by hanging drop vaporization with a protein:well solution ratio of 1:1 to screen crystallization conditions. Reservoir conditions included 28 % (v/v) PEG 4000, 200 mM lithium sulfate, and 100 mM Tris, pH 7.5. mhTS enzyme was co-crystallized with **15** by hanging drop vaporization with a protein:well solution ratio of 1:1 to screen crystallization conditions. Reservoir conditions included 40 % (v/v) PEG 400, and 100 mM imidazole, pH 8.0. mhTS enzyme (approximately 13 mg/ml) was incubated with 20 mM Bis-Tris, pH 7.0, 2 mM DTT, 2 mM dUMP, and 5 mM of inhibitor compounds on ice for 1 h before setting up drops. Crystals grew in approximately 1 week at 22 °C. All crystals were frozen with a cryosolution containing 25 % (v/v) ethylene glycol and 5 mM of the appropriate inhibitor compound and flash cooled with liquid nitrogen.

Diffraction data for *ChTS*-DHFR with **2**, **5**, **11**, **14**, **15**, **17**, **20**, and **23** and mhTS with **5**, **14**, **15**, and **23** were collected on beam line 24-ID-E, while diffraction data for *ChTS*-DHFR with **6**, **16**, and **25** was collected on beam line 24-ID-C through NE-CAT, using wavelength 0.979 Å. Diffraction data for *ChTS*-DHFR with **24** was collected on beam line 17-ID-FMX at NSLSII, using wavelength 0.979 Å. Data sets for best diffracting crystals were processed by XDS.[27] Phases were solved via molecular replacement using the program phaser.[28, 29] For *ChTS*-DHFR:compound a *ChTS*-DHFR structure in complex with four ligands (PDB ID 4Q0E) was used as the search model for molecular replacement. For mhTS:compound an apo mhTS structure (PDB ID 1HZW) was used as the search model for molecular replacement. The program COOT[30] was used for model building of the ligands into the electron density as well as residues 307–313 of mhTS. Structures were refined using Phenix[31] until acceptable R factors, geometry statistics (RMSDs for ideal bond lengths and angles), and Ramachandran statistics were achieved for the respective structures. Iterative build omit σ_A - weighted $2mFo-Fc$ electron density maps were generated using Phenix Autobuild.[32] Refinement statistics and PDB codes for structures are listed in Supplementary Table S2.

4.14. Molecular modeling

The computational procedures that were utilized are exactly the same as in earlier studies. [33–35] Starting from a crystal structure of the protein, the BOMB program[36] was used to build initial structures for the desired protein-ligand complex. Conjugate-gradient energy minimizations were performed to relax the structure, and Monte Carlo free-energy perturbation (MC/FEP) was carried out to compute relative free energies of binding. The calculations were performed with the MCPRO program[37] using the OPLS-AA force field for the protein,[38] OPLS/CM1A for the ligands,[39] and the TIP4P water model.[40]

Supplementary Material

Refer to Web version on PubMed Central for supplementary material.

Acknowledgments

This work was supported by the National Institutes of Health under Award Numbers (AI083146) to K.S.A., and (GM32136) to W.L.J. and Training Grant (5T32AI007404-23) to D.J.C. This work is based upon research conducted at the Northeastern Collaborative Access Team beamlines, which are funded by the National Institute of General Medical Sciences (NIGMS) from the NIH [P41 GM103403]. Crystals screening was conducted with supports in the Yale Macromolecular X-ray Core Facility [1S10OD018007-01]. This research used resources of the Advanced Photon Source, a U.S. Department of Energy (DOE) Office of Science User Facility operated for the DOE Office of Science by Argonne National Laboratory under Contract No. DE-AC02-06CH11357. This research used FMX beamline of the National Synchrotron Light Source II, a U.S. Department of Energy (DOE) Office of Science User Facility operated for the DOE Office of Science by Brookhaven National Laboratory under Contract No. DE-SC0012704. The Life Science Biomedical Technology Research resource is primarily supported by the NIH, NIGMS through a Biomedical Technology Research Resource P41 grant (P41 GM111244), and by the DOE Office of Biological and Environmental Research (KP1605010).

References

- [1]. Checkley W, White AC Jr., Jaganath D, Arrowood MJ, Chalmers RM, Chen XM, Fayer R, Griffiths JK, Guerrant RL, Hedstrom L, Huston CD, Kotloff KL, Kang G, Mead JR, Miller M, Petri WA Jr., Priest JW, Roos DS, Striepen B, Thompson RC, Ward HD, Van Voorhis WA, Xiao L, Zhu G, Hout R, A review of the global burden, novel diagnostics, therapeutics, and vaccine targets for cryptosporidium, *Lancet Infect Dis*, 15 (2015) 85–94. [PubMed: 25278220]
- [2]. Kotloff KL, Nataro JP, Blackwelder WC, Nasrin D, Farag TH, Panchalingam S, Wu Y, Sow SO, Sur D, Breiman RF, Faruque AS, Zaidi AK, Saha D, Alonso PL, Tamboura B, Sanogo D, Onwuchekwa U, Manna B, Ramamurthy T, Kanungo S, Ochieng JB, Omoro R, Oundo JO, Hossain A, Das SK, Ahmed S, Qureshi S, Quadri F, Adegbola RA, Antonio M, Hossain MJ, Akinsola A, Mandomando I, Nhampossa T, Acacio S, Biswas K, O'Reilly CE, Mintz ED, Berkeley LY, Muhsen K, Sommerfelt H, Robins-Browne RM, Levine MM, Burden and aetiology of diarrhoeal disease in infants and young children in developing countries (the Global Enteric Multicenter Study, GEMS): a prospective, case-control study, *Lancet*, 382 (2013) 209–222. [PubMed: 23680352]
- [3]. Miller CN, Panagos CG, Mosedale WRT, Kvac M, Howard MJ, Tsaousis AD, NMR metabolomics reveals effects of *Cryptosporidium* infections on host cell metabolome, *Gut Pathog*, 11 (2019) 13. [PubMed: 30984292]
- [4]. Kissinger JC, Evolution of *Cryptosporidium*, *Nat Microbiol*, 4 (2019) 730–731. [PubMed: 31015741]
- [5]. Martucci WE, Udier-Blagovic M, Atreya C, Babatunde O, Vargo MA, Jorgensen WL, Anderson KS, Novel non-active site inhibitor of *Cryptosporidium hominis* TS-DHFR identified by a virtual screen, *Bioorg Med Chem Lett*, 19 (2009) 418–423. [PubMed: 19059777]
- [6]. Mazurie AJ, Alves JM, Ozaki LS, Zhou S, Schwartz DC, Buck GA, Comparative genomics of *cryptosporidium*, *Int J Genomics*, 2013 (2013) 832756. [PubMed: 23738321]
- [7]. Laurent F, Lacroix-Lamande S, Innate immune responses play a key role in controlling infection of the intestinal epithelium by *Cryptosporidium*, *Int J Parasitol*, 47 (2017) 711–721. [PubMed: 28893638]
- [8]. Lee S, Ginese M, Girouard D, Beamer G, Huston CD, Osbourn D, Griggs DW, Tzipori S, Piperazine-Derivative MMV665917: an effective drug in the diarrheic piglet model of *Cryptosporidium hominis*, *The Journal of infectious diseases*, (2019).
- [9]. Ruiz V, Czyzyk DJ, Valhondo M, Jorgensen WL, Anderson KS, Novel allosteric covalent inhibitors of bifunctional *Cryptosporidium hominis* TS-DHFR from parasitic protozoa identified by virtual screening, *Bioorg Med Chem Lett*, 29 (2019) 1413–1418. [PubMed: 30929953]
- [10]. Borad A, Ward H, Human immune responses in cryptosporidiosis, *Future Microbiol*, 5 (2010) 507–519. [PubMed: 20210556]

- [11]. Martucci WE, Vargo MA, Anderson KS, Explaining an unusually fast parasitic enzyme: folate tail-binding residues dictate substrate positioning and catalysis in *Cryptosporidium hominis* thymidylate synthase, *Biochemistry*, 47 (2008) 8902–8911. [PubMed: 18672899]
- [12]. Kumar VP, Cisneros JA, Frey KM, Castellanos-Gonzalez A, Wang Y, Gangjee A, White AC Jr., Jorgensen WL, Anderson KS, Structural studies provide clues for analog design of specific inhibitors of *Cryptosporidium hominis* thymidylate synthase-dihydrofolate reductase, *Bioorg Med Chem Lett*, 24 (2014) 4158–4161. [PubMed: 25127103]
- [13]. Atreya CE, Anderson KS, Kinetic characterization of bifunctional thymidylate synthase-dihydrofolate reductase (TS-DHFR) from *Cryptosporidium hominis*: a paradigm shift for its activity and channeling behavior, *J Biol Chem*, 279 (2004) 18314–18322. [PubMed: 14966126]
- [14]. Martucci WE, Rodriguez JM, Vargo MA, Marr M, Hamilton AD, Anderson KS, Exploring novel strategies for AIDS protozoal pathogens: alpha-helix mimetics targeting a key allosteric protein-protein interaction in *C. hominis* TS-DHFR, *Medchemcomm*, 4 (2013).
- [15]. Yuthavong Y, Kamchonwongpaisan S, Leartsakulpanich U, Chitnumsub P, Folate metabolism as a source of molecular targets for antimalarials, *Future Microbiology*, 1 (2006) 113–125. [PubMed: 17661690]
- [16]. Kumar VP, Frey KM, Wang Y, Jain HK, Gangjee A, Anderson KS, Substituted pyrrolo[2,3-d]pyrimidines as *Cryptosporidium hominis* thymidylate synthase inhibitors, *Bioorg Med Chem Lett*, 23 (2013) 5426–5428. [PubMed: 23927969]
- [17]. Carreras CW, Santi DV, The catalytic mechanism and structure of thymidylate synthase, *Annu Rev Biochem*, 64 (1995) 721–762. [PubMed: 7574499]
- [18]. Benkovic SJ, Hammes-Schiffer S, A perspective on enzyme catalysis, *Science*, 301 (2003) 1196–1202. [PubMed: 12947189]
- [19]. Czyzyk DJ, Valhondo M, Jorgensen WL, Anderson KS, Understanding the Structural Basis of Species Selective, Stereospecific Inhibition for *Cryptosporidium* and Human Thymidylate Synthase, *FEBS Lett*, (2019).
- [20]. Doan LT, Martucci WE, Vargo MA, Atreya CE, Anderson KS, Nonconserved residues Ala287 and Ser290 of the *Cryptosporidium hominis* thymidylate synthase domain facilitate its rapid rate of catalysis, *Biochemistry*, 46 (2007) 8379–8391. [PubMed: 17580969]
- [21]. Aso K, Imai Y, Yukishige K, Ootsu K, Akimoto H, Pyrrolo[2,3-d]pyrimidine thymidylate synthase inhibitors: design and synthesis of one-carbon bridge derivatives, *Chem Pharm Bull (Tokyo)*, 49 (2001) 1280–1287. [PubMed: 11605654]
- [22]. Dahlgren MK, Schyman P, Tirado-Rives J, Jorgensen WL, Characterization of biaryl torsional energetics and its treatment in OPLS all-atom force fields, *J Chem Inf Model*, 53 (2013) 1191–1199. [PubMed: 23621692]
- [23]. Zhang G, Liu C, Yi H, Meng Q, Bian C, Chen H, Jian JX, Wu LZ, Lei A, External Oxidant-Free Oxidative Cross-Coupling: A Photoredox Cobalt-Catalyzed Aromatic C-H Thiolation for Constructing C-S Bonds, *J Am Chem Soc*, 137 (2015) 9273–9280. [PubMed: 26158688]
- [24]. Kim R, Kuduk SD, Liverton N, Zhuo G, N-Heteroarylethyldiamines as orexin receptor antagonists and their preparation, in: *Merck Sharp & Dohme Corp., USA*. 2016, pp. 116pp.
- [25]. Demmer CS, Rombach D, Liu N, Nielsen B, Pickering DS, Bunch L, Revisiting the Quinoxalinedione Scaffold in the Construction of New Ligands for the Ionotropic Glutamate Receptors, *ACS Chem. Neurosci*, 8 (2017) 2477–2495. [PubMed: 28872835]
- [26]. Pedersen-Lane J, Maley GF, Chu E, Maley F, High-level expression of human thymidylate synthase, *Protein Expr Purif*, 10 (1997) 256–262. [PubMed: 9226722]
- [27]. Kabsch W, Xds, *Acta Crystallogr D Biol Crystallogr*, 66 (2010) 125–132. [PubMed: 20124692]
- [28]. McCoy AJ, Solving structures of protein complexes by molecular replacement with Phaser, *Acta Crystallogr D Biol Crystallogr*, 63 (2007) 32–41. [PubMed: 17164524]
- [29]. McCoy AJ, Grosse-Kunstleve RW, Adams PD, Winn MD, Storoni LC, Read RJ, Phaser crystallographic software *J Appl Crystallogr*, 40 (2007) 658–674.
- [30]. Emsley P, Cowtan K, Coot: model-building tools for molecular graphics, *Acta Crystallogr D Biol Crystallogr*, 60 (2004) 2126–2132. [PubMed: 15572765]
- [31]. Adams PD, Afonine PV, Bunkoczi G, Chen VB, Davis IW, Echols N, Headd JJ, Hung LW, Kapral GJ, Grosse-Kunstleve RW, McCoy AJ, Moriarty NW, Oeffner R, Read RJ, Richardson

- DC, Richardson JS, Terwilliger TC, Zwart PH, PHENIX: a comprehensive Python-based system for macromolecular structure solution, *Acta Crystallogr D Biol Crystallogr*, 66 (2010) 213–221. [PubMed: 20124702]
- [32]. Terwilliger TC, Grosse-Kunstleve RW, Afonine PV, Moriarty NW, Adams PD, Read RJ, Zwart PH, Hung LW, Iterative-build OMIT maps: map improvement by iterative model building and refinement without model bias, *Acta Crystallogr D Biol Crystallogr*, 64 (2008) 515–524. [PubMed: 18453687]
- [33]. Lee WG, Gallardo-Macias R, Frey KM, Spasov KA, Bollini M, Anderson KS, Jorgensen WL, Picomolar inhibitors of HIV reverse transcriptase featuring bicyclic replacement of a cyanovinylphenyl group, *J Am Chem Soc*, 135 (2013) 16705–16713. [PubMed: 24151856]
- [34]. Bollini M, Domaol RA, Thakur VV, Gallardo-Macias R, Spasov KA, Anderson KS, Jorgensen WL, Computationally-guided optimization of a docking hit to yield catechol diethers as potent anti-HIV agents, *J Med Chem*, 54 (2011) 8582–8591. [PubMed: 22081993]
- [35]. Jorgensen WL, Bollini M, Thakur VV, Domaol RA, Spasov KA, Anderson KS, Efficient discovery of potent anti-HIV agents targeting the Tyr181Cys variant of HIV reverse transcriptase, *J Am Chem Soc*, 133 (2011) 15686–15696. [PubMed: 21853995]
- [36]. Jorgensen WL, Efficient drug lead discovery and optimization, *Acc Chem Res*, 42 (2009) 724–733. [PubMed: 19317443]
- [37]. Jorgensen WL, Tirado-Rives J, Molecular modeling of organic and biomolecular systems using BOSS and MCPRO, *J Comput Chem*, 26 (2005) 1689–1700. [PubMed: 16200637]
- [38]. Jorgensen WL, Maxwell DS, TiradoRives J, Development and testing of the OPLS all-atom force field on conformational energetics and properties of organic liquids, *Journal of the American Chemical Society*, 118 (1996) 11225–11236.
- [39]. Jorgensen WL, Tirado-Rives J, Potential energy functions for atomic-level simulations of water and organic and biomolecular systems, *Proc Natl Acad Sci U S A*, 102 (2005) 6665–6670. [PubMed: 15870211]
- [40]. Jorgensen WL, Chandrasekhar J, Madura JD, Impey RW, Klein ML, Comparison of Simple Potential Functions for Simulating Liquid Water, *J Chem Phys*, 79 (1983) 926–935.

Highlights

Twenty-six novel antifolate analogues were synthesized

Biochemical and X-ray studies were performed to determine *ChTS* inhibition

2-phenylacetate methylene linker important for optimal position in *ChTS* active site

Active site rigidity driving force of inhibitor selectivity

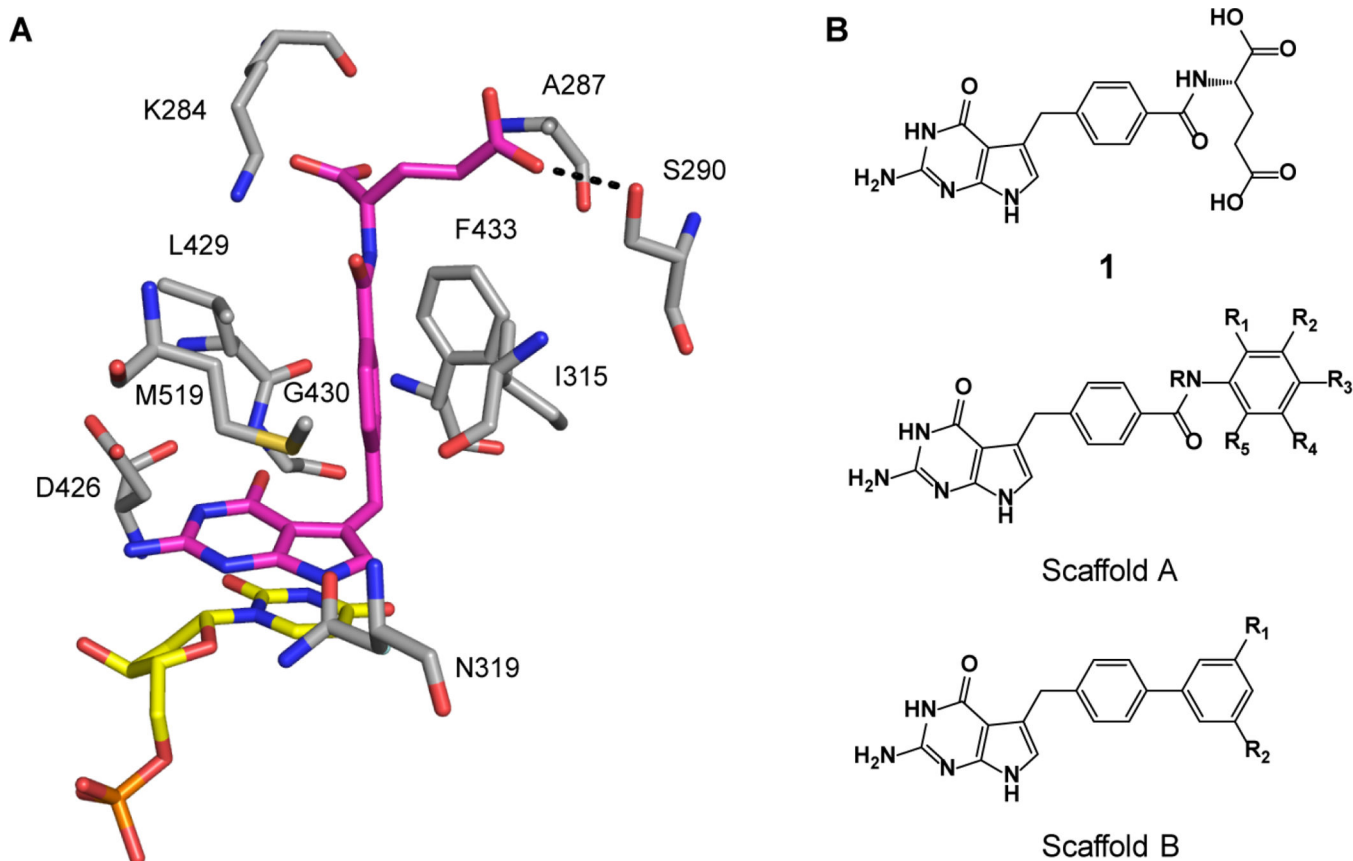


Figure 1. Lead optimization guided by crystal structure of compound **1** bound to *ChTTS*. A. Compound **1** bound in *ChTTS* active site, hydrogen bond between γ -carboxylate with S290 denoted by black dotted line. B. Structure of compound **1** and scaffolds used for lead optimization.

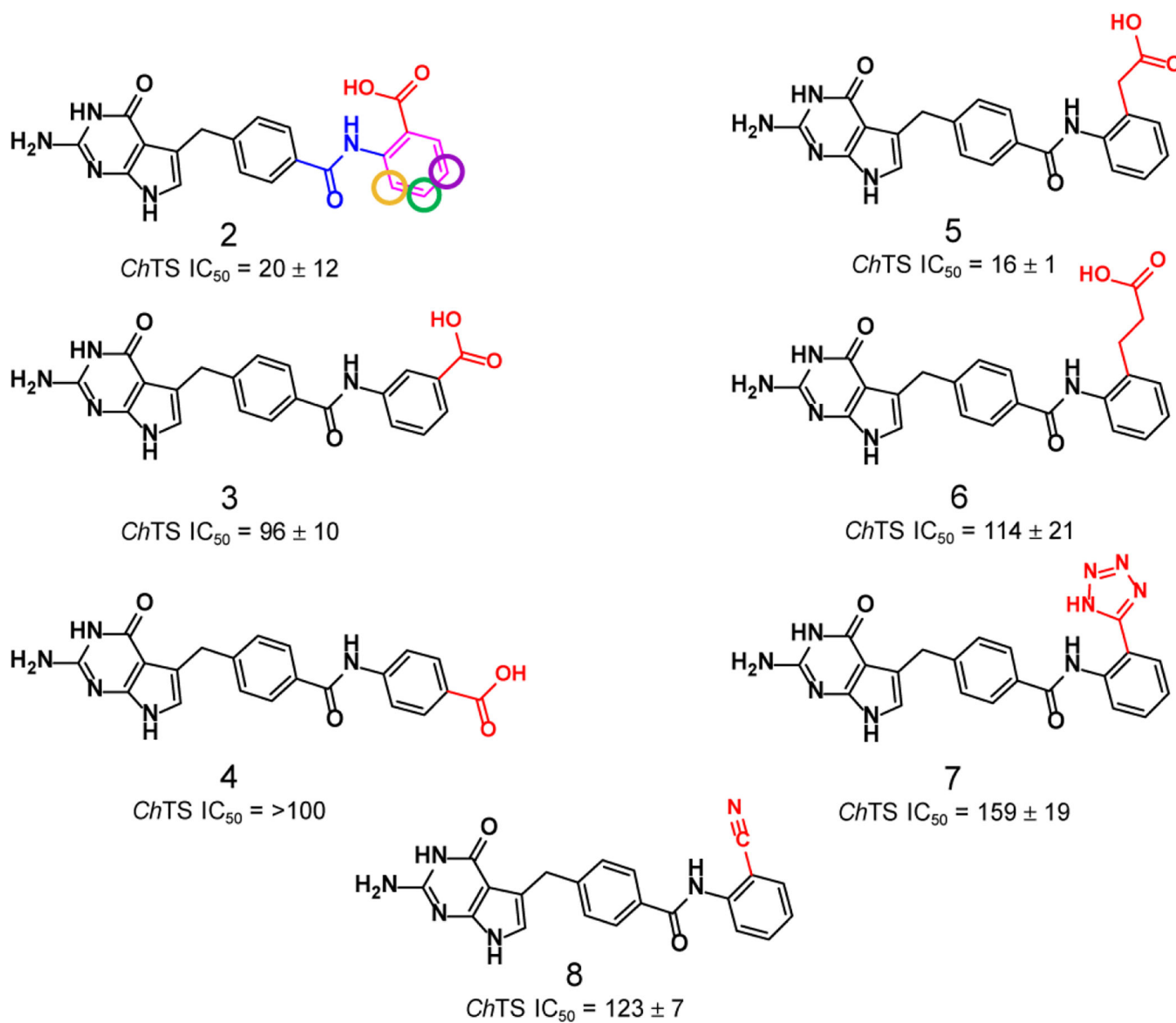
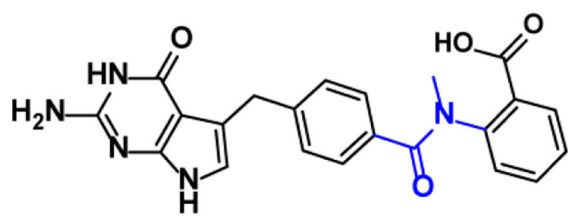
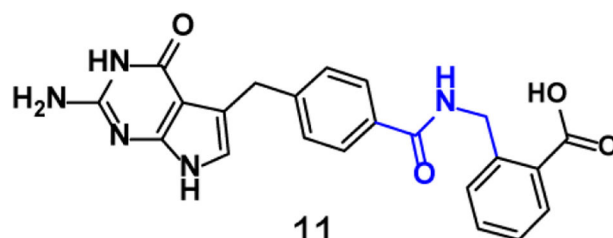


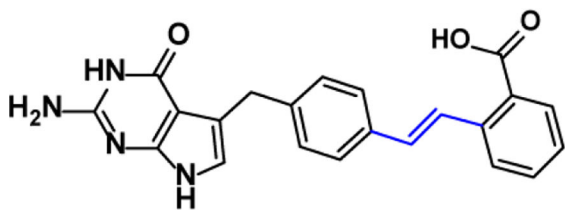
Figure 2. Structure and *ChTS* IC_{50} values for compounds 2–8, modifications made to carboxylate (red). Coloration of compound 2 denotes modifications made during SAR, amide linker moiety (blue), aromaticity (pink), carboxylate (red), and substitutions to C-3, C-4, and C-5 positions (purple, green, and gold, respectively).



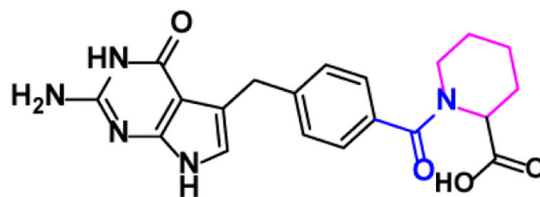
9

 $ChTS\ IC_{50} = 210 \pm 81$ 

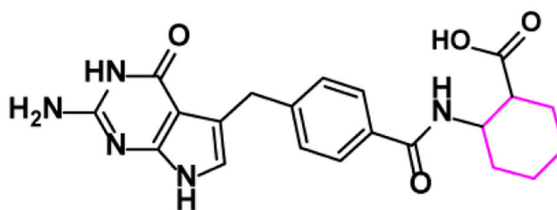
11

 $ChTS\ IC_{50} = 119 \pm 13$ 

10

 $ChTS\ IC_{50} = >100$ 

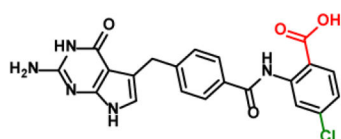
12

 $ChTS\ IC_{50} = >500$ 

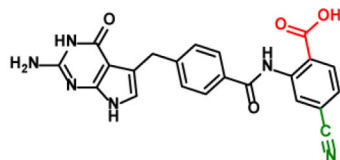
13

 $ChTS\ IC_{50} = 63 \pm 8$

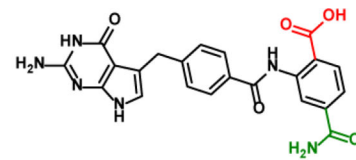
Figure 3. Structures and $ChTS\ IC_{50}$ values for compounds 9–13, modifications made to the amide linker moiety (blue), and aromaticity (pink).



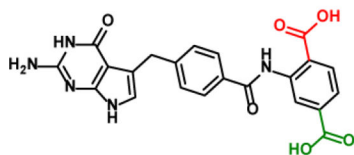
14

 $ChTS\ IC_{50} = 28 \pm 6$ 

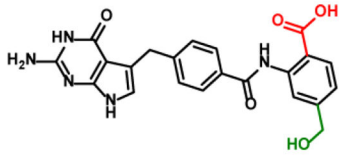
17

 $ChTS\ IC_{50} = 11 \pm 1$ 

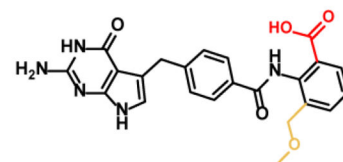
20

 $ChTS\ IC_{50} = 20 \pm 4$ 

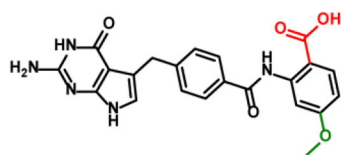
15

 $ChTS\ IC_{50} = 18 \pm 2$ 

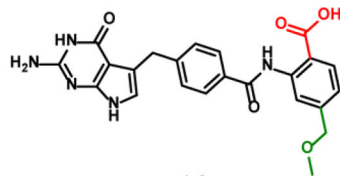
18

 $ChTS\ IC_{50} = 68 \pm 12$ 

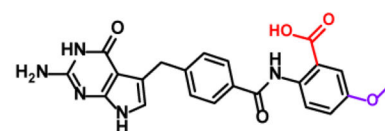
21

 $ChTS\ IC_{50} = 222 \pm 77$ 

16

 $ChTS\ IC_{50} = 50 \pm 8$ 

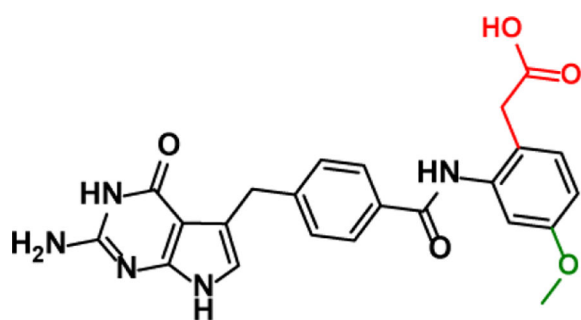
19

 $ChTS\ IC_{50} = 181 \pm 32$ 

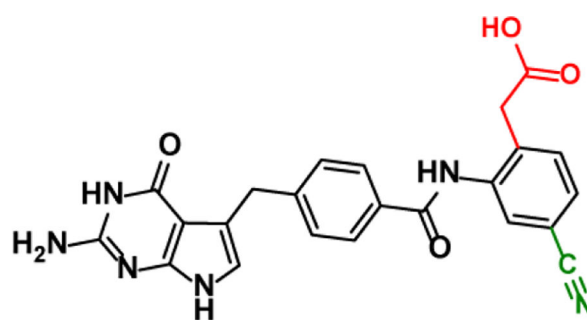
22

 $ChTS\ IC_{50} = >100$ **Figure 4.**

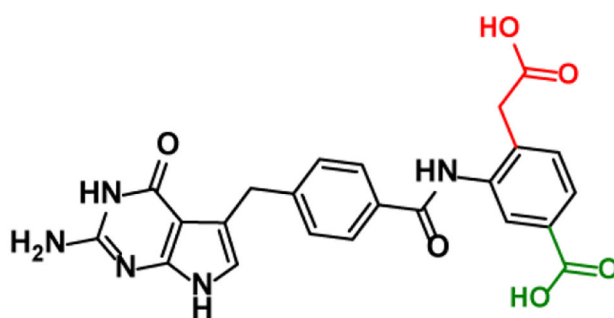
Structures and $ChTS\ IC_{50}$ values for compounds **14–22**, modifications made to the C-3 (purple), C-4 (green), and C-5 (gold) positions.



23
 $ChTS IC_{50} = 11 \pm 1$

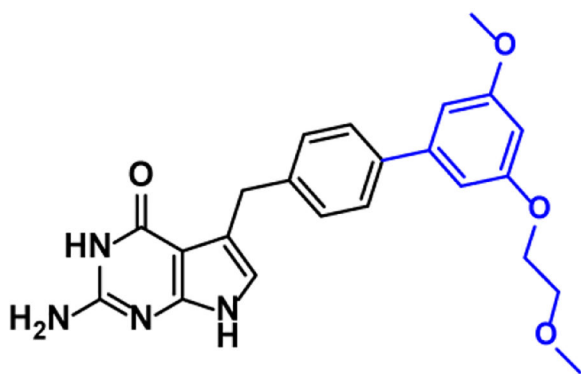


24
 $ChTS IC_{50} = 9.1 \pm 0.7$

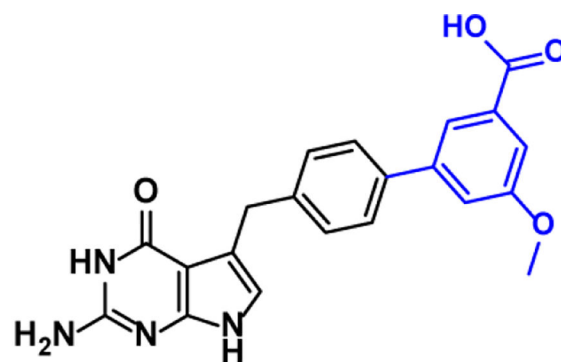


25
 $ChTS IC_{50} = 10 \pm 1$

Figure 5.
Structures and $ChTS IC_{50}$ values for compounds 23–25, modifications made carboxylate (red), and C-4 (green) positions.



26

 $ChTS\ IC_{50} = 97 \pm 44$ 

27

 $ChTS\ IC_{50} = >500$

Figure 6.
Structures and *ChTS* IC_{50} values for compounds 26–27.

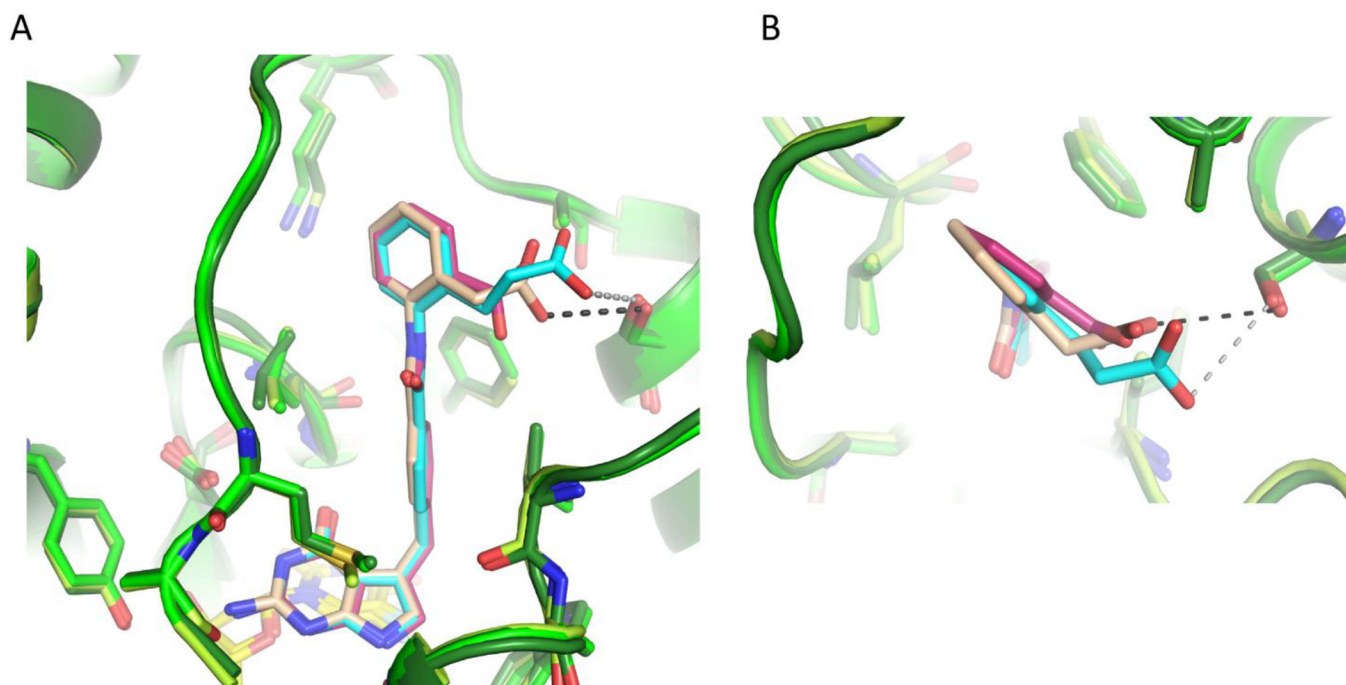


Figure 7. Comparison of *ChTS* bound to **2** (light green/warm pink), *ChTS* bound to **5** (green/tan) and *ChTS* bound to **6** (dark green/cyan) with dUMP (yellow) (PDB: 6PF7, 6PF9, and 6PFB). A. Comparison of **2**, **5**, and **6** bound in *ChTS* active site, hydrogen bonds to **5** in black and to **6** in gray. B. Top view of benzoic acid, 2-phenylacetic acid, and 3-phenylpropanoic acid moiety for **2**, **5**, and **6**, respectively.

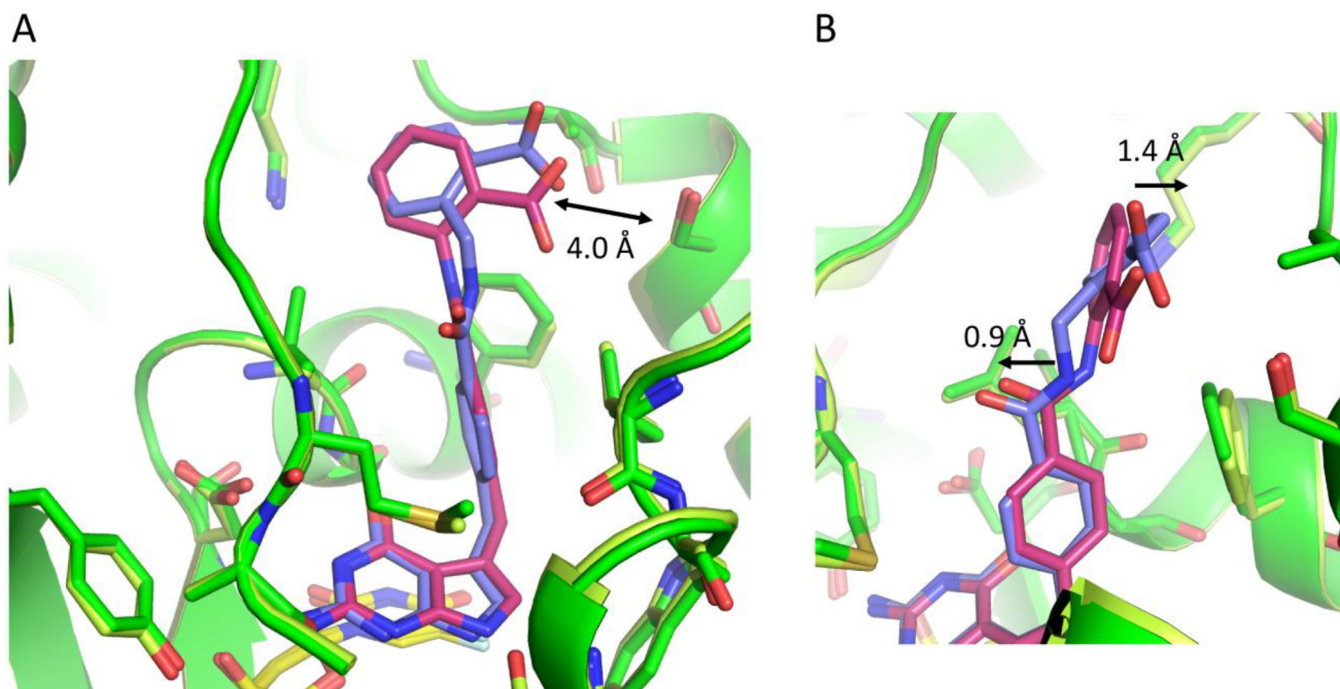


Figure 8.

Comparison of *ChTS* bound to **2** (green/warm pink) and *ChTS* bound to **11** (dark green/lavender) with dUMP (yellow) (PDB: 6PF7, and 6PFA). A. Comparison of **2** and **11** bound in *ChTS* active site, carboxylate group for both compounds are similar distance from S290
B. Zoom in view of **11** benzoic acid moiety compared to **2**.

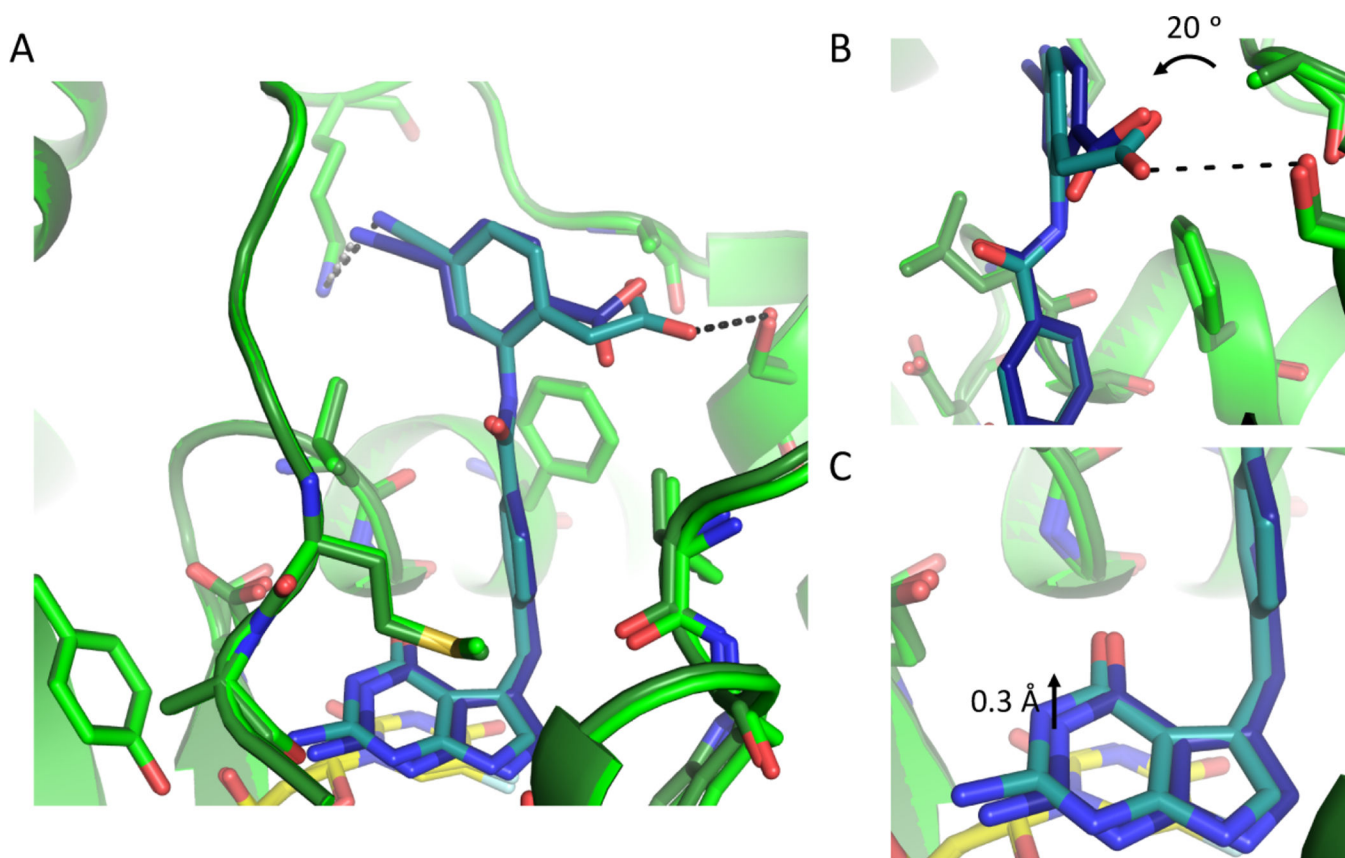


Figure 9. Comparison of *ChTS* bound to **17** (green/navy) and *ChTS* bound to **24** (dark green/teal) with dUMP (yellow) (PDB: 6PFF, and 6PFH). A. Comparison of **17** and **24** bound in *ChTS* active site, hydrogen bonds to **17** in gray and to **24** in black. B. Zoom in view rotation of **24** 2-phenylacetic acid moiety with respect to **17** benzoic acid moiety. C. Zoom in view of shift of pyrrolo[2,3-d]pyrimidine moiety of **17** and **24**.

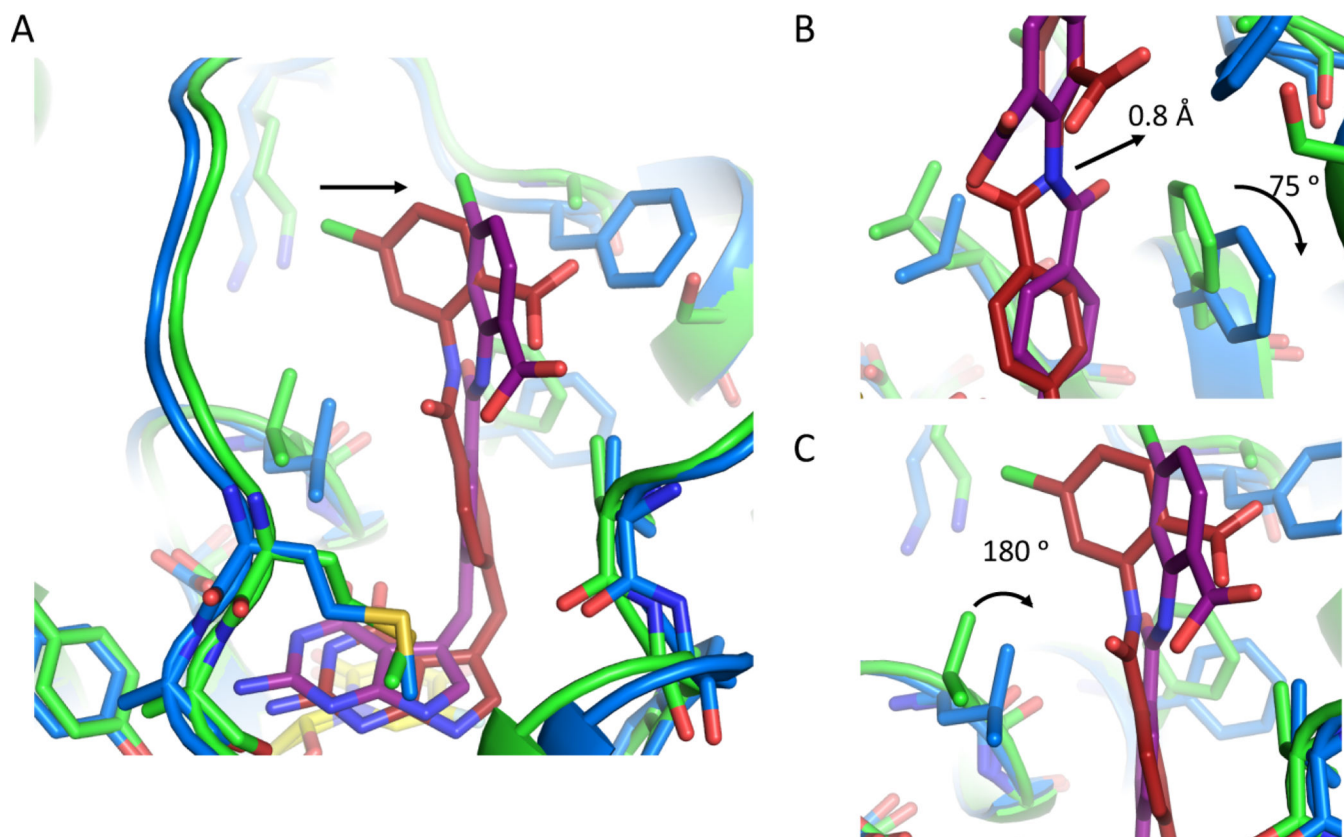
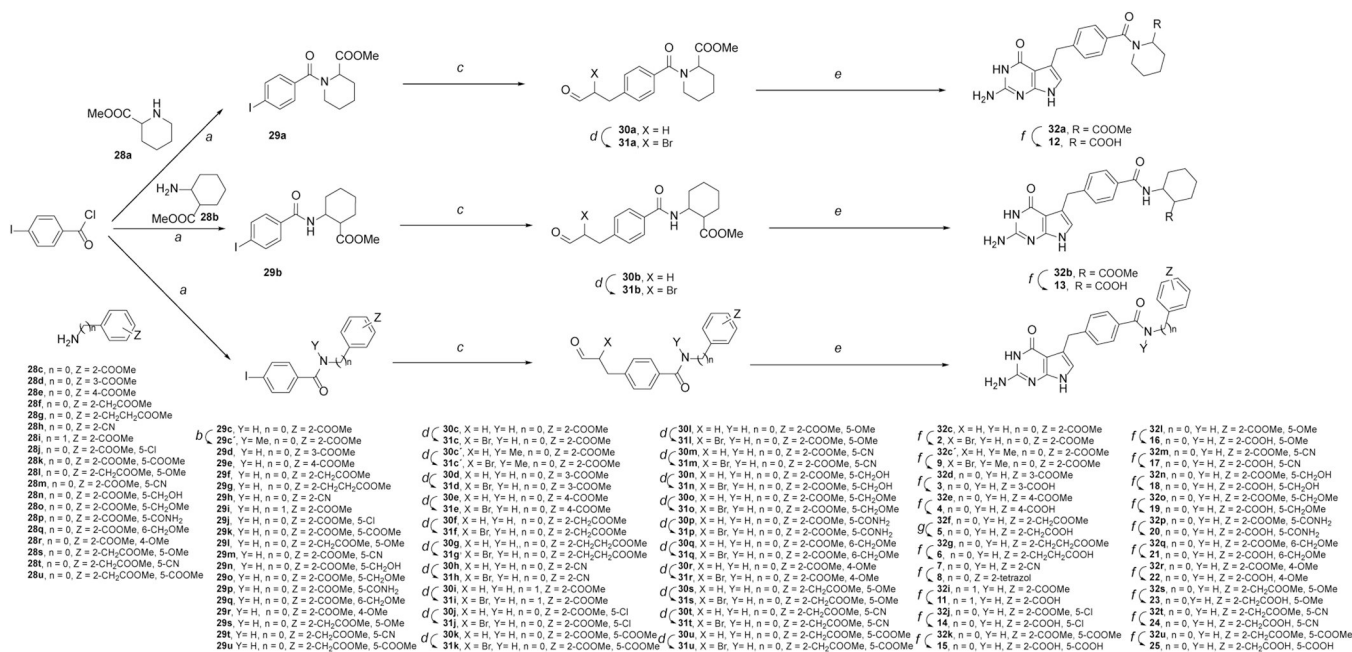
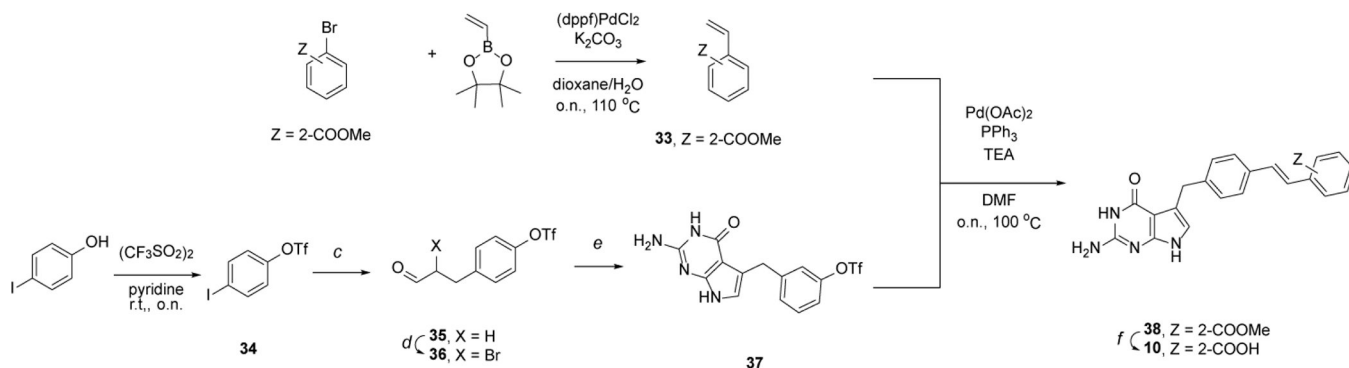


Figure 10. Comparison of hTS bound to **14** (blue/dark red) and ChTS bound to **14** (green/purple) with dUMP (yellow) (PDB: 6PF8, and 6PF3). A. Comparison of **14** bound in hTS and ChTS active site. B. Zoom in view hTS residue F225 and ChTS residue F433 position upon binding **14**. C. Zoom in view hTS residue L221 and ChTS residue L429 position upon binding **14**.

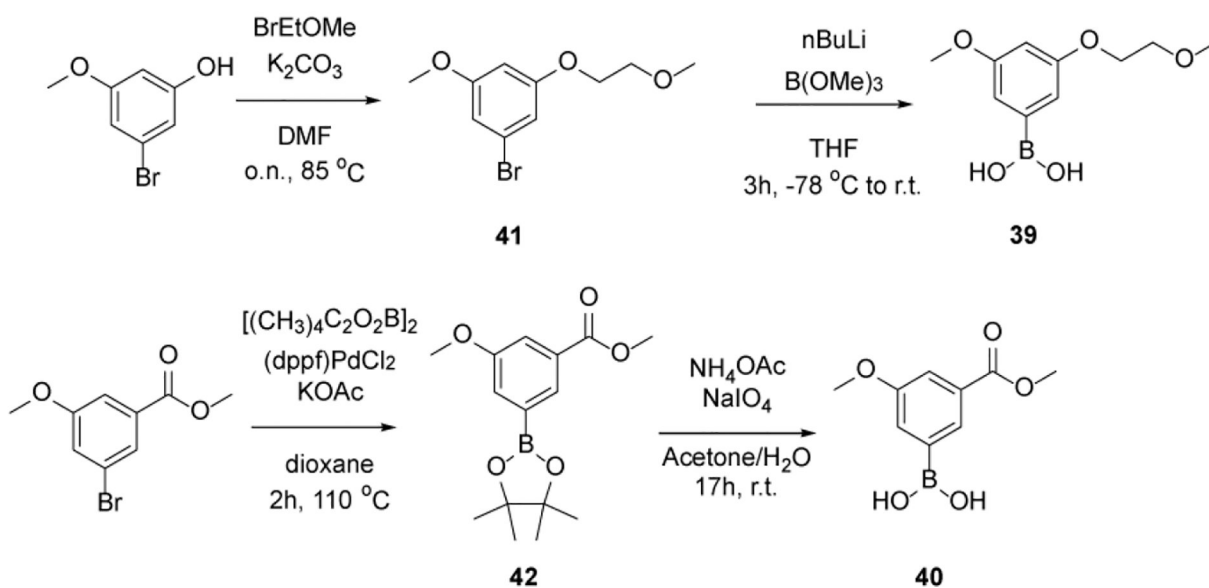
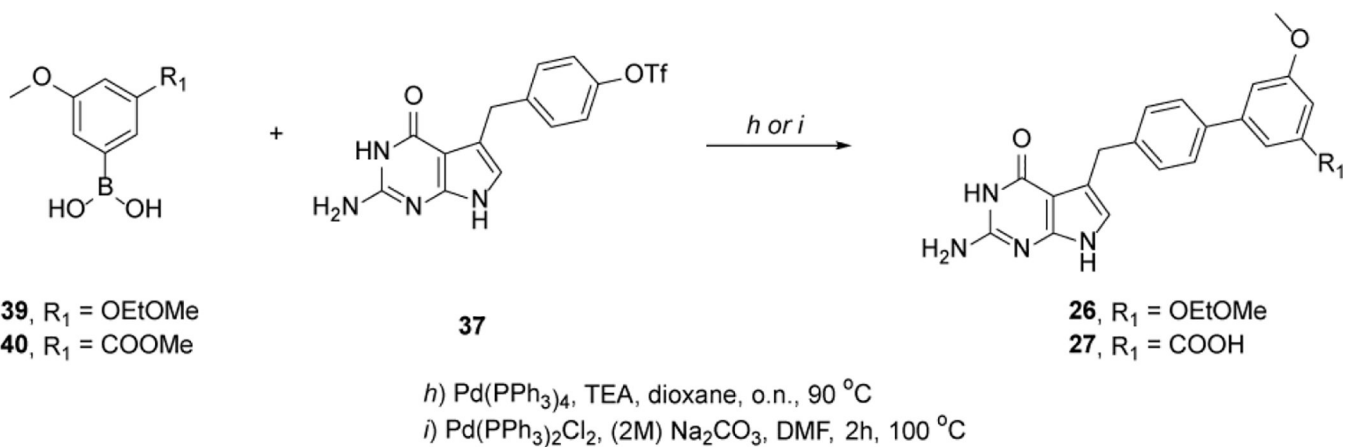
**Scheme 1.**

General scheme for the synthesis of compounds **2–9** and **11–25**.

^aReagents, conditions: (a) Et₃N, DCM, r.t., o.n.; (b) MeI, NaH, DMF, r.t., o.n.; (c) Allyl alcohol, NaHCO₃, Pd(OAc)₂, Bu₄NCl, 70°C, o.n.; (d) 5,5-dibromo meldrum's acid, HCl, THF, r.t., 18h; (e) 2,6-diaminopyrimidin-4-ol, NaOAc, MeOH/H₂O, 45 °C, 2h; (f) 2N NaOH, MeOH/H₂O, 60°C, 1h; (g) NaN₃, DMSO, 100°C, o.n.

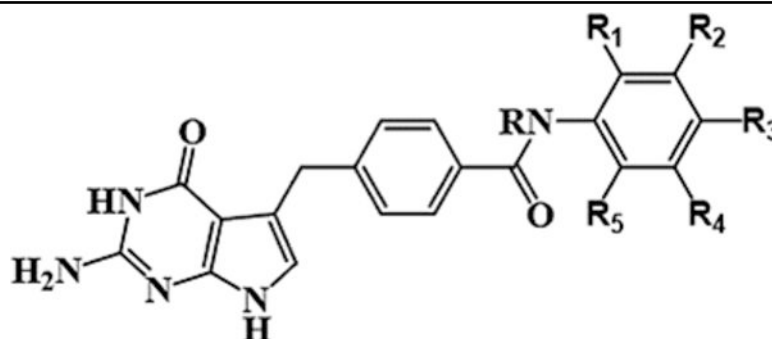


Scheme 2.
General scheme for the synthesis of compound 10.

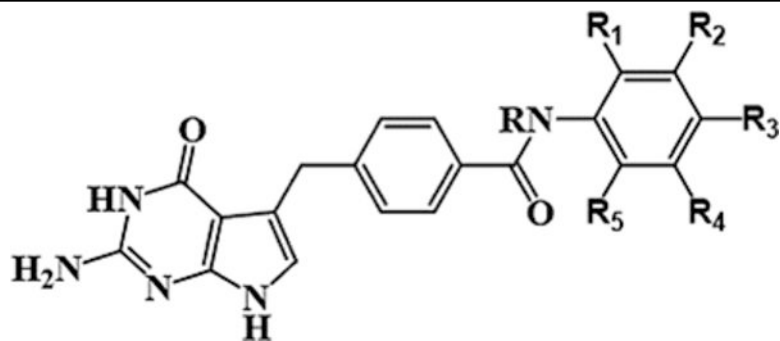
**Scheme 3.**

General scheme for the synthesis of compounds **26** and **27**.

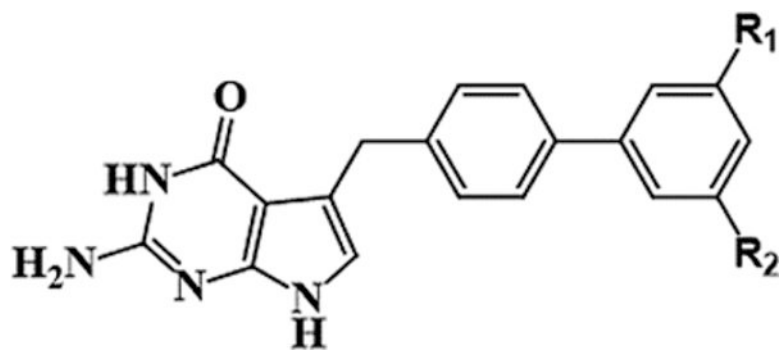
Table 1.

Compound 2–8 and 14–27 IC₅₀ (μM) for *ChTS*

Compounds	R ₁	R ₂	R ₃	R ₄	R ₅	<i>ChTS</i> IC ₅₀ (μM)	ClogP
2	COO ⁻	H	H	H	H	20 ± 12	2.63
3	H	COO ⁻	H	H	H	96 ± 10	2.47
4	H	H	COO ⁻	H	H	>100	2.49
5	CH ₂ COO ⁻	H	H	H	H	16 ± 1	1.96
6	(CH ₂) ₂ COO ⁻	H	H	H	H	114 ± 21	2.48
7	Tetrazole	H	H	H	H	159 ± 19	1.96
8	CN	H	H	H	H	123 ± 7	2.29
14	COO ⁻	H	H	Cl	H	28 ± 6	3.28
15	COO ⁻	H	H	COO ⁻	H	18 ± 2	2.51
16	COO ⁻	H	H	OCH ₃	H	50 ± 8	2.66
17	COO ⁻	H	H	CN	H	11 ± 1	2.36
18	COO ⁻	H	H	CH ₂ OH	H	181 ± 32	1.94
19	COO ⁻	H	H	CH ₂ OCH ₃	H	68 ± 12	2.56
20	COO ⁻	H	H	CONH ₂	H	20 ± 4	1.42
21	COO ⁻	H	H	H	CH ₂ OCH ₃	>100	1.60
22	COO ⁻	H	OCH ₃	H	H	222 ± 77	2.66
23	CH ₂ COO ⁻	H	H	OCH ₃	H	11 ± 1	1.99
24	CH ₂ COO ⁻	H	H	CN	H	9.1 ± 0.7	1.69

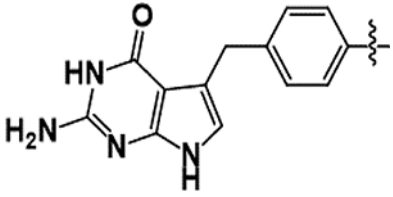
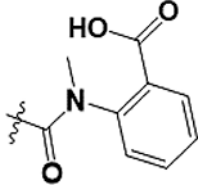
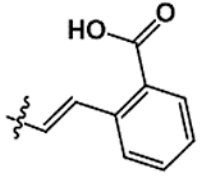
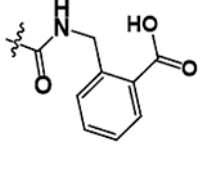
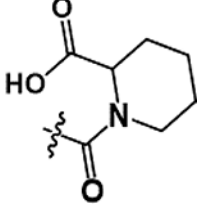
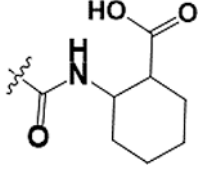


Compounds	R ₁	R ₂	R ₃	R ₄	R ₅	ChTS IC ₅₀ (μM)	ClogP
25	CH ₂ COO ⁻	H	H	COO ⁻	H	10 ± 1	1.85



26	O(CH ₂) ₂ OCH ₃	OCH ₃	~ ~	~ ~	~ ~	97 ± 44	3.42
27	COO ⁻	OCH ₃	~ ~	~ ~	~ ~	>500	3.38

Table 2.Compound 9–13 IC₅₀ (μM) for *ChTS*

Compound	<i>ChTS</i> IC ₅₀ (μM)	ClogP
		
	210 ± 81	2.87
	>100	3.60
	119 ± 13	1.81
	>500	-0.66
	63 ± 8	1.90